5105-157
Solar Thermal Power Systems Project
Parabolic Dish Systems Development

DOE/JPL-1060-93
Distribution Category UC-62

Projected Techno-Economic Characteristics of Solar Thermal Parabolic Dish-Electric Power Modules

T. Fujita
J. Bowyer
W. Gates
L. Jaffe
W. Revere

September 15, 1985

Prepared for
U.S. Department of Energy
Through an Agreement with
National Aeronautics and Space Administration
by
Jet Propulsion Laboratory
California Institute of Technology
Pasadena, California

JPL Publication 85-87

5105-157
Solar Thermal Power Systems Project
Parabolic Dish Systems Development

DOE/JPL-1060-93
Distribution Category UC-62

Projected Techno-Economic Characteristics of Solar Thermal Parabolic Dish-Electric Power Modules

T. Fujita
J. Bowyer
W. Gates
L. Jaffe
W. Revere

September 15, 1985

Prepared for
U.S. Department of Energy
Through an Agreement with
National Aeronautics and Space Administration
by
Jet Propulsion Laboratory
California Institute of Technology
Pasadena, California

JPL Publication 85-87

Prepared by the Jet Propulsion Laboratory, California Institute of Technology, for the U.S. Department of Energy through an agreement with the National Aeronautics and Space Administration.

The JPL Solar Thermal Power Systems Project is sponsored by the U.S. Department of Energy and is part of the Solar Thermal Program to develop low-cost solar thermal and electric power plants.

ABSTRACT

Using test results from the operation of parabolic dish modules and the background gained in fabrication of these test modules, a techno-economic assessment of parabolic dish technology is made. Tests encompass dish modules employing organic-Rankine, Stirling, and Brayton engines. These tests indicate that early modules achieve efficiencies of 15 to 25% in converting sunlight to net-delivered electricity. Evolutionary improvements include: (1) conversion efficiency and operation and maintenance resulting from technology development activities already underway; and (2) cost reductions, due to design improvements of dish concentrators that parallel the advances made in heliostats for central receivers. These improvements are used as the basis for projecting future production module characteristics; that is, module costs determined as a function of production volume. Considering markets of isolated loads, small community power systems, and central power stations in conjunction with financing arrangements representative of municipal utilities, investor-owned utilities, and third-party investors, a value analysis is employed to determine breakeven costs for dish systems. The achievement of these breakeven costs is associated with establishing a level of production for the projected dish modules that will reduce costs to the breakeven value. If fossil fuel prices escalate to the upper bound limit of projections made in 1983, breakeven values are achieved for the most advanced systems projected on the basis of evolutionary development. If such upper bound fuel-price escalations occur, the assessment indicates that these markets represent potential opportunities which can be exploited through evolutionary development of the parabolic dish modules that are currently in the test and evaluation stage. When the nominal or intermediate projections made in 1983 for fuel-price escalations are used, results indicate that further major advances in technology leading to considerably higher performance and lower costs will be needed to penetrate all but the least competitive markets.

ACKNOWLEDGMENTS

The editorial and publication aspects of this report were handled by Peggy Panda. The authors wish to express their appreciation for her special effort, invaluable contributions, and enthusiastic support. The authors also express their gratitude to Marion Rice for preparation of draft manuscripts.

This report is based on work accomplished by the Solar Thermal Power Systems (TPS) Project at the Jet Propulsion Laboratory (JPL). The following project managers provided inputs and guidelines regarding the formulation of material presented in this report: Vince Truscello, Project Manager, and John Lucas and Al Marriott, Assistant Project Managers. This report was completed during JPL phase-out and transition of the program to Sandia National Laboratories, with John Lucas serving as Project Manager during this period. The authors wish to thank these managers for their contributions and support.

The TPS Project was one of many energy-related projects under an Energy Program area directed by Dr. Marshall Alper. The policies established by Dr. Alper regarding transfer of information and documentation during the phase-out and transition period made it possible to prepare this report. Furthermore, Dr. Alper provided significant contributions in reviews of report manuscripts. The authors wish to express their appreciation for this effort as well as the overall direction that was provided during the entire period of the TPS Project at JPL.

GLOSSARY

Acronyms

ac	alternating current
ACC	Applied Concepts Corp.
ACRS	Accelerated Cash Recovery System
AGT	Advanced Gas Turbine
ASE	Automotive Stirling Engine
dc	direct current
DOE	U.S. Department of Energy
EIA	Energy Information Administration
EPRI	Electric Power Research Institute
ESOR	Experimental Solar-Only Receiver
ETS	Edwards Test Station, Edwards, California
FACC	Ford Aerospace and Communications Corp.
JPL	Jet Propulsion Laboratory
MTBF	Mean Time Between Failures
NASA	National Aeronautics and Space Administration
O&M	Operation and Maintenance
OPEC	Organization of Petroleum Exporting Countries
PCA	Power Conversion Assembly
PCS	Power Conversion Subsystem
PCU	Power Conversion Unit
PDC	Parabolic Dish Concentrator
PDTS	Parabolic Dish Test Site
PKI	Power Kinetics, Inc.
SAGT	Solar Advanced Gas Turbine
SCE	Southern California Edison Co.
SKI	Solar Kinetics, Inc.
SNLA	Sandia National Laboratories, Albuquerque, New Mexico
TAP	Turbine/Alternator/Pump
TBC	Test Bed Concentrator
TEFRA	Tax Equity and Fiscal Responsibility Act of 1982
TPS	Solar Thermal Power Systems Project
USAB	United Stirling AB of Sweden

Units and Measurements

Btu	British thermal units
cm	centimeter
deg	degrees (angular)
°C	degrees Celcius
°F	degrees Fahrenheit
ft	foot, feet
h	hour
hp	horsepower
Hz	Hertz
in.	inch
kHz	kiloHertz
kVA	kilovolt amperes
kW	kilowatt
kWe	kilowatt-electric
kWt	kilowatt-thermal
kg	kilogram
lb	pound
m	meter
m^2	square meter
mi	mile
min	minute
MJ	megajoule
mm	millimeter
MPa	megapascal
mrad	milliradian
MWe	megawatt-electric
%	percent
psi	pounds per square inch
psia	pounds per square inch absolute
rev/min	revolutions per minute
s	second
V	volt
wk	week
yr	year

CONTENTS

Figures

Tables

SECTION I

INTRODUCTION

A. BACKGROUND

From 1976 to 1984, the Jet Propulsion Laboratory (JPL) was responsible for a Solar Thermal Power Systems (TPS) Project sponsored initially by the U.S. Energy Research and Development Administration and later by the successor to ERDA, the U.S. Department of Energy (DOE). The TPS Project concerned the development of solar thermal power systems for terrestrial use.

Much of the TPS Project effort centered about the development of power systems using parabolic dish modules. Each module consists of a parabolic dish solar concentrator, a receiver-engine-generator assembly mounted near its focal point, and the associated accessories (Figure 1-1). The concentrator optical elements rotate about two axes to follow the sun; they focus the incident sunlight on the receiver. The receiver has an aperture through which the concentrated solar flux enters and impinges on receiver internal surfaces. The solar energy absorbed by these internal surfaces is converted to heat which is then transferred to the working fluid of the engine. The engine drives the generator to produce electrical energy.

The project was organized around the development of three basic options, differing in the type of engine used: organic-Rankine, Stirling, or Brayton. The pursuit of options based on three different types of engines provided the dish program with the ability to select engines on the basis of suitability and availability for a particular system. In particular, if a production engine representing any one of the three basic types were to be developed for a non-solar application, the project would be oriented toward developing the technological basis for adapting this engine for use on solar dish systems.

This report provides an assessment of the techno-economic characteristics of parabolic dish systems based on development activities conducted by JPL. Test results and the experience gained in fabricating test hardware have provided the basis from which the performance and cost characteristics have been projected for production modules that incorporate evolutionary improvements to present test hardware. An assessment of system economic viability was obtained by evaluating potential markets for and manufacturing costs of the projected production systems and by comparison of these solar thermal power systems with systems that use fossil fuels.

B. OBJECTIVES

The overall purpose of this report is to provide an assessment of parabolic dish systems that reflects the status as of 1983 to 1984 time frame, at which time the responsibility for the program was transferred from JPL to the Sandia National Laboratories, Albuquerque, New Mexico (SNLA). The assessment is to be based primarily on the findings of the JPL development team and their projections based on these findings.

Specific objectives of the study are to:

(1) Project the performance and cost characteristics of parabolic dish systems based on hardware development experience and testing activities.

(2) Estimate the market potential of parabolic dish systems through value analysis and breakeven cost analysis, where projected cost characteristics as a function of production volume are combined with breakeven costs and market size to assess the potential for market penetration.

(3) Delineate the effects of uncertainties in projecting system characteristics and in estimating markets, and identify the key developmental and economic factors that have the greatest effects on the assessment.

C. SCOPE AND MAJOR CAVEATS

The primary focus of the parabolic dish and other solar thermal programs has been on technical development activities. For the purpose of assisting in formulating management policies and in making technical decisions that would provide the most beneficial expenditure of government resources, assessment studies that were scoped to provide the needed first-order insights were undertaken. This report reflects the findings of these limited scope activities.

A major caveat of the assessment given in this report is that it is based on developmental experience gained at JPL up to the 1983 to 1984 time frame. The developmental program is continuing under the technical direction of SNLA. Thus, this report should be viewed as an assessment of parabolic dish systems at a particular stage in their developmental history.

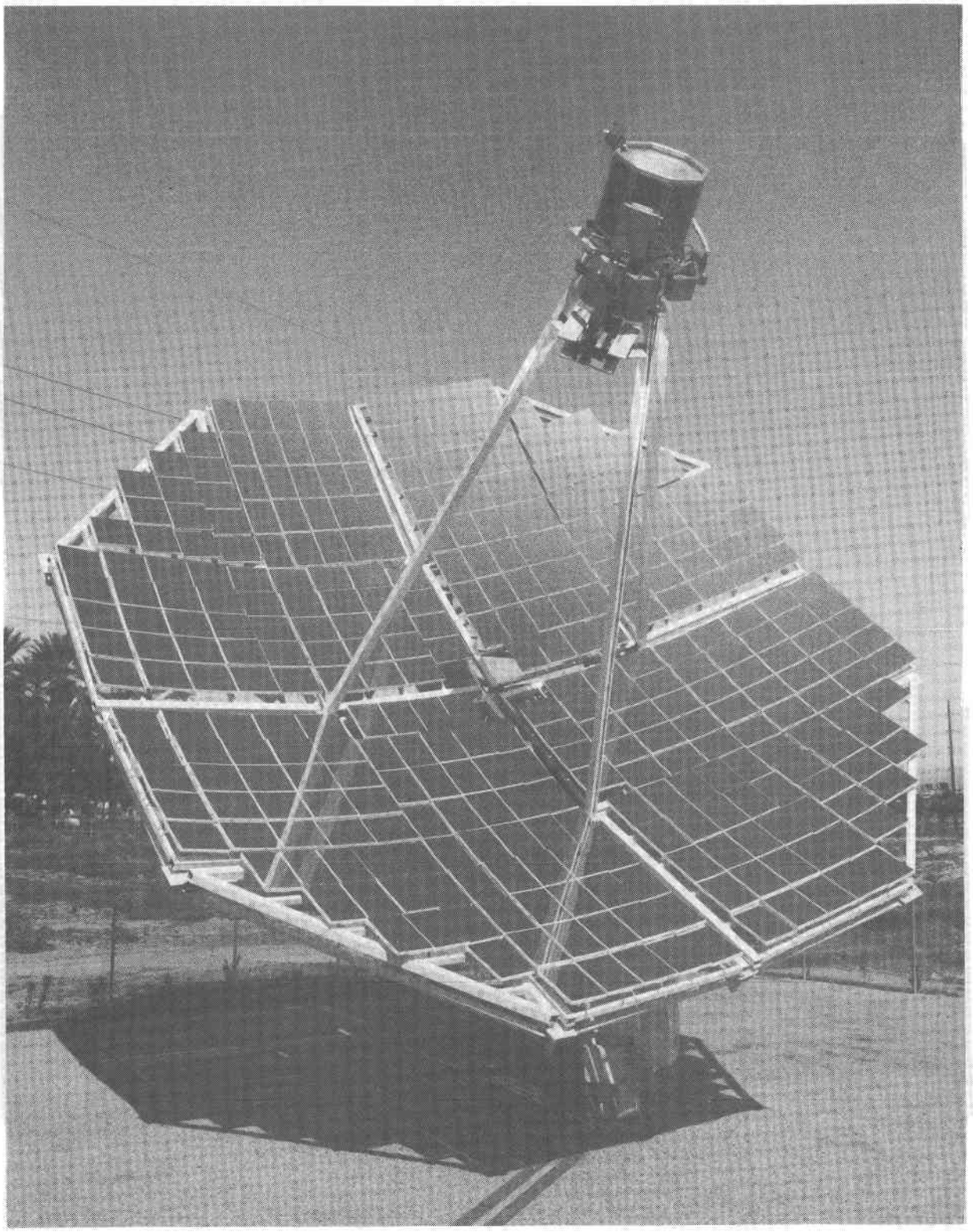

Figure 1-1. Advanco Stirling Module at Rancho Mirage, California

SECTION II

TESTS OF EXPERIMENTAL MODULES

The Solar Thermal Power Systems (TPS) Project at JPL conducted many tests: tests of materials, components, subsystems, assemblies of subsystems, and complete experimental modules. This section primarily describes tests of experimental modules and assemblies of subsystems, with less complete accounts of tests of lower-level items (more detailed accounts of the tests may be found in the references cited). It covers experimental modules that represent each of the three basic options. The experience gained in developing the experimental hardware and the test results of this section provide a major part of the basis for projecting system characteristics discussed in Section III.

A. TEST SITES

Tests of experimental modules were performed at three principal sites:

(1) JPL's Parabolic Dish Test Site (PDTS) at Edwards, California. Rankine and Stirling modules were tested at the PDTS.

(2) A Southern California Edison Co. (SCE) site at Rancho Mirage, near Palm Springs, California, and adjacent to the SCE's Santa Rosa substation. A Stirling module was tested at Rancho Mirage (see Figure 1-1).

(3) A Sanders Associates, Inc., site adjacent to their manufacturing facilities at Merrimack, New Hampshire. An experimental Brayton module was tested at Merrimack.

The Rancho Mirage and Merrimack tests included concentrators intended to be part of the complete experimental module. At the PDTS, however, the modules were tested with a Test-Bed Concentrator (TBC) rather than with a concentrator intended to be used later as part of the module. The TBCs are described in Section II.F. Some tests of subsystems and components were carried out at the PDTS; most were made at the systems contractors' or suppliers' sites.

B. ORGANIC-RANKINE TESTS

1. Ford Aerospace and Communications Corporation's System

The organic-Rankine assembly tested was designed and assembled by Ford Aerospace and Communications Corporation (FACC). Principal elements included a FACC receiver, a Barber-Nichols Rankine engine with a Simmonds Precision alternator, and power-conditioning equipment assembled by FACC. The assembly was planned to be combined with a General Electric Co. or Acurex Corp. concentrator to form a complete module, but was tested at the PDTS with

a TBC (Figure 2-1). A group of modules was intended to form the basis for a Small Community Solar Thermal Power Experiment, providing power to an electric utility on an experimental basis (Reference 1).

The cavity receiver was designed to heat toluene, the working fluid, to a temperature of 400°C (750°F) and a pressure of 4.2 MPa (600 psi). The toluene was contained in a single coiled tube of stainless steel, brazed to the exterior of a cylindrical copper shell, which served to distribute the heat evenly (Figure 2-2). The core assembly of tube and shell was nickel-plated and painted black on its interior to improve absorption of the incoming sunlight, and was surrounded by thermal insulation (Figure 2-3). The receiver aperture diameter was 380 mm (15 in.).

The receiver and power conversion subsystem constituted a power conversion assembly, schematized in Figure 2-4 and sketched in Figure 2-5. The power conversion subsystem was built around a turbine/alternator/pump (TAP) unit. Other major elements (Figure 2-5) included a regenerator, a condensor, start and boost pumps, valving, and a rectifier. The TAP (Figure 2-6) was 125 mm (5 in.) in diameter; its rotating parts were mounted on a single shaft turning at a design speed of 60,000 rev/min. The (feed) pump pressurized toluene to 3.9 to 4.2 MPa (550 to 600 psi), and delivered it to the regenerator where it was preheated. The toluene went to the receiver where it was heated and vaporized, then to a vapor control valve, which controlled the toluene flow so as to keep the turbine inlet temperature close to its design value despite variations in insolation. The toluene then drove the turbine, exiting to the low-pressure side of the regenerator, then to an air-cooled condenser where it was cooled and condensed, and then to a boost pump that returned it to the feed pump. The power conversion assemblies were evacuated to remove oxygen before being filled with toluene and then sealed.

The turbine was a single-stage impulse type. The permanent magnet alternator used samarium-cobalt armature magnets and produced 3-kHz, three-phase, 500 to 600 V output at design speed. The TAP was a sealed unit, designed to prevent loss of toluene or any inflow of air that could oxidize the hot toluene. For bearing lubrication, it utilized toluene internally fed through a hole down the center of the shaft. Radial bearings used tilting pads; thrust bearings used radially grooved, gimballed, flat bronze washers.

The 3-kHz power went to a rectifier mounted on the concentrator. The dc output was intended to be connected in parallel with that from other modules and delivered to a controlled inverter for conversion to 60 Hz, three-phase. The inverter had a controlled duty cycle that maintained the preset voltage across the dc bus regardless of changes in ac load. The test inverter, built by Nova Electric Manufacturing Corp. was designed to handle 30 kVa. For a full-sized powered plant it was expected that much larger inverters, each handling the output from many modules, would be used.

The 60-Hz power went through a switchboard that delivered it either to the Southern California Edison Co. distribution grid at the PDTS or to a local load bank. The load bank was provided for test purposes and to absorb the generated power if the system was accidentally disconnected from the grid or

if grid failure occurred while the system was generating power. The inverter, switchboard, load bank, grid interface equipment, and power cabling constituted the energy transport subsystem.

Control was provided by a master plant controller (designed to control a number of modules) connected to a remote control interface assembly that formed part of the module. These units were designed to accept operator commands and cycle the plant and modules through appropriate modes, including startup and shutdown. Because the TBC was PDTS facility equipment, it was controlled separately during the tests. Figure 2-7 is a schematic of this test setup at the PDTS.

2. System Tests Conducted

The PDTS test of the organic-Rankine equipment was performed as a verification test of the power conversion assembly prototype and as a qualification test of the energy transport subsystem prototype. Its primary objective was to validate the design of these items. This required that the module be operated under a wide range of conditions and be subjected to artificially imposed perturbations. It operated on-sun for a total of 33.6 h.

Before the test, the TBC mirror facets were adjusted to produce a flux distribution at the receiver similar to that predicted for Parabolic Dish Concentrator No. 1 (PDC-1) designed by General Electric (Reference 2). It should be noted that the power conversion assembly was designed for an input of 96.5 kWt. The TBC could provide only 76 kW at an insolation of 1 kW/m^2, and the insolation was this high only once during the test period. Thus, the receiver, turbine, pumps, alternator, rectifier, and inverter operated at less-than-design conditions. Also, because of some earlier data, the inverter was generally set to maintain 500 V on the dc bus, rather than the 600 V used for system design. The result was that the TAP generally operated at significantly less than design speed.

The tests provided data for (1) the evaluation of module performance at various levels of solar input to the receiver, (2) the transients caused by abrupt changes in solar input, (3) the effect of various voltage settings for the dc bus and (4) the operation of the system in all control modes. The effect of a second module on inverter and control performance was simulated by placing a dc power supply in parallel with the dc produced by the test module.

3. System Test Results: Performance

Test results are given in References 1 and 3; highlights are summarized as follows. Efficiency and output were calculated for the module and for the system, which included both module and inverter. Both gross and net efficiencies and outputs were calculated; that is, before and after deduction of parasitic power, such as that used to drive the boost pump, condenser fan, concentrator, etc.

An example representative of steady-state operation with near-maximum solar input was Run 13 (Test No. 8) at 12:00 noon on 3 March 1982. The measured direct normal insolation was 0.983 kW/m^2. The measured module

power delivered into the inverter was 16.2 kW gross or 15.5 kW net. The measured system output from the inverter was 13.5 kW gross or 12.8 kW net. Parasitics were 0.69 kW. Corresponding efficiencies for the module were 18.6 gross and 17.8 net; for the system, 15.5 gross and 14.7 net. These efficiencies were calculated without correction for circumsolar radiation (see Reference 1).

Subsystem efficiences were:

Concentrator	0.85 (gross)
Receiver	0.95
Power conversion subsystem	0.23 (gross)
Inverter	0.83
Parasitic loss factor	0.95

Subsystem performance is shown in a "waterfall chart," Figure 2-8.

In interpreting these results, it should be noted that the input power to the various subsystems and components was well below their design points. The receiver was rated at 95 kW input and received only 74.2 kW; the power conversion subsystem (PCS) was rated at 92.4 kW input and received only 70.8 kW; the inverter was rated for 30 kVa input and received only 16.2 kW. Subsystem tests showed that their efficiencies would be considerably higher when operated at their design points (see Reference 3). Further, the inverter was much smaller than one designed for plant use and was operated below design voltage; again these factors would be expected to reduce its efficiency. The measured efficiency of the inverter was 83.3% in the test mentioned.

The tests verified proper operation of the system, including its automatic control subsystem, in many design modes and under transient conditions. They provided many desired performance data. Power at 60 Hz was delivered to the Southern California Edison grid.

4. System Test Results: Malfunctions

Malfunctions in the units under solar test included the following:

(1) The servo-operated vapor control valve of the engine stuck. This failure was traced to contamination in the commercial servo unit.

(2) The inverter failed, ending the test series.

In addition, damage to the bearings of the TAP unit was found in post-test examination. This problem is discussed in Section II.7.

5. Ford Aerospace and Communications Corp. Subsystem Tests

Prior to the system tests at the PDTS, FACC carried out tests of the receiver, the energy transport subsystem, the control subsystem, and the power conversion assembly (receiver with power conversion subsystem).

Barber-Nichols, the engine manufacturer, carried out tests of the power conversion subsystem and of its subassemblies.

The alternator and inverter were tested by their respective manufacturers, Simmonds Precision and Nova Electric Manufacturing Corp. After the solar tests of the system, Barber-Nichols performed considerable development work and testing on the TAP unit.

6. Subsystem Test Results: Performance

The receiver performed as designed (Reference 4). No local hot spots or instabilities were found, even when the toluene pressure was lowered to 3.2 MPa (450 psi) where two-phase flow would occur. (At the design pressure toluene is super-critical.) Receiver efficiency was 95.4% at 85% of rated power.

The power conversion subsystem also generally performed well (Reference 5). Figure 2-9 shows the efficiency versus input power measured both in subsystem tests and in the system test on-sun. The maximum measured power conversion efficiency was 23% net; the maximum net power output from the power conversion subsystem was 21.6 kWe. As a result of tests and analyses, FACC concluded that efficiency could be improved if the fluid dynamics of the turbine and regenerator nozzles and of the feed pump were modified and the alternator diameter increased to improve the magnetic path.

The control and energy transport systems, with the exception of the inverter, behaved well (Reference 6). Measured part-load efficiency of the inverter is shown in Figure 2-10.

7. Subsystem Test Results: Malfunctions

The dc/ac power inverter, which performed a key control function, failed several times in test and did not operate properly. Part of the difficulty was traced to incorrect internal wiring. In later development of the organic Rankine system for use in Small Community Solar Experiment 1, the Nova inverter was replaced by a different inverter.

Some power conversion subsystem malfunctions were traced to a dirty toluene filter. Frequent opening of the sealed toluene system during development was considered a major contributor.

Wear and damage to the bearings of the TAP unit were found in many of the tests. Changes made to correct this included going from internal (through the shaft) to external (through the bearings) hydrodynamic toluene lubrication and changing the radial bearings to another tilting-pad design. The most important source of damage, however, appeared to be electrical arcing from rotor to stator in the vicinity of the bearings. This was stopped by insulating the bearings. Thereafter, no wear or damage was found in 300 h of bearing test under the JPL TPS Project (Reference 7). Further tests have been conducted by Barber-Nichols for Small Community Solar Experiment 1.

C. STEAM-RANKINE SYSTEMS

Steam-Rankine systems were not a major focus of the JPL TPS Project; it was believed that a sealed toluene system would require much less maintenance. Nevertheless, tests were run on: (1) a steam-Rankine system built by the Omnium-G Co.; (2) a steam collector heating system built by Applied Concepts Corp. and Power Kinetics, Inc.; (3) a steam receiver built by Garrett AiResearch Manufacturing Co.; and (4) two steam engines built by Jay Carter Enterprises, Inc.

1. Omnium-G System

This system incorporated a concentrator, receiver, reciprocating steam engine, and control subsystem, all built by Omnium-G, plus an alternator and auxiliaries. Figure 2-11 is a schematic of this system. The concentrator (Figure 2-12) used 16 pie-shaped panels of polyurethane foam forming a 6-m-diameter paraboloid with focal ratio of 0.67. The reflecting surface was polished anodized aluminum sheet. Metal trusses supported the panels, which rested on a central elevation bearing on top of a pedestal. The pedestal rotated in azimuth by wheels on a track. Both axes were driven by electric motors, using chain and friction drive. Rough sun pointing was controlled by a clock; fine pointing by sun sensors through an analog loop.

The cavity receiver consisted of a single coil of stainless steel buried in an aluminum block inside an Inconel housing. The aluminum was designed to melt during operation to provide heat distribution and thermal storage. The receiver aperture was 100 mm (4 in.) in diameter.

The Omnium-G engine was a single-cylinder reciprocating steam engine designed by Roy F. Ferrier Co. and built by Omnium-G. It was a two-cylinder, double-acting engine designed to operate up to about 1000 rev/min and to provide about 34 kW (45 shaft hp) from 315°C (600°F) steam at 2.5 MPa (350 psia). Exhaust steam preheated the feedwater going to the receiver, then passed through a water-cooled condenser and oil separator. The engine drove a 10-kW, three-phase induction generator. The system was in limited commercial production.

2. Omnium-G System Test Results

Despite several years of effort, JPL was unable to get the Omnium-G system installed at the PDTS to operate properly. The concentrator and receiver did not provide enough steam to drive the engine except for short bursts. No measurements of steady-state performance could be made.

Malfunctions included sun-tracker drift and failures, elevation-drive failures to hold position in winds, engine piston seizure in the cylinder, and piston rods bending due to accumulation of water in the cylinder.

3. Omnium-G Subsystem Tests

Calorimeter and flux-mapper tests of the Omnium-G concentrator at the PDTS showed that it delivered 7 kWt through a 100-mm (4-in.) aperture and 12 kWt through a 180-mm (7.1-in.) aperture at an insolation of 1 kW/m^2 (Figure 2-13). These results were obtained with clean, newly replaced and aligned reflector panels. The hemispherical reflectance of new, clean panels was measured as 84% (Reference 8).

Measurements were also made of the concentrator and receiver together, known as the collector. This collector delivered about 4 kWt, normalized to an insolation of 1 kW/m^2 at 325°C (615°F) (see Figure 2-13). A series of changes was made, including a new tracking subsystem; a redesigned elevation drive using a jackscrew; adding insulation to the steam lines; and a new receiver. This receiver had a solid brass heat sink and a 200-mm (8-in.) diameter aperture. The heat collected was slightly above 10 kWt at 1 kW/m^2 insolation (Reference 9).

Tests of the Omnium-G engine were run using steam supplied by the Garrett steam receiver, heated by a TBC. (The Garrett receiver and the TBC are described below.) This provided more steam than the Omnium-C concentrator/receiver and the engine was run successfully. The maximum efficiency measured for this engine/generator assembly was 3.5% (see Reference 9).

4. Applied Concepts Corp./Power Kinetics, Inc. Steam Heating System Tests

Applied Concepts Corp. (ACC) was responsible for system design and integration of an experimental steam heating system that used a concentrator and receiver designed and built by Power Kinetics, Inc. (PKI). The system was designed to deliver steam for industrial heating, rather than for the generation of electricity.

The optical portion of the PKI concentrator (Figure 2-14) consisted of a 9-m square array of 864 flat facets of second-surface silver on glass, each 300-mm (12-in.) square. The focal ratio was 0.9. The mirror facets were backed by polyurethane foam and supported by metal frames. These formed a series of curved horizontal slats, one row of facets per slat. Each slat rotated individually in end plates to provide elevation pointing. This assembly was mounted on a framework resting on a track; the track rotated in azimuth over fixed wheels. The steam receiver consisted of parallel steel tubes, insulated and mounted in a steel box, with a 60-cm (24-in.) aperture. The receiver was mounted to the rotating framework to move in azimuth with the concentrator, but its elevation angle was fixed. The assembly was driven by electric motors, using a chain cable for the azimuth drive and worm gears for the slat elevation drive. Azimuth rough pointing was based on previous tracking data stored in a microprocessor. Fine pointing used sun sensors in an analog loop.

Two units were installed and tested as part of the JPL TPS Project. One was installed on concrete piers at the Mid-Temperature Test Facility of Sandia National Laboratories at Albuquerque, New Mexico, and was later transferred to

Hill Air Force Base in Utah. The other was installed on a roof-top platform at the Capitol Concrete Co., Topeka, Kansas. This unit received its feedwater from the feedwater supply provided for a much larger fuel-fired steam unit, and delivered its output to the main steam line or, when steam was not needed, to the feedwater heater. The Topeka installation was a technical feasibility test in an industrial environment.

5. Applied Concepts Corp./Power Kinetics, Inc. Steam Heating System Test Results

In tests at Albuquerque, the system delivered up to 200,000 Btu/h (59 kWt) of saturated steam at 150°C (305°F), for an overall plant thermal efficiency of 84%, averaged over an operating day, at an average insolation of 0.930 kW/m^2 (Reference 10). The unit at Topeka was run for 231 h over a 122-day test period under the cognizance of DOE Albuquerque Operations Office. On a day with an insolation of 0.880 to 0.940 kW/m^2, hourly output was about 100 MJ (28 kWt average) at an output temperature averaging 139°C (282°F) and a thermal efficiency of 42 to 50%. Over a 107-h period when insolation was above 600 W/m^2, average output was above 75,000 Btu/h (22 kWt), and conversion efficiency was above 37%. Plant availability (August through November) was 75% (Reference 11). System ownership was transferred to Capitol Concrete Co., which to date has run it for an additional 3 years. Capitol Concrete decided, however, not to run the system under winter conditions.

The unit at Hill Air Force Based was tested under Air Force sponsorship. Efficiency for this test was not calculated on the basis of output divided by solar input during operation, but instead the denominator used was the solar input available over the entire day, including that available outside of the 6 h when the system operated. On this basis, the highest daily efficiency at Hill Air Force Base was 0.31 (Reference 12).

Malfunctions included breakage of mechanical components, switch and control failures, EMI failures caused by lightning, freezing, and improper focus at low sun angles, plus some software and instrumentation malfunctions. Maintenance at Topeka was reported to average 1 hour per week; it was higher at Hill Air Force Base.

The system at Topeka was generally operated without operator attention, and operated during weekends with no one at the plant.

6. Garrett Steam Receiver

A prototype steam receiver was designed and built by the Garrett AiResearch Manufacturing Co. of California under the JPL TPS Project. The receiver consisted (Figure 2-15) of two single-layered helical coils of stainless steel tubing mounted end-to-end in an insulated steel box. The coils were coated with oxides to increase absorptivity. Design solar input was 85 kWt through an aperture of 203 to 254 mm (8 to 10 in.). Two separate coils were installed to permit one to be used for primary steam production and the other for reheat.

The receiver was tested on a TBC at the PDTS. The two coils were connected in series for these tests. Superheated steam at up to 735°C (1355°F) and 14 MPa (2000 psia) was produced. Measured efficiencies scattered badly. For output temperatures above 260°C (500°F), efficiencies ran from 80 to 95%.

Malfunctions included shattering of the silicon carbide aperture cone and rear plate because of thermal shock. They were replaced by an end plate of nickel-chromium steel and an aperture assembly of graphite (grade CS).

7. Carter Steam Engines

Two reciprocating engines designed and built by Jay Carter Enterprises were tested. These were developmental prototypes for automotive applications. The smaller was a single-cylinder, single-acting engine (Figure 2-16) with a nominal speed of 1800 rev/min and rated shaft output of 6 kWe (8 hp). Design was conventional except for the inlet valve; this was a spring-return valve in the engine head opened by a spike attached to the piston. A positive displacement pump supplied feedwater. In the tests described here, the engine drove a 3.7-kWe (5-hp) induction generator, which delivered power to the local grid.

The single-cylinder engine was tested on the ground at the PDTS, using steam supplied by a TBC and the Garrett steam receiver. Maximum measured power output of the engine/generator was 2.25 kWe net, from an input of 23.2 kWt of steam at 402°C (757°F), for a power conversion efficiency of 9.7% net and an engine efficiency of 11.9% (Figure 2-17). Maximum efficiency was measured at a lower power level: 13.2 kWt input at 390°C (730°F), electrical output of 1.45 kWt, power conversion efficiency of 11.0% net, engine efficiency of 14.5%. Operating time totaled 5 h (References 9 and 13).

Disassembly after the runs revealed (1) fractures in the metal O-ring that sealed the head to the cylinder, (2) wear on the intake valve seat, (3) scratches on the crank-shaft journal, (4) scoring of the cylinder, and (5) bulging of the cylinder head (see Reference 9).

The larger Carter engine was a two-cylinder, single-acting engine with a rated shaft power of 17 kW (23 hp) and a nominal speed of 3600 rev/min. Its design, including the inlet valving, was similar to the single-cylinder engine. Exhaust steam passed through a feedwater preheater before going to a water-cooled condenser (Figure 2-18). The engine drove a 18.7-kWe (25-hp) induction generator that delivered power to the local grid. This engine was tested at the manufacturer's site at Santa Barbara, California, using steam from a fuel-fired steam generator, and on the ground at the PDTS using steam provided by a TBC and the Garrett steam receiver. In the fuel-fired tests, maximum electrical output was 15.5 kWe net (16.3 kWe gross) at an input of 87.3 kWt of 565°C (1050°F) steam, for a power conversion efficiency of 17.8% net at an expansion ratio of 14.4/1. Maximum measured power conversion efficiency was 19.6% net with an input of 78.6 kwt of 540°C (1000°F) steam and an expansion ratio of 10/1, a net electrical output of 15.4 kWe and gross

electrical output of 15.7 kwe were measured (Figure 2-19). Malfunctions observed included leak of input steam through a blow-down valve and leakage of the cast aluminum exhaust manifold (see References 9 and 13).

In the tests at the PDTS, the maximum measured power conversion efficiency was about 20% net, at inlet temperatures of 540 to 565°C (1000 to 1050°F) (see Reference 9). It was believed that performance would be increased if leaks were corrected and the inlet valve enlarged.

D. BRAYTON SYSTEM TESTS

Brayton tests included a test of a system integrated by Sanders Associates, and separate tests of a receiver designed and built by AiResearch Manufacturing Co. and a solarized automotive gas turbine built by Garrett Turbine Engine Co.

1. Sanders Brayton System

The Sanders system (Figure 2-20) used a LaJet concentrator, a Sanders receiver, an engine/alternator from Garrett AiResearch, an inverter from Abacus Controls and a Sanders module control subsystem. The LaJet concentrator uses 24 disks of aluminized mylar film for its optical element, each 1.5 m (60 in.) in diameter. Each disk is mounted on an aluminum ring and shaped to an approximately spherical contour by atmospheric pressure. A vacuum pump lowers the pressure in the space between each reflecting membrane and a backing membrane. The membrane shape is determined by the position of a tube, located on the axis of symmetry of each disk, through which the pumping is done; the reflector membrane is pushed down until it contacts the end of the tube and shuts off the vacuum line (Figure 2-21). Overall focal length is about 5.3 m (17.4 ft). The circumferential disk rings are supported on a space frame that rests on bearings providing rotation in declination. These bearings are supported by a polar axis tube that rotates in right ascension on a cantilever truss and tripod resting on concrete piers (see Figure 2-21). Coarse pointing control in right ascension is by a clock, in declination by a record of past tracking. Fine pointing is by sensors and microprocessor.

The Sanders receiver (Figure 2-22) uses a silicon carbide honeycomb on which the concentrated sunlight falls and is absorbed. Air is blown through the honeycomb and picks up the heat. The cavity aperture, 280 mm (11 in.) in diameter, is sealed by a fused silica window.

The Garrett AiResearch subatmospheric Brayton-cycle engine has a turbine, compressor, and permanent magnet alternator mounted on a common shaft (Figure 2-23). The shaft is driven by hot air entering the radial turbine. Turbine exhaust goes in turn through a recuperator (heat exchanger), an air-cooled radiator (sink heat exchanger), the centrifugal compressor, the recuperator, the receiver, and the turbine (Figure 2-24). The engine is hybrid; that is, it can be operated on sunlight, fuel, or both simultaneously: a combustor between the receiver and the turbine permits addition of heat from the burning of natural gas. A portion of the air loop is just above atmospheric pressure, permitting exhaust of combustion products. The portion of the loop between turbine exhaust and compressor

inlet is at an absolute pressure of about one-half of an atmosphere. High-frequency ac power from the alternator is full-wave rectified, then inverted to single-phase 60 Hz.

The Sanders control subsystem, based on a commercial microprocessor, controls the engine and inverter, commands the concentrator, and provides operator interface.

2. Brayton System Test

A series of development tests of the Brayton system (Figure 2-25) were run at the Sanders plant at Merrimack, New Hampshire, after cognizance of the work was transferred from JPL to SNLA. Early tests used fuel alone or fuel plus solar as a source of heat; later tests included some with only the sun as a source. In the solar-only tests, system efficiency was a few percent, less 2% for parasitics[1] (Reference 14). It was believed that performance could be improved substantially by correcting a number of deficiencies described below under the subsystems. The control system worked well[1].

3. Subsystem Tests of Brayton System Elements

a. LaJet Concentrator. The concentrator used in the Sanders system was a production Model 460 LaJet concentrator modified by Sanders. Modifications included strengthening of the structure to support the engine weight, installing a counterweight, and providing for inverted stow. Optical tests by Sanders of the modified concentrator showed that the total solar power delivered by the concentrator was about 33 kWt, corrected to a normal insolation of 1 kW/m^2. The intercept factor was 0.85 + 0.15, -0.20 for a 280-mm (11-in.)-diameter aperture and 0.65 $\pm$0.20 for a 180-mm (7-in.) aperture (Figure 2-26).

Many of the mirrors were of fair to poor quality; wrinkles, delamination, and loss of reflecting layers occurred. Air leaks developed through the bond between the reflecting film and its support rings. Sanders believed that the concentrator performance could be improved considerably by improving mirror quality and mirror alignment procedures. Other malfunctions included software problems, connector and insulation wiring failures, breakage of a drive sensor, a loose shaft coupling, and a voltage regulator failure.

[1]K. Linker, private communication, Sandia National Laboratories, Albuquerque, New Mexico, November 1985.

b. Sanders Receiver Tests. Several versions of the Sanders air receiver were tested using combustion heat on a test-bench at Merrimack and using solar and combustion heat on concentrators at the PDTS and Merrimack. One solar test of the version used in the system test was made with a receiver output temperature of 540°C (1000°F) and a thermal input of 21.8 kW to the receiver; receiver efficiency measured by Sanders was 78.3%. [The receiver was designed for power input of 34 kWe and an output temperature of 870°C (1600°F).] A fuel-fired test at an inlet temperature of 396°C (764°F) showed receiver losses of 4.1 kWe (Reference 15). Air leaks in the receiver were noted (see Reference 14).

Another version of the Sanders receiver, designed for higher power (75 kWe input), was found in bench tests to have an efficiency of about 83% at 870°C (1600°F) (Reference 16).

An earlier version was designed for 60 kWe output, higher temperature (1370°C, 2500°F), and elevated pressure (300 kPa absolute, 43 psia). It incorporated thermal buffer storage. Measurements on a TBC at the PDTS showed receiver efficiencies ranging from 81% at an outlet temperature of 885°C (1625°F) and thermal input of 70.1 kW to 60% at 1120°C (2050°F) and 77 kW input (Reference 17). Receiver malfunctions included damage to ceramic components at the highest temperatures and breakage of the silica window.

It is believed that performance of receivers of these types can be significantly improved by changing the frame of the silica window and adding thermal insulation to reduce conductive losses, modifying the cavity geometry to reduce radiative losses, and fixing air leaks (see Reference 16).

c. Garrett Subatmospheric Engine Tests. Several versions of the engine were tested at the Garrett AiResearch plant at Torrance, California, using heat from the combustion of fuel. One assembly of the engine with a Sanders receiver was also bench-tested, using fuel. The version used in the system test was Mark IIIA, a developmental prototype. In bench tests at Garrett, the measured engine/generator efficiency was 17%. However, in later tests at Sanders, the efficiency decreased to 13.4% at the rated turbine inlet temperature of 870°C (1600°F). Garrett expected that the performance could be improved by correcting a compressor/turbine mismatch and reducing air and thermal leakage. Bench tests by Garrett of a later version (Mark IIIB) gave an efficiency of 20%; significant leakage was still occurring.

Malfunctions observed in Sanders' testing of the Mark IIIA version included oil contamination of the bearing air supply, bearing over-temperature, a loose linkage, and a relay failure. Sanders also noted that a large amount of intake air, intended for combustion, bypassed the engine, recuperator, and receiver (see Reference 14).

Garrett tests of the generator and rectifier alone at an output of 3.1 to 3.8 kWe showed a generator efficiency of about 80% and a rectifier efficiency of 98% (Reference 18).

d. Abacus Inverter. This inverter was designed for 8-kW input. At 8 kW input, the measured efficiency was 90%; at 5 kW input, it was 86%; at 2.2-kW input, it was 80%.

4. Garrett AiResearch Brayton Receiver Tests

This receiver, a development prototype from Garrett AiResearch, used a cylindrical-plate/fin-metallic heat exchanger (Figure 2-27). Sunlight passing through the aperture was absorbed at the inner surfaces of the cylinder. Air passed axially through the segmented heat exchanger and was heated. The design input power was 85 kW, the pressure was 225 kPa (37 psia), and the output temperature was 815°C (1500°F). The receiver was tested on a TBC at the PDTS. Measured efficiency was approximately 70% at an outlet temperature of 815°C (1500°F) and 80% at 595°C (1100°F), not including the power needed to blow the air through the receiver. Malfunctions included cracking at the inner surface of the receiver (see Reference 9).

5. Garrett Solar Advanced Gas Turbine Engine Tests

The Solar Advanced Gas Turbine (SAGT) engine, designed and built by Garrett Turbine Engine Co., is a solarized version of the Garrett Advanced Gas Turbine being developed for automotive applications (Figure 2-28). The engine is hybrid, incorporates a single-stage radial turbine and single-state centrifugal compressor with variable inlet guide vanes, and drives a 25-kWe induction generator through a gear train and belt. Regeneration is by direct contact of air with a rotating ceramic disk.

A bench test by Garrett of an SAGT-1A engineering development model, using fuel and a turbine inlet temperature of 925°C (1700°F), gave an engine efficiency of 29.8% and an overall power conversion efficiency of 20.4%. Later tests gave a poorer performance, attributed to higher leakage, particularly at regenerator seals, and the installation of an oil damper to control subsynchronous whirl associated with a foil bearing. Other difficulties encountered were mechanical interferences and dynamic instabilities (Reference 19).

E. STIRLING TESTS

The Stirling tests included in the JPL TPS Project used solarized variants of the Model 4-95 kinematic Stirling engine developed for automotive use by United Stirling AB (USAB) of Sweden. Most tests also used some version of USAB's experimental solar-only receiver (ESOR); a few tests used a hybrid receiver designed and built by Fairchild/Stratos Division. The tests may be divided into two groups:

(1) Tests at Rancho Mirage, California, of a prototype Stirling module designed by Advanco Corp.

(2) Tests at the PDTS aimed at development of Stirling receivers, engines, and power conversion assemblies, but also including a complete module.

1. Advanco System

This module (Figures 1-1 and 2-29), installed at Rancho Mirage and tested by Advanco, included an Advanco concentrator, USAB receiver and engine, alternator and electric power system supplied by Onan Corporation, and system and concentrator controls by Electrospace Systems, Inc. System integration and concentrator elements were provided by Rockwell International.

The concentrator used a paraboloidal array of 336 second-surface silver on glass mirrors to form a 10.6-m-diameter reflector with a focal ratio of 0.58. The mirrors were bonded to spherically shaped cellular glass substrates to form facets that were supported on metal racks mounted on trusswork. The trusswork was supported by an "exocentric" gimbal mechanism incorporating two nonperpendicular rotation axes. This mechanism was mounted on a steel pedestal sunk into the ground and encased in concrete. The drive was powered by electric motors with gear reducers. The pointing was controlled by a microprocessor using stored ephemeris and sun sensors.

The USAB cavity receiver had a 200-mm (8-in.) diameter aperture. Sunlight was absorbed by 72 heating tubes of a chromium-nickel-cobalt-iron alloy, bent to an involute conical shape and containing the hydrogen working fluid. Eighteen tubes were connected to each of the four cylinder heads of a modified USAB 4-95 engine. The 4-95 was an experimental engine originally designed for fuel firing (Figure 2-30). The engines used in the solar program were "solarized;" one modification was provision of a lubrication system that would operate properly when the engine attitude changed during solar concentrator rotation. The engine incorporated cartridge-type regenerators. The four engine cylinders were arranged in a square; their pistons drove two crankshafts (Figures 2-31 and 2-32). In the Advanco module, the crankshafts drove a 22.5-kW induction generator operating at 1800 rev/min and connected to the local electricity grid via switchgear. The receiver, engine, and alternator constituted the power conversion unit (PCU).

2. Advanco System Test Results: Performance

In the module tests at Rancho Mirage, instantaneous performance at a direct normal insolation of 0.850 kW/m^2 was reported to include a gross output of 20.1 kWe, net output of 18.5 kWe, gross module efficiency of 27.3%, and net module efficiency of 25.2%. Component efficiences included 82.8% gross for the concentrator and 33.0% gross for the power conversion unit, with a parasitics factor of 92.0% (Reference 20). An approximate breakdown of the power conversion efficiency, based on calibration and measurements at low insolation, indicated that the receiver efficiency was about 84%, the engine efficiency was about 42% gross, and the alternator efficiency was about 94% (Reference 20) (Figure 2-33). This is at an engine temperature of 720°C (1330°F), using hydrogen as the working fluid.

Later measurements included a module output of 27.1-kWe gross and 25.6-kWe net at an insolation of 1 kW/m^2, and a net module efficiency of 29.4% (Reference 21).

The gross power output, for quasi-steady conditions, was found to vary linearly with insolation as shown in Figure 2-34. The net power was about 1.7 kWe less than the gross. On cloudy days, insolation transients were frequent; output and efficiency were lower (see Reference 20).

Measured performance over a whole day at summer solstice included 13.25 h of operation at an average insolation of 0.821 kW/m^2, average module efficiency of 27.4% gross and 25.2% net, and net energy output of 2.52 kWh/m^2 of projected area of the reflective surface. Average system efficiency over 15 consecutive days near summer solstice, including 3 mostly cloudy days, was 25.1% gross, 22.5% net; net energy output was 29.0 kWh/m^2 over 164.3 running hours at an insolation averaging 0.785 kW/m^2. The module solar availability over this time was stated to be over 99%, presumably calculated for sunny periods only (see Reference 20).

Between February 1984 and the end of January 1985, the module delivered power to the grid for 1173 h. Test operations continued until July 25, 1985 (see Reference 21).

The pointing and control equipment consumes 0.53 kW parasitic power even when the concentrator is stowed. During a month with only 7 clear days, the module produced 2209 kWh gross, but parasitics consumed 924 kWh (see Reference 21).

On many days, the module operated fully automatically from sunrise to sunset, including sun acquisition and engine start-up and shutdown (see Reference 20).

3. Advanco System Test Results: Malfunctions and Maintenance

Among the problems encountered in operation were delamination of some mirror facets from their substrate, malfunctions and other difficulties with the gravity-activated emergency stow mechanism, problems with cables, sensors, and control hardware and software, receiver material degradation, leaks in the hydrogen supply equipment, broken oil pump and speed sensor shafts, excessive gear wear in the main drive gears and in the oil pump, repeated failures of the "uninterruptable power supply" that provided emergency power to the controls, and operator error. The module operated during weekdays and most weekends, except when operation was prevented by clouds, for 40 consecutive days with no forced outages (see Reference 20). Temperature differences were found among the four quadrants of receiver tubes. These differences were believed to have lowered engine performance. Tests indicated that convection within the receiver cavity, deflection of the

concentrator structure by gravity, and local soiling of the mirrors probably caused these temperature differences. (The mirrors that were closest to the ground during stow soiled the fastest.)

During 25 summer days without rain or washing of the mirrors, their reflectivity was found to have decreased from 92.5 to 74%. Washing, requiring 2 h, restored the reflectivity to 92%. On another occasion, 10 min of light rain increased the reflectivity from 86.8 to 90.7%. Heavier, longer rain brought the reflectivity back to 92% (see Reference 20).

4. Advanco and USAB Subsystem Tests

a. Advanco Concentrator

Measured power delivered by the Advanco concentrator into a 200-mm (8-in.) diameter aperture was 73 kWe, and into a 380-mm (15-in.) aperture was 74 kWe. These are values normalized to a direct normal insolation of 1 kW/m^2. Corresponding optical efficiencies, including intercept factor, were 85.3% and 86.4%. Hemispherical reflectance of the facets when new and clean was measured as 93.5%; this fell to 92% after repeated cycles of exposure to the weather and washing. Specularity was reported to be 0.25 mrad. Facet slope error was measured as 0.95 mrad; structural deflection of the whole concentrator under gravity as 0.61 mrad; deflection of the facet racks under simulated wind loading as 0.81 mrad; and pointing error as 0.02 mrad. The corresponding standard deviation in the angle of sunlight leaving a local area of a mirror facet was 2.03 mrad. This does not include spread caused by the angular spread in incoming sunlight or, apparently, in imperfect facet alignment. The intercept factor for a 200-mm (8-in.)-diameter aperture was measured as about 0.97 (see Reference 20).

b. United Stirling Receiver and Power Conversion Subsystem

A number of variants of the United Stirling receiver were tested on-sun, using the PDTS TBCs. The variants differed primarily in the shape to which the gas heater tubes were bent and in the size and manifolding of these tubes. Also, several variants of the engine and several different alternators were used.

The heat delivered from the receiver to the engine was not measured, so receiver and engine performance were not measured separately. Power output was measured as alternator output; the alternator performance was measured separately in bench tests, and this permitted calculation of receiver-engine performance.

A test using hydrogen as the working fluid gave a power conversion unit (PCU) output of 24.2 kW gross, about 20.2 kW net, at an insolation of 0.960 kW/m^2; PCU efficiency was 33.6% gross, about 28% net. Corresponding efficiencies for the module were 28.4% gross, about 23% net (Reference 22).

In another test, the working fluid was helium and the engine cooling was changed to reduce parasitic loss. PCU output was 23.2 kW gross, 22.2 kW net, at an insolation of 0.940 kW/m^2. PCU efficiency was 32.8% gross, 31.4% net for this test. Module efficiency was 27.8% gross, 25.9% net (Reference 23).

PCU efficiency averaged over a full operating day reached 30%. The module ran 13.5 h that day, producing over 250 kWh (gross). The total operating time of the module exceeded 250 h. Two modules were run in parallel, connected to and delivering power to the local grid. Alternator efficiency was measured as about 92% when delivering 23 to 24 kW (References 24 and 25). Performance was significantly lower at high wind speeds (Reference 25). Also, performance in these TBC tests may have been reduced somewhat because the USAB PCU was too large to fit inside the mounting ring of the concentrators. It was, therefore, not possible to place the receiver at the design focus of the concentrator.

Temperature differences among the four quadrants of receiver tubes caused malfunctions and degraded performances (see Reference 22). Other problems included control difficulty during wind fluctuations (which affected receiver losses) (see Reference 24). On several occasions, the engine cranking did not start promptly, when insolation rose, because of fuse outages, low oil pressure, etc; overheating and failure of receiver tubes resulted in these instances (see Reference 24). Other receiver tube failures resulted from fabrication defects. Loss of grid power stopped the cooling water pump and radiator fan (see Reference 22). On these occasions, an operator error led to receiver tube failure. Engine failures included a broken piston rod.

Piston rings, seals, and O-rings were changed frequently during these development tests, so no real information on their lifetime under representative power plant operating conditions was obtained (see Reference 22).

5. Fairchild Receiver Tests

This hybrid receiver was designed and built by Fairchild Industries/Stratos Division. Concentrated sunlight passed into the cavity receiver and was absorbed at the inner surface of a thin copper cone. In the copper were embedded nickel alloy tubes containing the helium working fluid (Figure 2-35). When fuel was used, the combustion products heated the outer surface of the cone. Portions of the tubes extending from the cone to the engine regenerator were enclosed in copper sleeves clad with nickel alloy; the combustion gases passed through this tube array before reaching the cone. Exhaust gases heated a pre-heater that warmed the air coming into the combuster (Reference 26).

Proper operation of the receiver in the fuel-fired mode were verified by tests at the manufacturer's plant. The receiver was then integrated with a USAB engine and tested at the PDTS in both fuel-fired and hybrid modes using 25 and 50% of full solar power input from a TBC. Because of instrumentation and receiver malfunctions, meaningful test data were not obtained (see References 22 and 23).

Malfunctions occurred in the combustion controls. The brazed joints at the ends of the receiver tubes failed repeatedly (see Reference 22). It appeared that a design change to reduce the thermal stresses at the joints would be necessary to permit sustained operation.

F. CONCENTRATORS

The JPL TPS Project tested three concentrators at the PDTS that were not developed as part of any specific power system: two TBCs and Parabolic Dish Concentrator 1 (PDC-1). The TPS Project also tested optical elements of three other concentrators designed by Acurex Corp. (PDC-2), Boeing Engineering Services, and Entech, Inc.

1. Test Bed Concentrators

Two TBCs (Figure 2-36) were installed at the PDTS for solar testing of other solar power subsystems. Optically, each consisted of 224 spherical reflector segments of second-surface silver on glass, forming a paraboloidal array, 11 m in diameter, with a focal ratio (f/D) of 0.6. Each reflector was bonded to a contoured block of foamed glass to form a mirror segment. These mirror segments, made by JPL, are attached to a mount designed and built by E-Systems, Inc. The metal framework supporting the mirrors pivots on elevation bearings and the assembly rotates in azimuth on wheels, running on a track that rests on a concrete pad. Electric motors drive an azimuth wheel and a linear elevation actuator. Rough sun pointing is controlled by an ephemeris or past tracking data stored in a microprocessor; fine pointing is controlled by sun sensors and the microprocessor. Each mirror can be individually adjusted. This permits tailoring the flux pattern to accommodate the needs of each test. A detailed description of the TBCs is given in Reference 22.

Measurements made within the first year after installation of the concentrators gave the flux distribution in the focal plane shown in Figure 2-37. This was with all the facets focused on a point. The center third of the facets were then defocused to a 100-mm (4-in.)-diameter circle about the focal point. The power delivered was measured at 80 to 82 kWt, normalized to direct normal insolation of 1 kW/m^2, through apertures of 254 and 560 mm (10 and 22 in.). Subsequent installation of a larger receiver mounting ring increased the blockage of incoming sunlight; this was calculated to reduce the delivered power by about 2 kWt (see References 22 and 27 and footnote 2).

Measurements made 3-1/4 years after concentrator installation showed 71.8 kWt delivered through a 152-mm (6.0-in.)-diameter aperture, 75.5 kWt through a 203-mm (8.0-in.)-diameter aperture, and 76 kWt through a 510-mm (20.5-in.) diameter aperture, all normalized to 1 kW/m^2. The decrease from the earlier value for comparable apertures was attributed to mirror degradation (Reference 22).

---

[2]W. Carley, "TBC Characterization," JPL private communication, April 6, 1982.

Measured reflectance was 95 to 96%, through apertures of 15 to 46 mrad, for new clean mirror facets. Facets stored 1.5 yr inside or on top of a building showed the same reflectance after cleaning; a facet stored 3 years on top of the building showed 94.5% after cleaning. Facets used on a TBC for 1.5 yr averaged 92.5% after 6 wk of dirt accumulation. Two panels that had 91.5 to 92% reflectance were washed using a detergent solution; their reflectance increased to 94%.[3]

Measurements of the slope error of a sample facet showed a standard deviation of approximately 0.5 mrad from a spherical shape. This is small compared to the deviation of the spherical facet shapes from a paraboloid (calculated as about 1.5 mrad). (Groups of facets were ground to three different radii and placed on the paraboloid at different distances from the axis to minimize the deviation between the spherical and local paraboloidal curvature).[4]

Malfunctions included control system problems (water in connectors and software errors), speckling and cracking of mirror facets, overheating of structure and wiring near the receiver during sun acquisition and deacquisition, fraying of cables at the pivots, loosening of an elevation sensor from its axis, seizing of a drive motor brush, and cracking of the support wheels. Considerable trouble was also encountered with the elevation jackscrews. This was believed to be due primarily to overloading. The concentrators were designed to support 500 kg (1100 lb) of added mass at the receiver/engine position but 840 to 900 kg (1850 to 2000 lb) of added mass was often installed.

The jackscrews were greased frequently -- as often as daily in cold weather. Most other lubrication was done monthly.[5]

2. Parabolic Dish Concentrator No. 1

Parabolic Dish Concentrator No. 1 (shown in Figure 2-38) was designed by General Electric Co. measuring 12 m in diameter with a focal ratio of 0.5. Its paraboloidal mirror consists of 36 sandwich panels with a balsa-wood core and fiberglass facing, impregnated with a polyester resin. The sunward surface was covered with acrylate sheet and a reflective layer of aluminized polyester film. The mirror panels were clamped to steel ribs within the paraboloid. This structure rotates in elevation on trunnions supported by two pedestals. The pedestals rotate in azimuth about a central pivot on wheels that roll on a track. The track and pivot rest on concrete piers. Drive is by electric motors via cables. Coarse pointing control is by a microprocessor with stored ephemeris; fine pointing is by analog control using sun sensors. The concentrator was built and installed at the PDTS by FACC and its subcontractors, except for the mirror panels (made by Design Evolution 4) and the control system (built by General Electric and JPL).

---

[3]E. Dennison and M. Argoud, "Reflectance Measurements Taken at ETS April 19, 1982," JPL private communication, April 17, 1982.

[4]L. Wen and T. Carroll, "Test Bed Concentrator (TBC) Optical Performance Evaluation (Part II)," JPL private communication, August 8, 1979.

[5]D. Ross and R. W. Vincent, JPL private communications, 1985.

Solar tests showed that power delivered through a 520-mm (20.5-in.)-diameter aperture was 72.5 kWt, normalized to insolation of 1 kW/m^2. Through a 380-mm (15-in.) aperture, it was less than 65.2 kWt. Performance was quite sensitive to ambient temperature: When the ambient temperature was much different from that at which the mirrors were assembled to the ribs, the concentrated sunlight was spread over a larger area. This was believed to be due to a mismatch in thermal expansion between the sandwich mirror panels and the steel ribs (Reference 28).

Malfunctions included: (1) the panels pulling away from their clamps and falling off the ribs, (2) delamination of some mirror panels, (3) gravity--produced sag as the dish rotated in elevation, (4) permanent deformation of the panels after installation, (5) slippage of the cables on their pulleys, and (6) wear of the pivot bearing, sideslip of the wheels on the track and damage to the wheel bearings (see Reference 28). Control problems included a motor control relay, a control card failure, moisture condensation problems in the sun sensors, and various errors in the software (Reference 29).

One set of three panels (inner, middle, and outer) was tested optically at JPL using a source with a spread of 0.9 mrad. Resulting intercept factors are shown in Figure 2-39[6] (Reference 30).

3. Acurex Parabolic Dish Concentrator No. 2 Reflector Panels

Several versions of Parabolic Dish Concentrator No. 2 (Figure 2-40) were carried through most of the design stage by Acurex Corp. but were not built under the JPL TPS Project. (Further work on this concentrator has been contracted for by DOE). Seven reflector panels were, however, fabricated (Figure 2-41). These were designed for an 11-m-diameter paraboloid; the complete mirror would have consisted of 64 panels.

One of the panels fabricated by Budd Corp. for Acurex used second-surface silver on glass bonded to a substrate of glass fiber and epoxy. The remaining panels, made by Acurex, used second-surface silver on glass bonded to a substrate of cellular glass. The back of the substrate was partially capped with sheet glass (Figure 2-42).

Several of the panels were tested optically at JPL using the 0.9 mrad source. The epoxy-glass panel twisted out of shape and had to be constrained to get good optical performance. When so constrained, the measured slope error over most of the surface was about 1.5 mrad (Reference 31). Tests of a subsize panel showed some instability of optical performance when the panel was heated from 21°C (70°F) to 49°C (120°F); this was attributed to inadequate curing of the resin (Reference 32).

The optical tests of the cellular glass panels gave the intercept factors shown in Figure 2-39.[6]

---

[6]Dennison, E.W., "Preliminary Report on 25-ft Space Simulator Data," JPL private communication, December 21, 1981.

4. Boeing Concentrator Reflector Panels

Boeing Engineering and Construction designed and fabricated two subsize test panels, 60 x 70 cm, with a 6.45-m focal length, matching the dimensions of the TBC mirror segments. These panels were made of formed steel sheet, stiffened by hat sections, and with a reflective surface of aluminized polyester film.

Optical tests showed, for the better panel, 27% of the concentrated sunlight through a 38-mm aperture, 73% through 78 mm, 96.8% through 156 mm, 98.4% through 322 mm, and over 99.9% through 310 mm. Temperature variations from 12 to 41°C (54 to 105°F) appeared to have no significant effect. Tests on smaller coupons shows a specular reflectance of 0.85 and a specularity of 1.5 mrad (1 sigma, half angle). Some film delamination occurred in coupons heated to 50°C (122°F) (Reference 33).

5. Entech Fresnel Concentrator Lens Panel

Entech, Inc., designed, assembled, and tested an 0.67 x 1.2-m (2 x 4-ft) panel for a Fresnel lens concentrator of about 8-m (27-ft) focal length. It consisted of an array of 0.1 x 0.6-m (4 x 24-in.) linear prismatic elements made of acrylic sheet bonded to a superstrate of smooth acrylic sheet (Figures 2-43 and 2-44). The prisms were designed so the angle of incidence of sunlight would be equal to its exit angle from the material (see Figure 2-44). (The prismatic sheet was made by 3M Corp.) The panel was assembled flat and bent into a conical segment for test. In use, a series of similar panels would form a conical ring, and a series of conical rings (with prisms of differing angles) would form a dome-shaped Fresnel lens, 11 m (36 ft) in diameter (see Figure 2-43). The test panel was designed for a position of 30 deg from the optical axis as viewed from the focal point (Reference 34).

Entech reported a measured optical efficiency of 82% into a 690-mm (27.3-in.)-diameter receiver aperture in a solar test. Intercept factors are shown in Figure 2-45 (Reference 34).

6. University of Chicago Secondary Concentrator

The University of Chicago designed and built three secondary concentrators, each shaped as a hyperbolic trumpet (Figure 2-46). The concentrators had an entrance aperture of 770 mm (31 in.), an exit aperture of 141 mm (5.5 in.), and a length of 399 mm (16 in.). Two concentrators had mirrors of vapor-deposited aluminum on a substrate of aluminum sheet. One of these was water-cooled, the other cooled by free air convection. The third concentrator had a mirror of silver electroplate on copper sheet and was water cooled.

The secondary concentrators were designed for use with an Omnium-G concentrator, but were first tested at the PDTS on a TBC adjusted to simulate an Omnium-G concentrator; the outer mirror segments were covered. Power delivered to a 141-mm (5.5-in.)-diameter aperture was increased from 17.9 kW without a secondary to 23.8 kW with the silver-plated secondary. The

silver-plated secondary had an efficiency of 96%. Performance of the aluminized concentrators was somewhat lower; the air-cooled one melted locally (Reference 35).

The silver-plated secondary was later tested on an Omnium-G concentrator at the University of Queensland, at Queensland, Australia. (This test was not part of the JPL TPS Project.) Power into a 141-mm (5.5-in.)-diameter aperture was increased by a factor of 1.72 when the secondary was used. Power transmittance of the secondary was again measured as 96% (Reference 36).

G. APERTURE MATERIALS TESTS

Tests of materials that might be used for uncooled receiver aperture plates were made with a PDTS TBC. Requirements for these materials were based on estimates for the FACC organic-Rankine module as it was then conceived. They included: (1) the ability to withstand walk-off conditions of 7000 kW/m^2 locally for 15 min, (2) the ability to withstand many thousands of cycles of 1- to 2-s exposures to the same peak flux during routine sun acquisition and deacquisition, and (3) many years of exposure, at the edge of the aperture plate, to spillage of 100 to 300 W/m^2. Tests were made on a TBC defocused to provide a peak flux density of about 7000 kW/m^2 under a typical insolation of 0.720 kW/m^2.

Types of materials tested under conditions simulating walk-off included graphite, silicon carbide, silica, various silicates, alumina, zirconia, aluminum, copper, steel, and polytetrafluorethylene, mostly as samples about 250 mm (1 in.) thick. Of these, the only material that neither cracked nor melted was grade G-90 graphite. Grade CS graphite cracked halfway across but did not fall apart. Samples of high-purity, slip-cast silica survived 1.5 to 4 min before slumping. Oxidation loss for the graphite grades mentioned varied from 0.2 to 8 mm (0.008 to 0.3 in.) of thickness, from 2 to 22% of the mass. The amount of oxidation varied strongly with the wind speed (Reference 37).

Grade CS graphite was also tested for up to 2000 cycles simulating 1-s periods of acquisition. Oxidation loss in moderate to high winds was about 5 mm (0.20 in.) in thickness, or 0.15% of the sample mass. Tests under simulated spillage conditions were limited to measurements of the temperature of the lip of a simulated aperture plate of grade CS graphite. They showed a temperature of about 175°C (345°F) at a lip flux of 400 kW/m^2. The oxidation rate calculated for this temperature, based on data in the literature, was less than 1 μm/yr (see Reference 37).

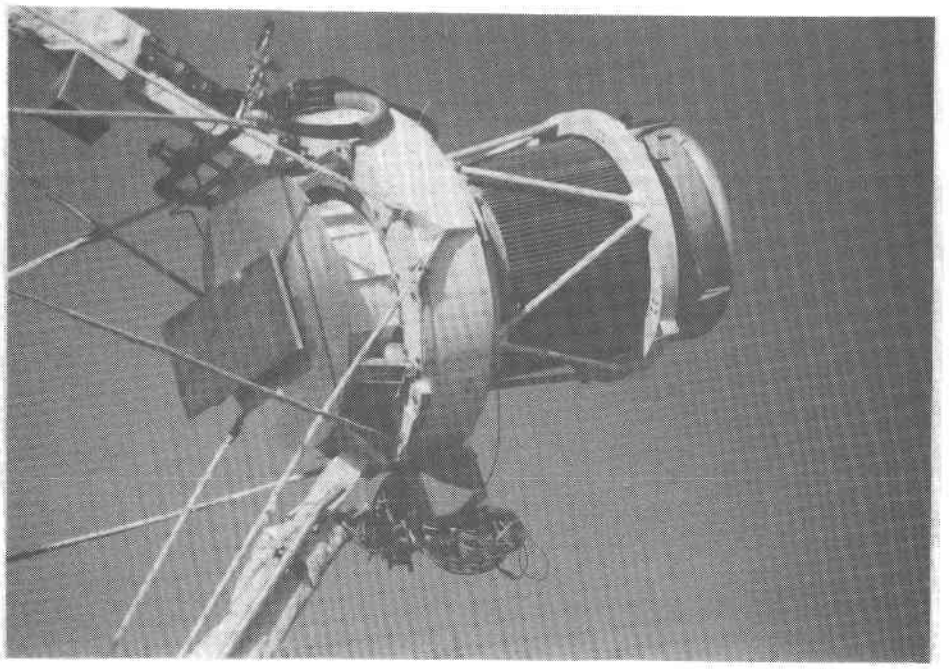

Figure 2-1. FACC Organic-Rankine-Cycle Power Conversion Assembly on Test Bed Concentrator at the PDTS

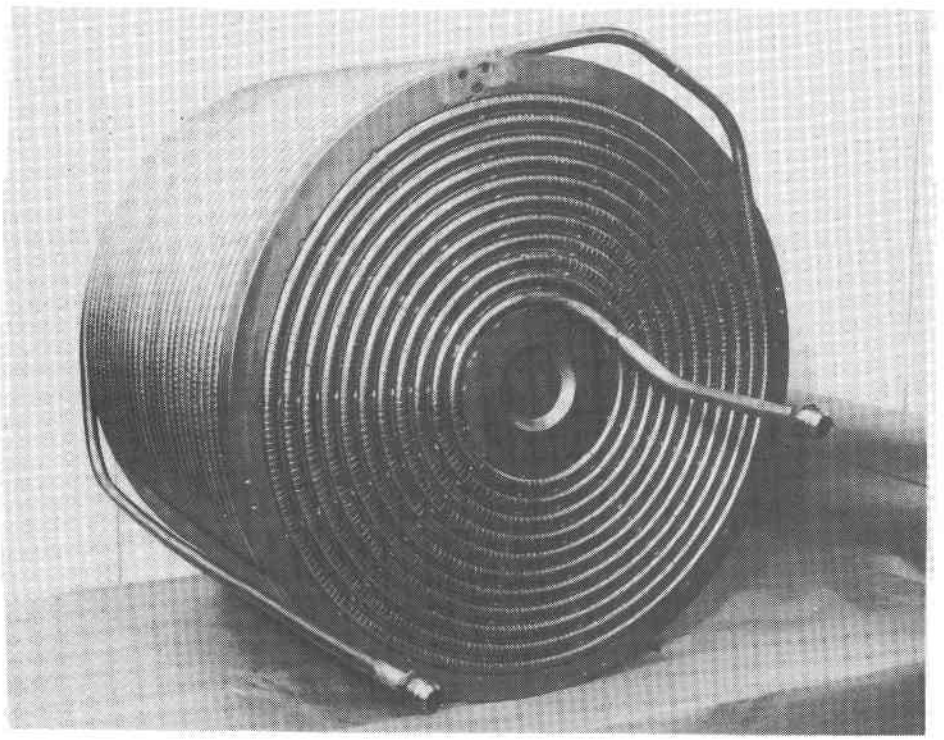

Figure 2-2. Core of FACC Organic-Rankine-Cycle Receiver

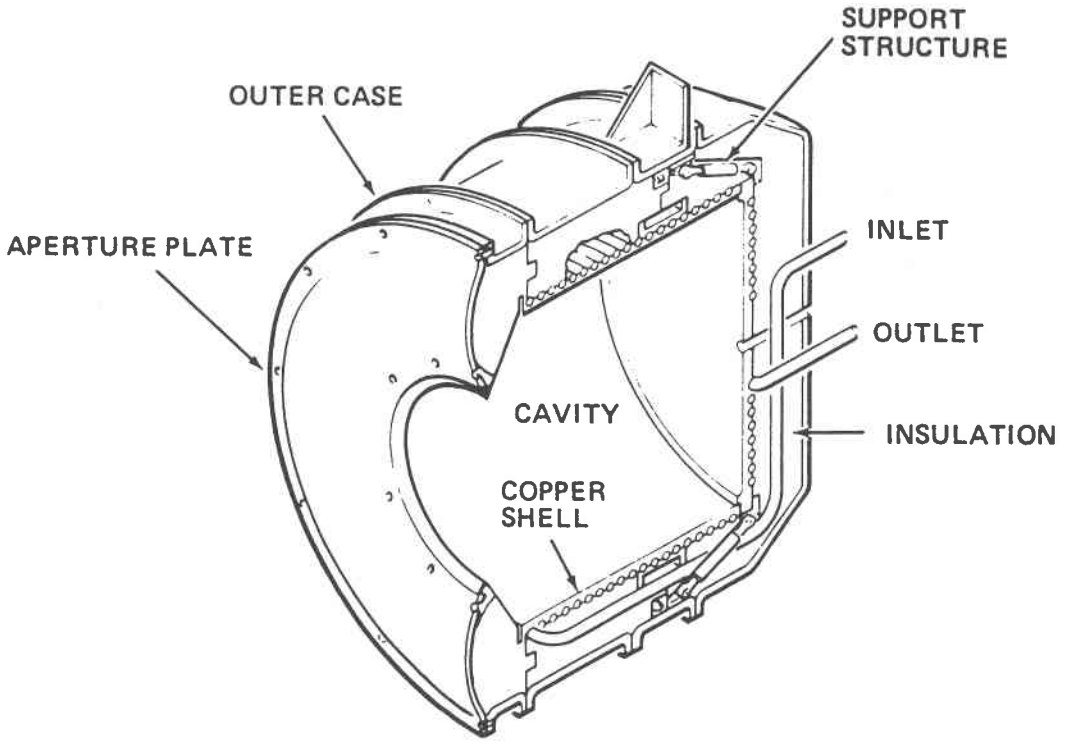

Figure 2-3. Cut-Away View of FACC Organic-Rankine-Cycle Receiver

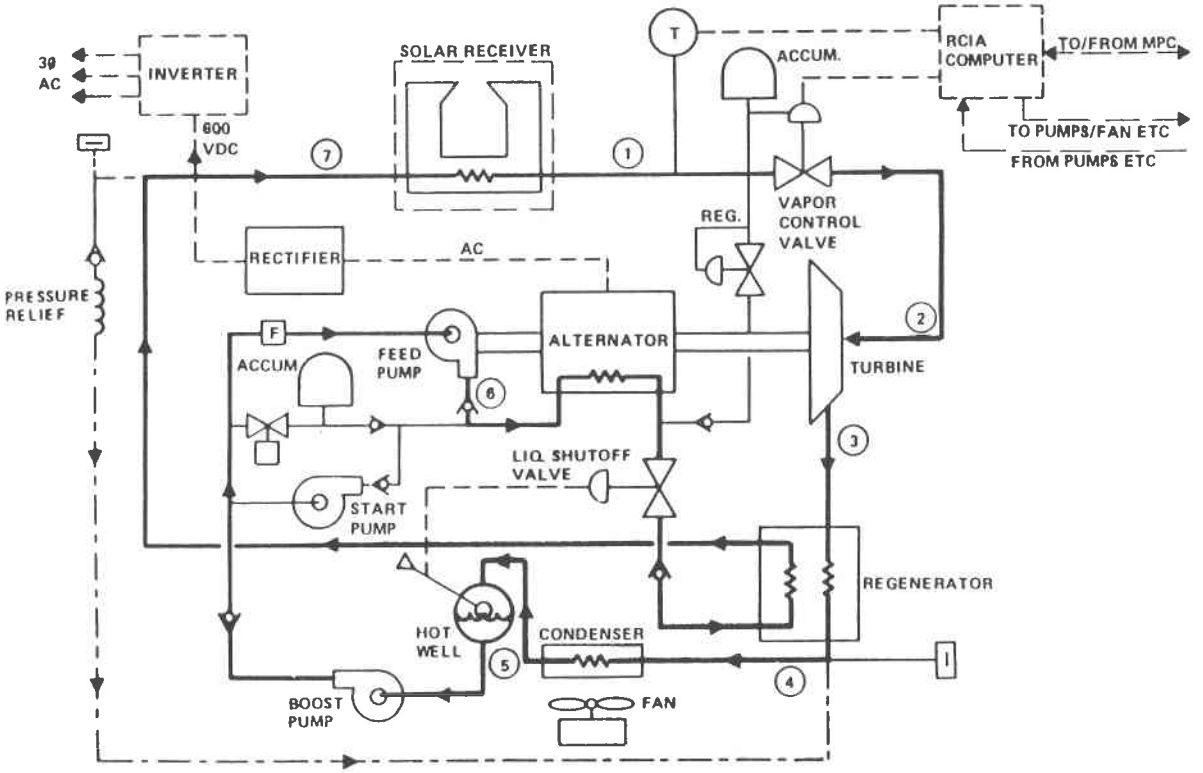

Figure 2-4. Schematic of FACC Organic-Rankine-Cycle Power Conversion Assembly

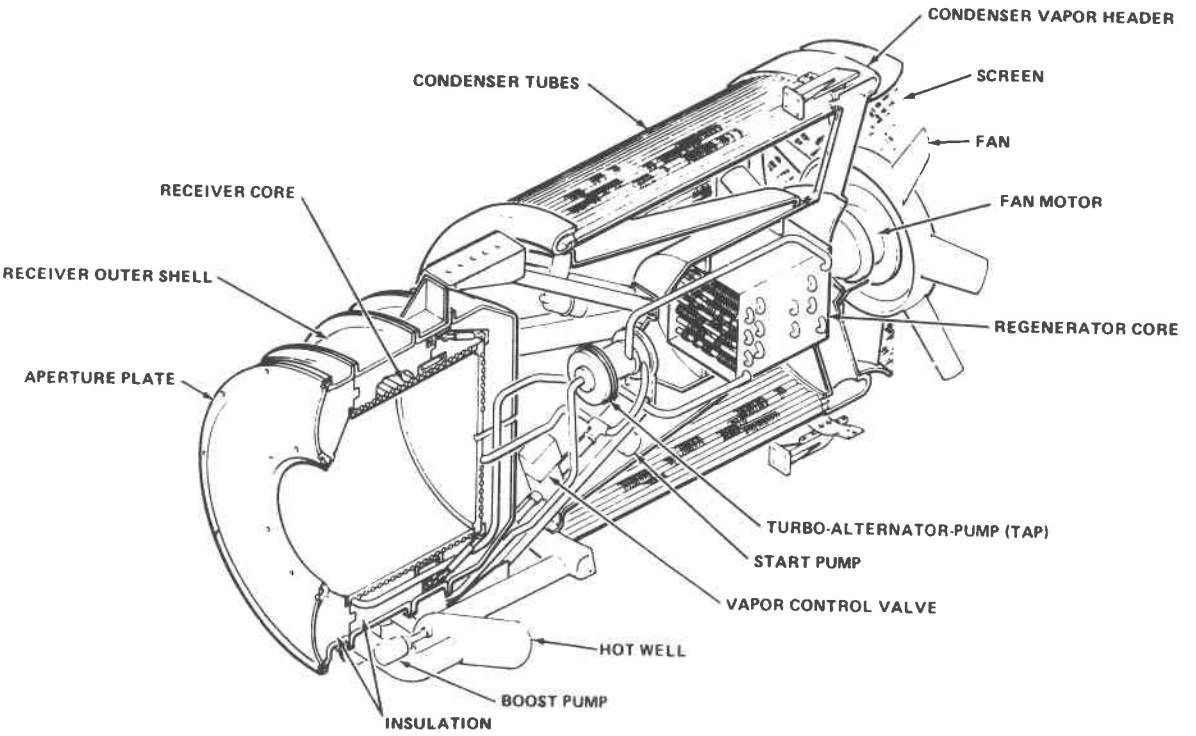

Figure 2-5. FACC Organic-Rankine-Cycle Power Conversion Assembly

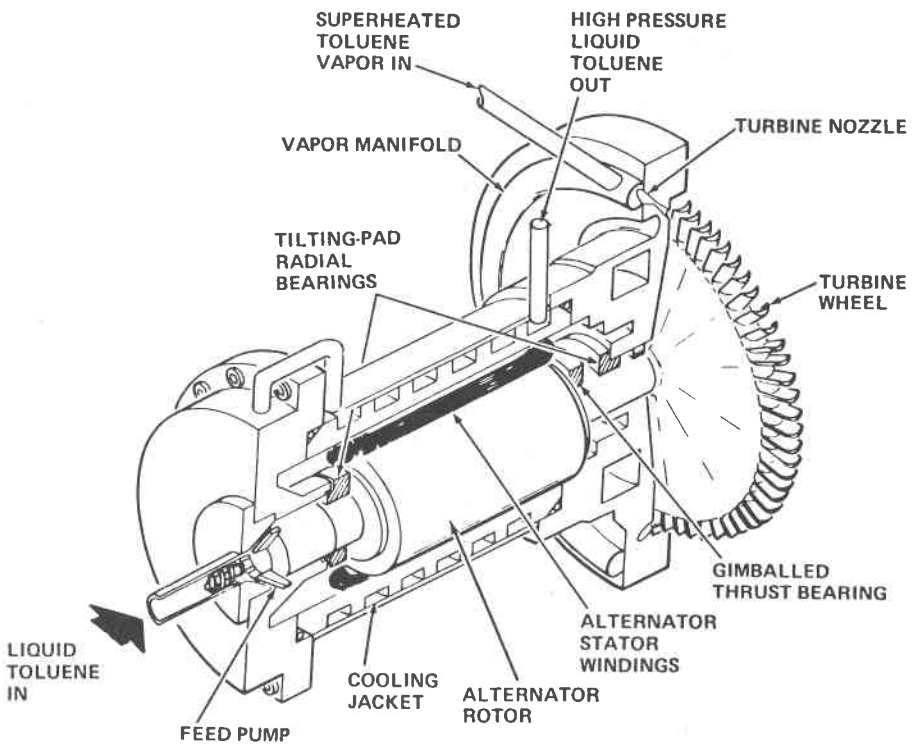

Figure 2-6. Turbine/Alternator/Pump (TAP) Assembly of Barber-Nichols Organic-Rankine-Cycle Engine

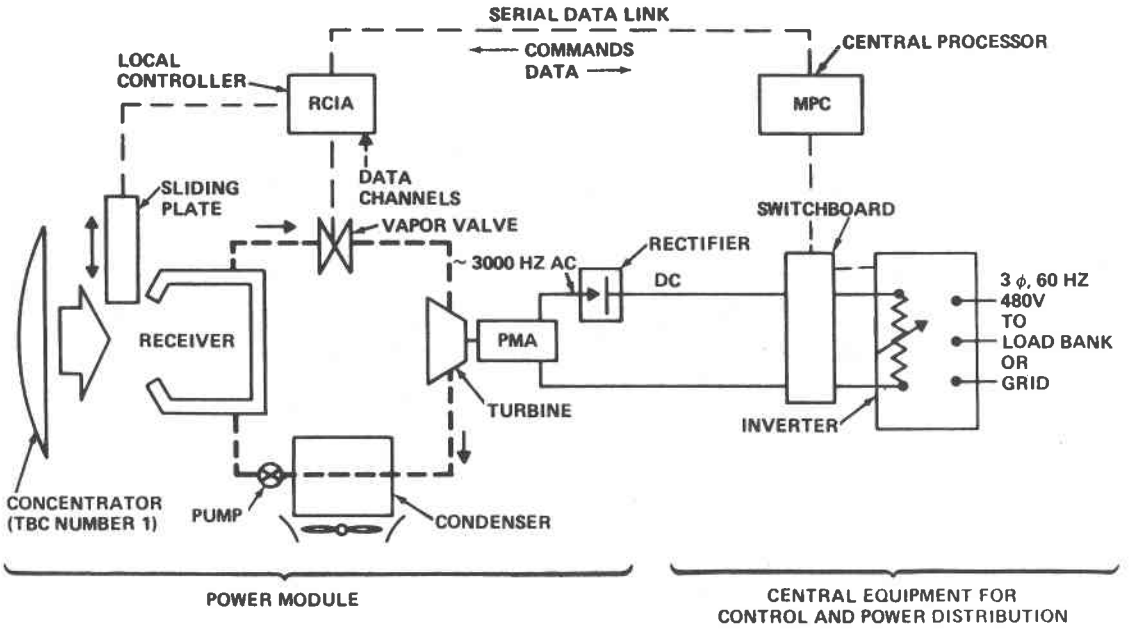

Figure 2-7. Simplified Schematic Diagram of FAAC Organic-Rankine-Cycle Tests at the PDTS

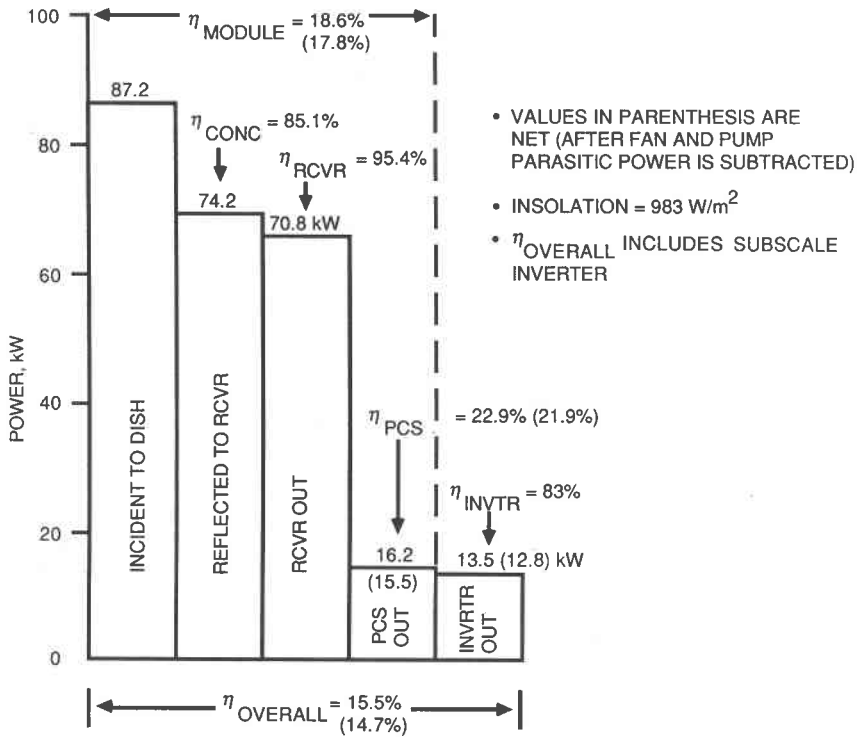

Figure 2-8. Measured Subsystem, Module, and System Performance of FACC Organic-Rankine System in Typical Test (modified from Reference 1)

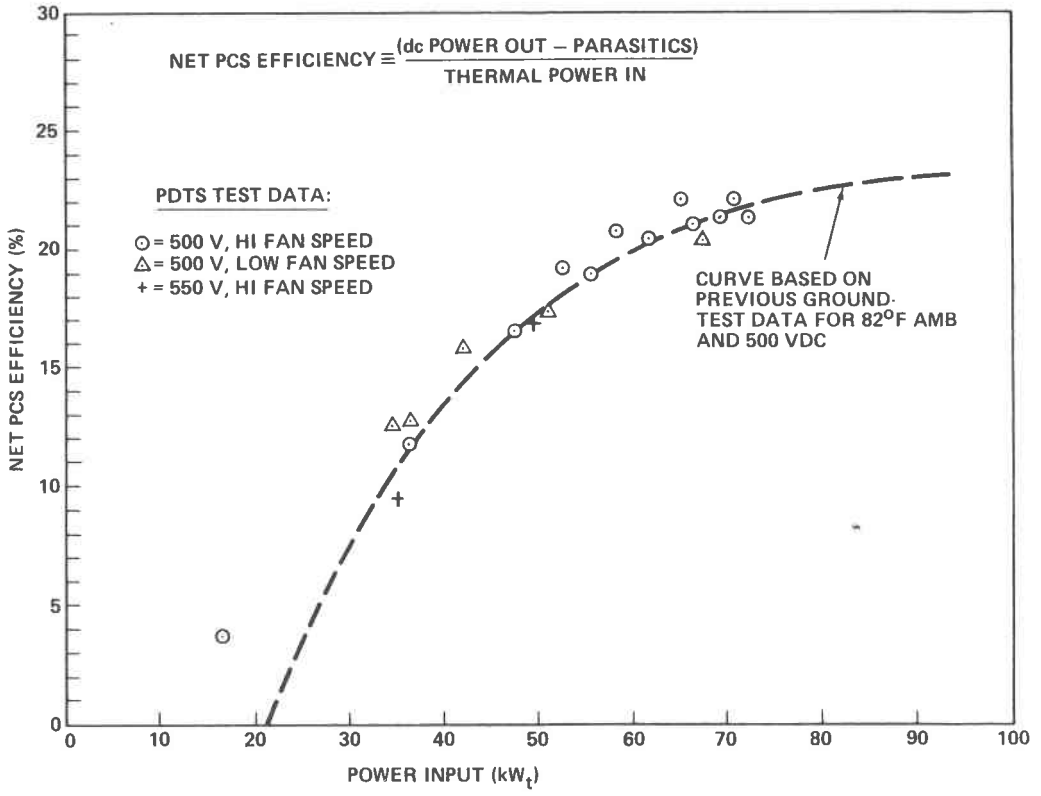

Figure 2-9. Measured Efficiency of FACC Organic-Rankine Power Conversion Subsystem (Net after Parasitic Power Subtracted) (Reference 1)

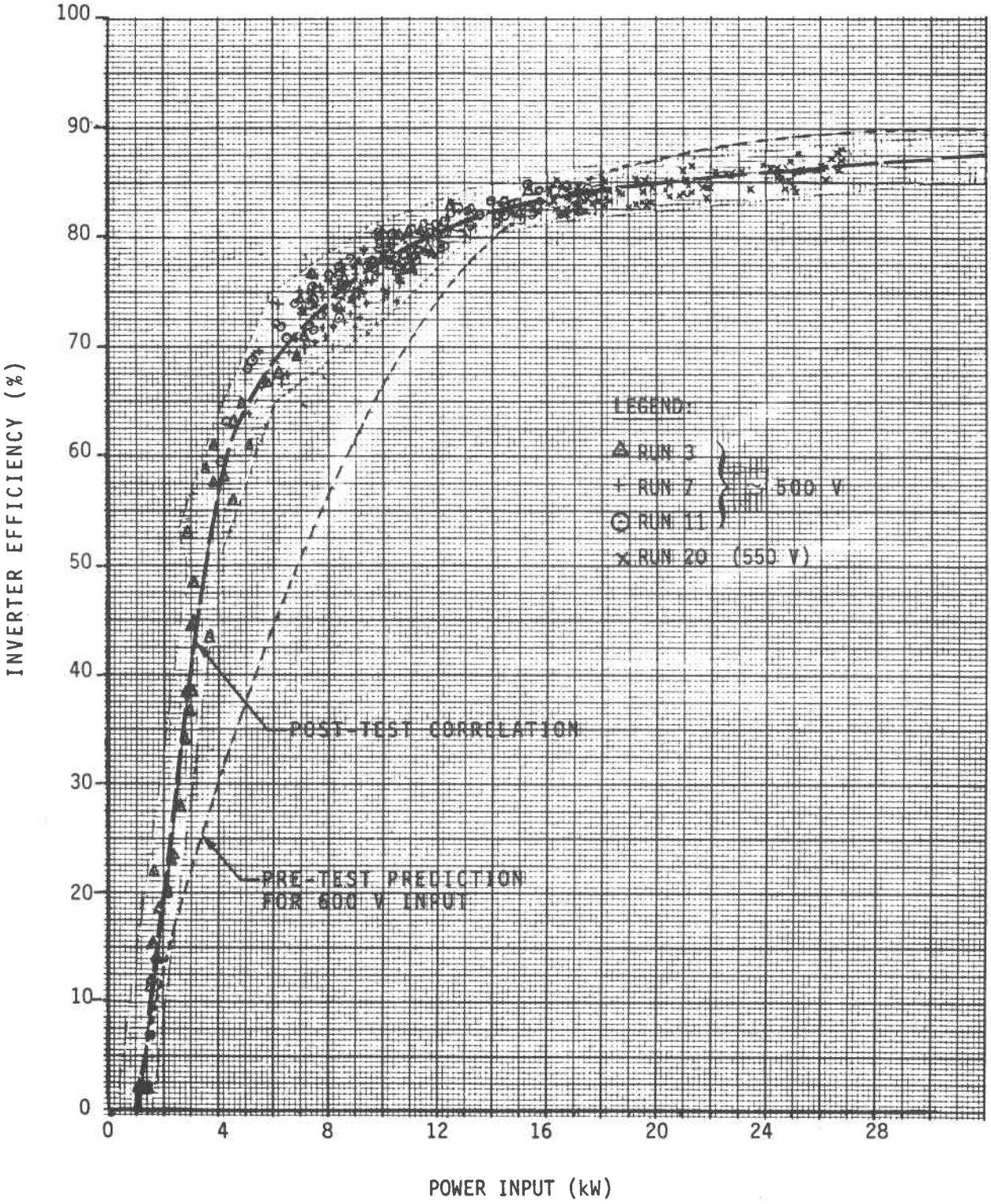

Figure 2-10. FACC Organic-Rankine Module: Inverter Efficiency Data (Reference 1)

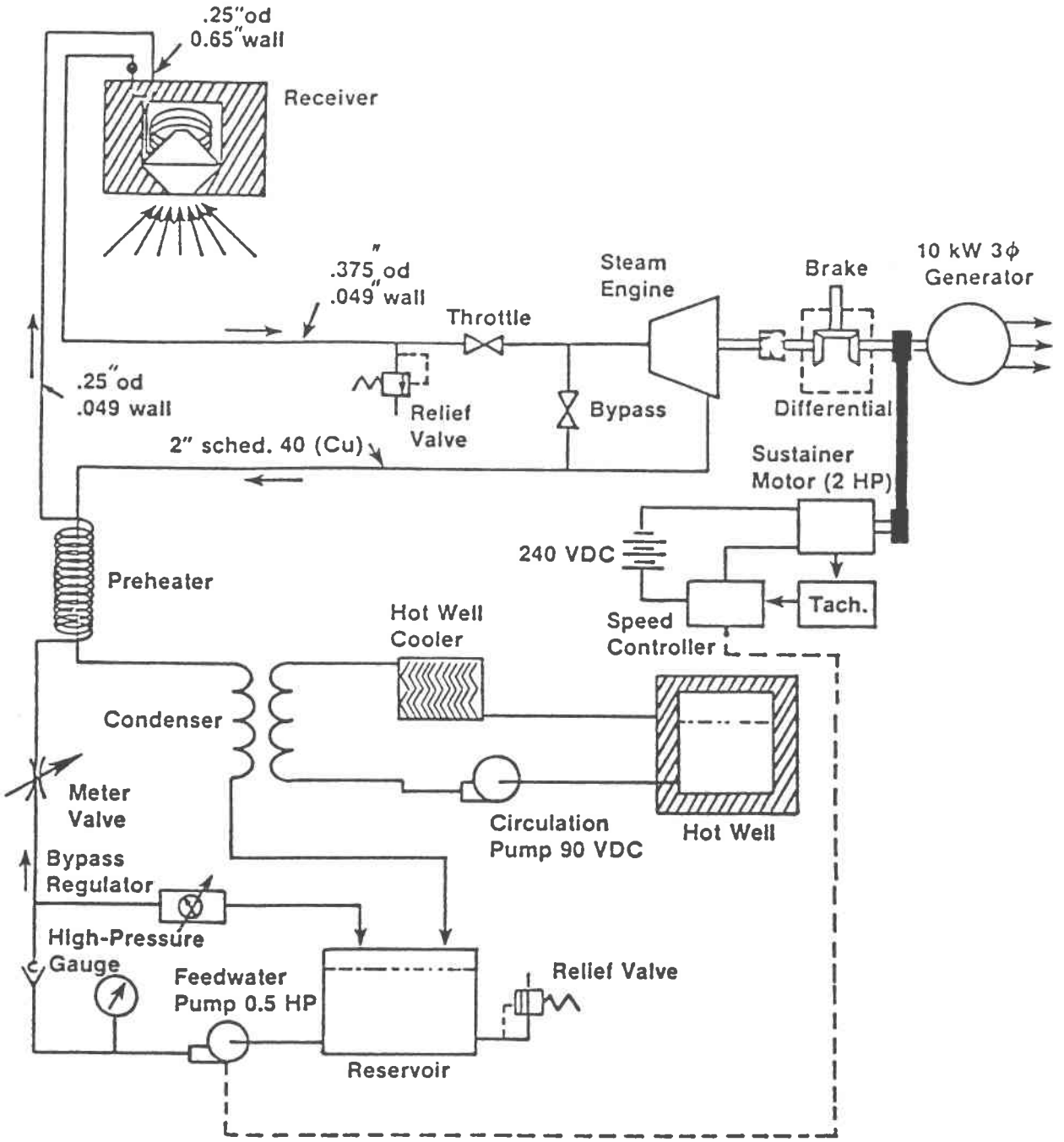

Figure 2-11. Schematic of Omnium-G Steam-Rankine-Cycle System

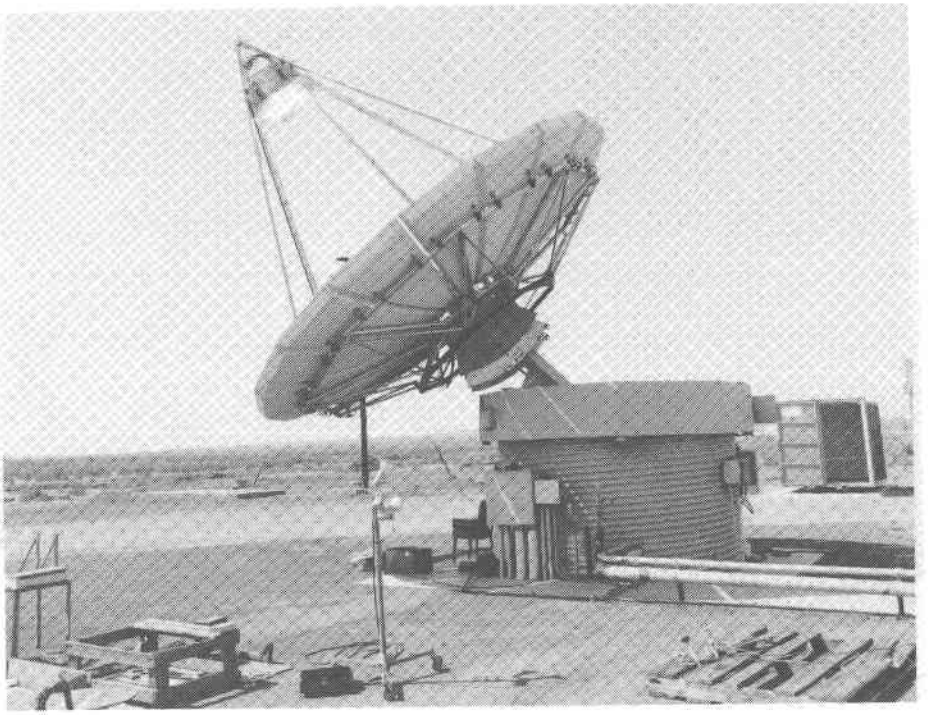

Figure 2-12. Omnium-G Steam-Rankine-Cycle System at the PDTS

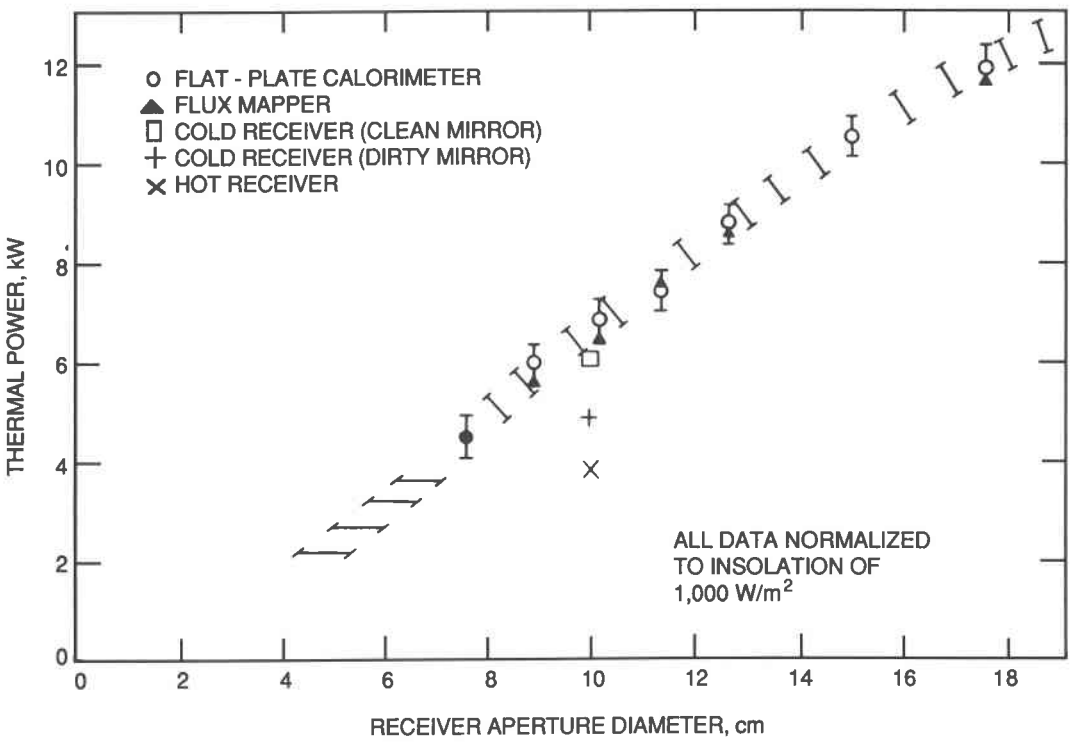

Figure 2-13. Omnium-G Collector Test Results (Reference 9)

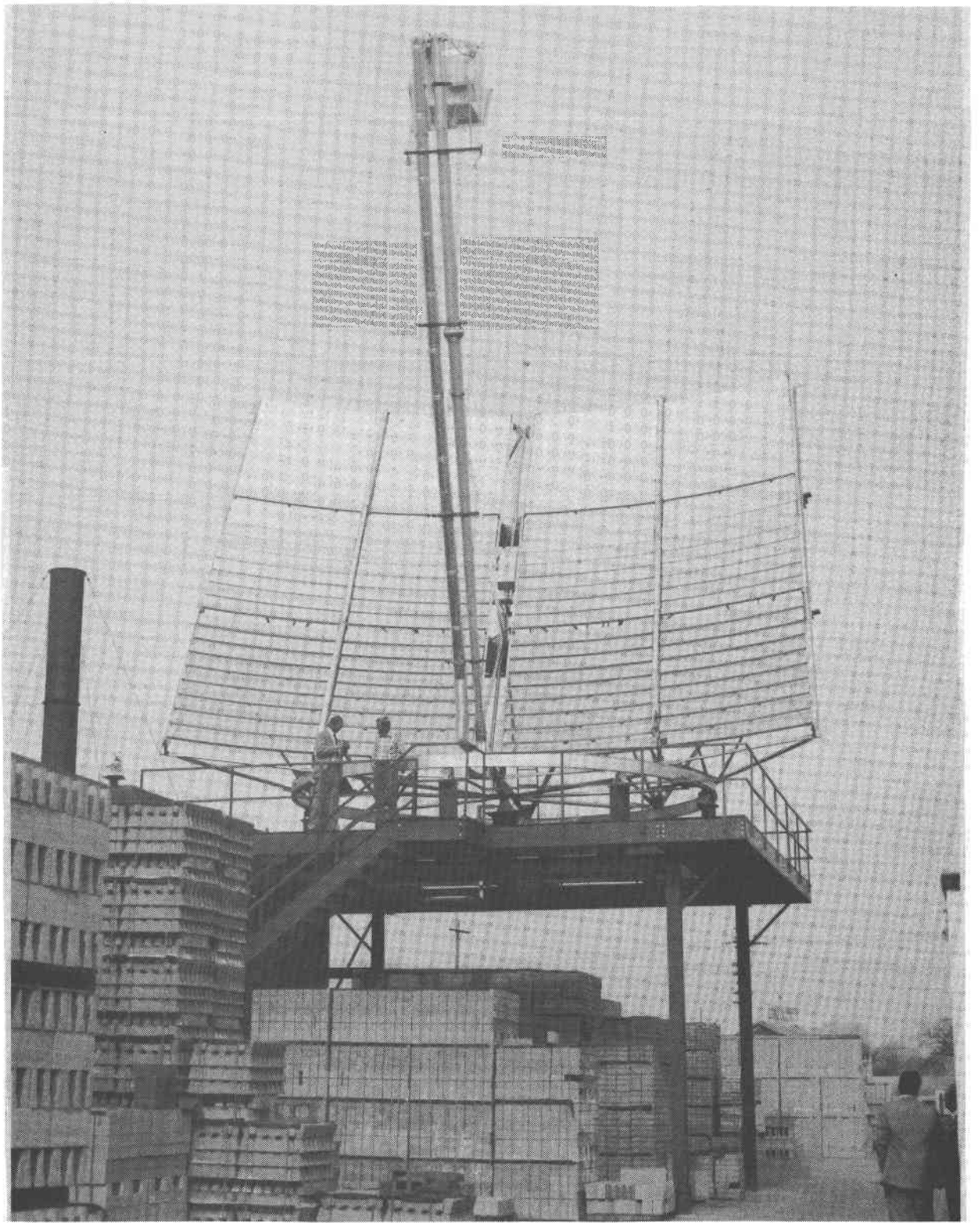

Figure 2-14. PKI Collector at Capital Concrete Products Co.

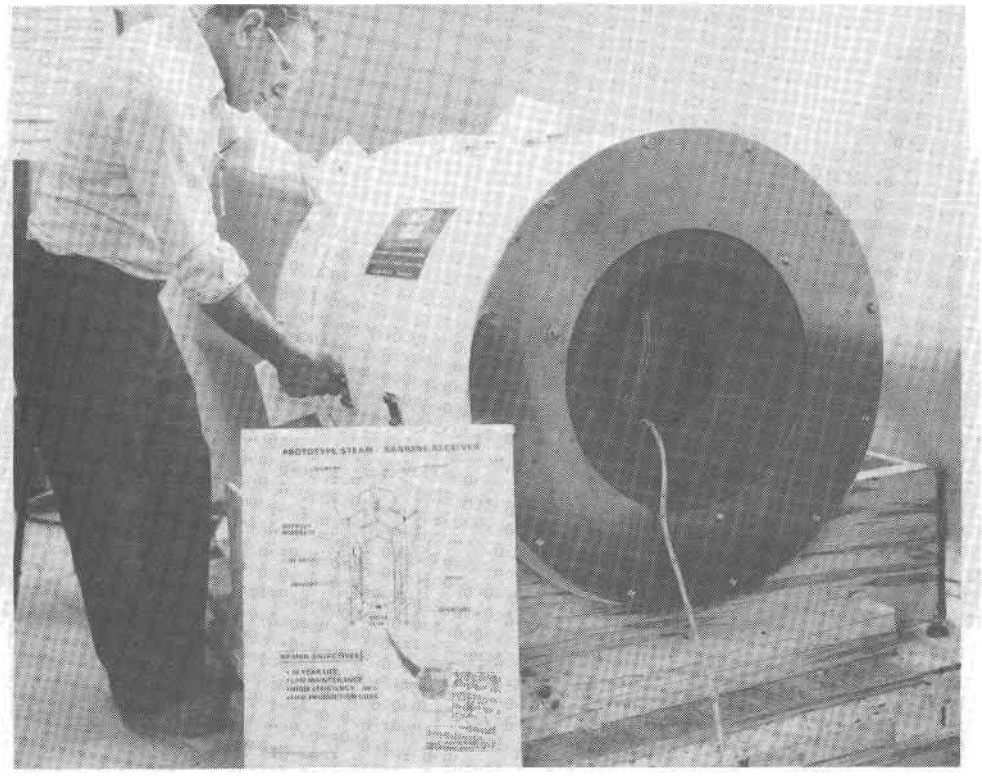

Figure 2-15. Garrett Steam Receiver

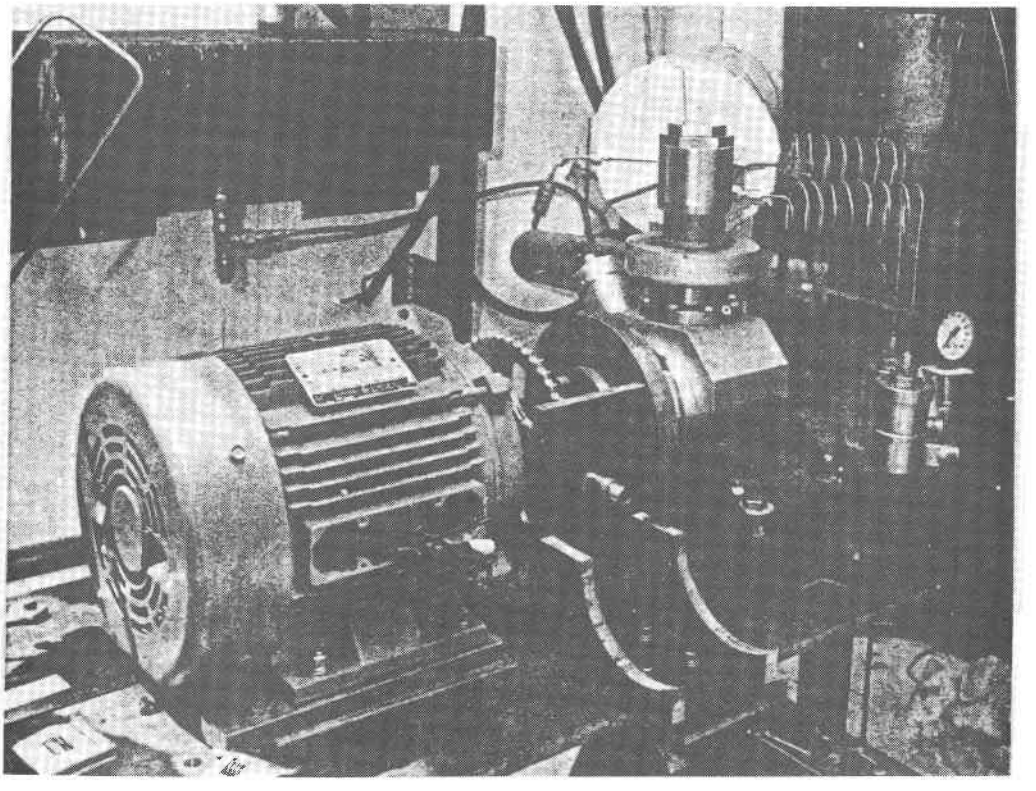

Figure 2-16. Jay Carter Single-Cylinder Developmental Prototype Automobile Steam Engine with Generator

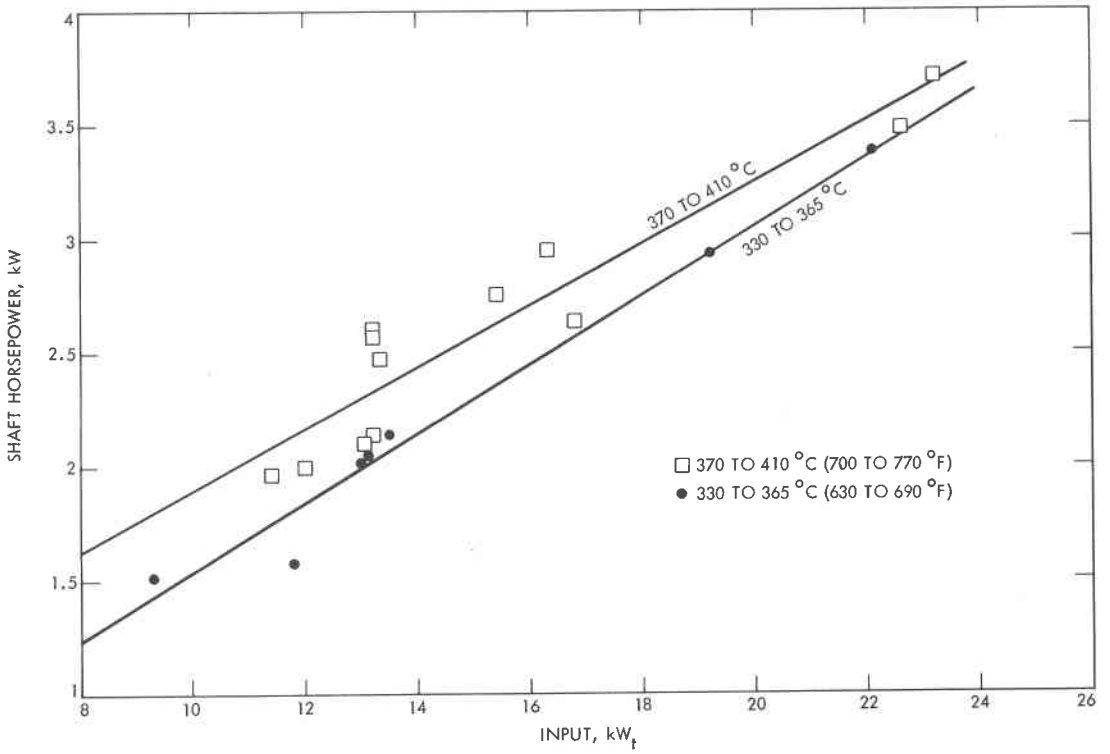

Figure 2-17. One-Cylinder Carter Steam Engine Performance (Reference 9)

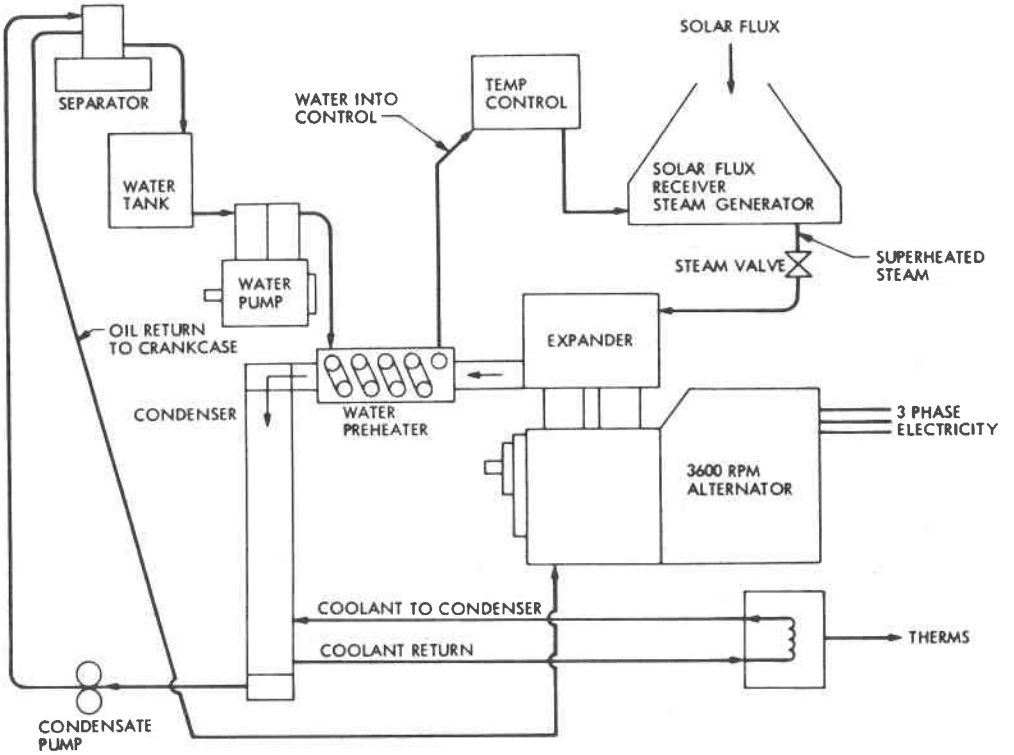

Figure 2-18. Schematic of Solar Test Setup of Carter Two-Cylinder Steam Engine

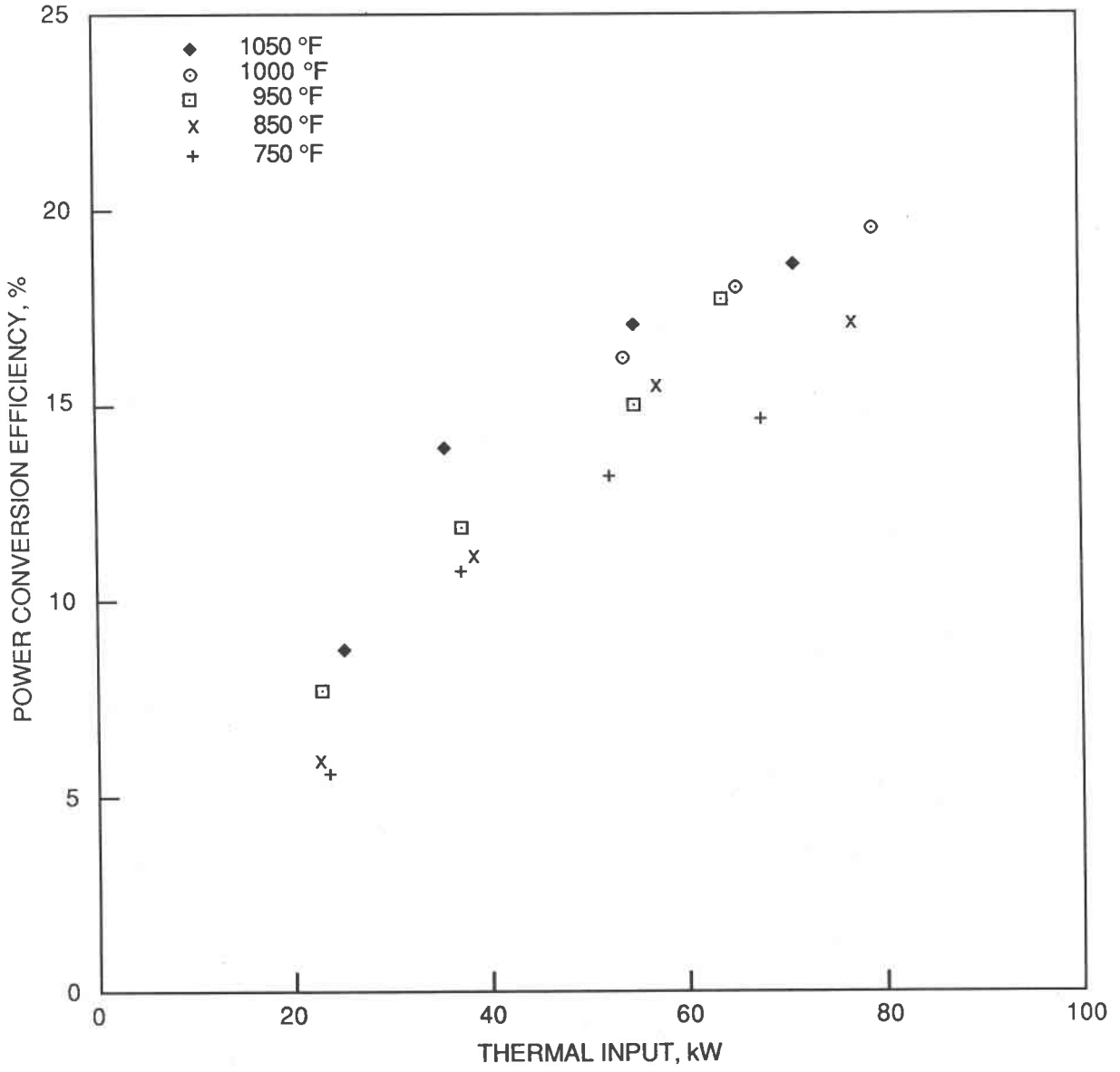

Figure 2-19. Test Results for Jay Carter Enterprises Two-Cylinder Steam Engine (Expansion Ratio 10:1) (modified from Reference 1)

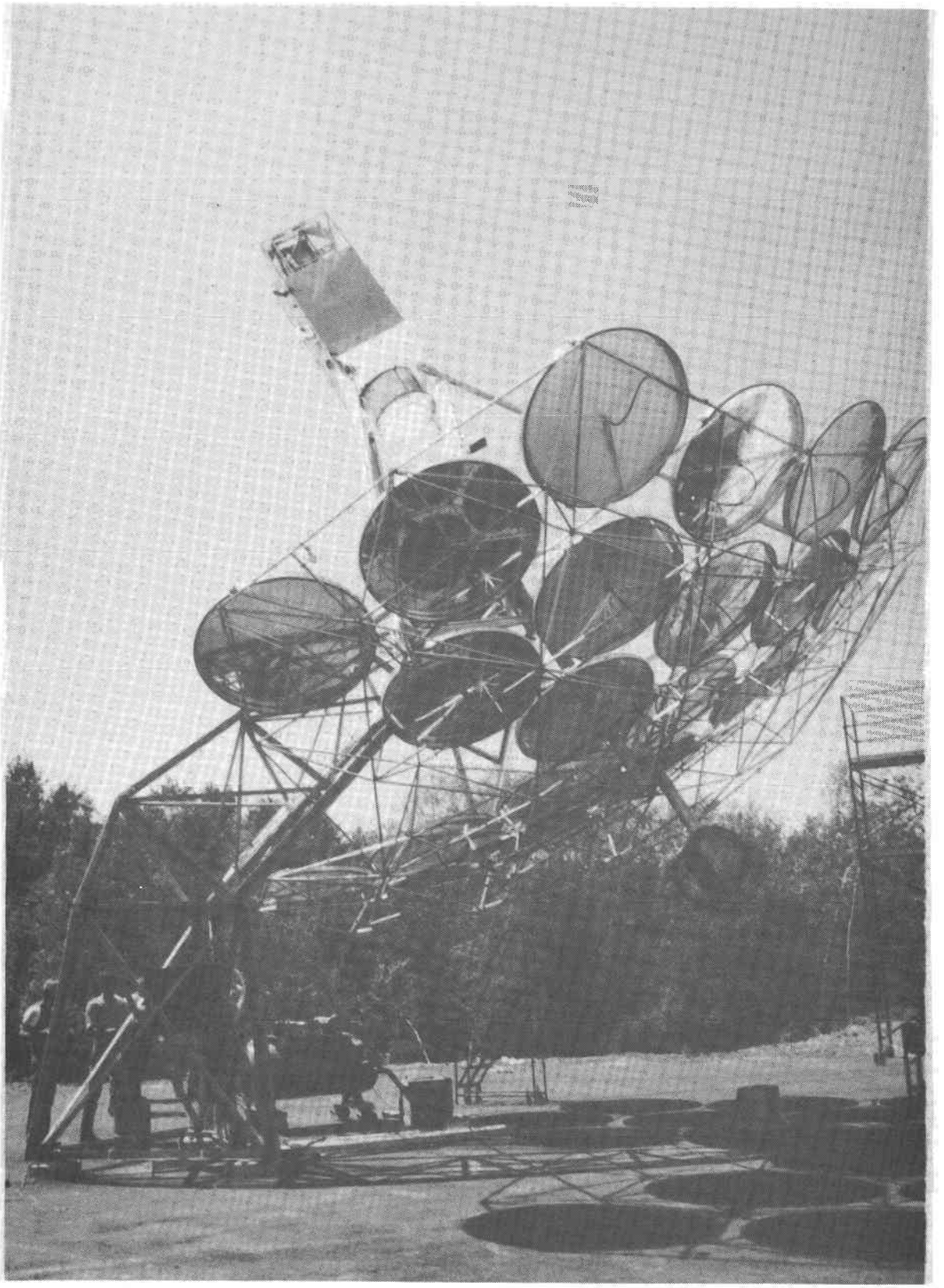

Figure 2-20. Sanders Brayton Module at Merrimack, New Hampshire

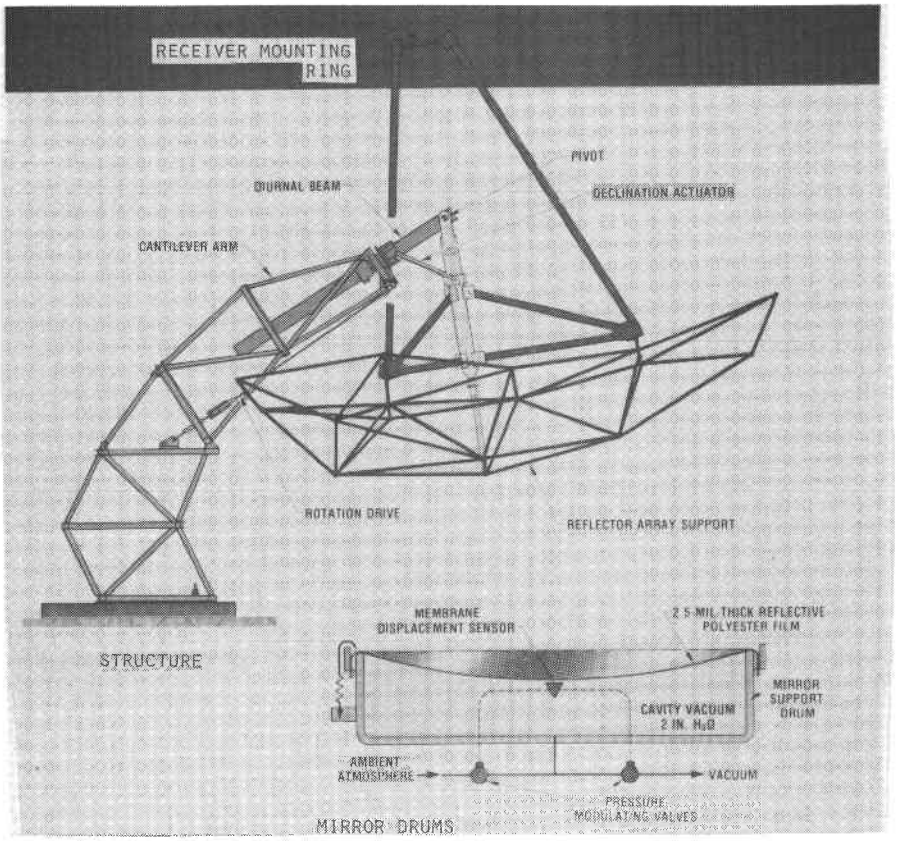

Figure 2-21. Sketch of LaJet Concentrator

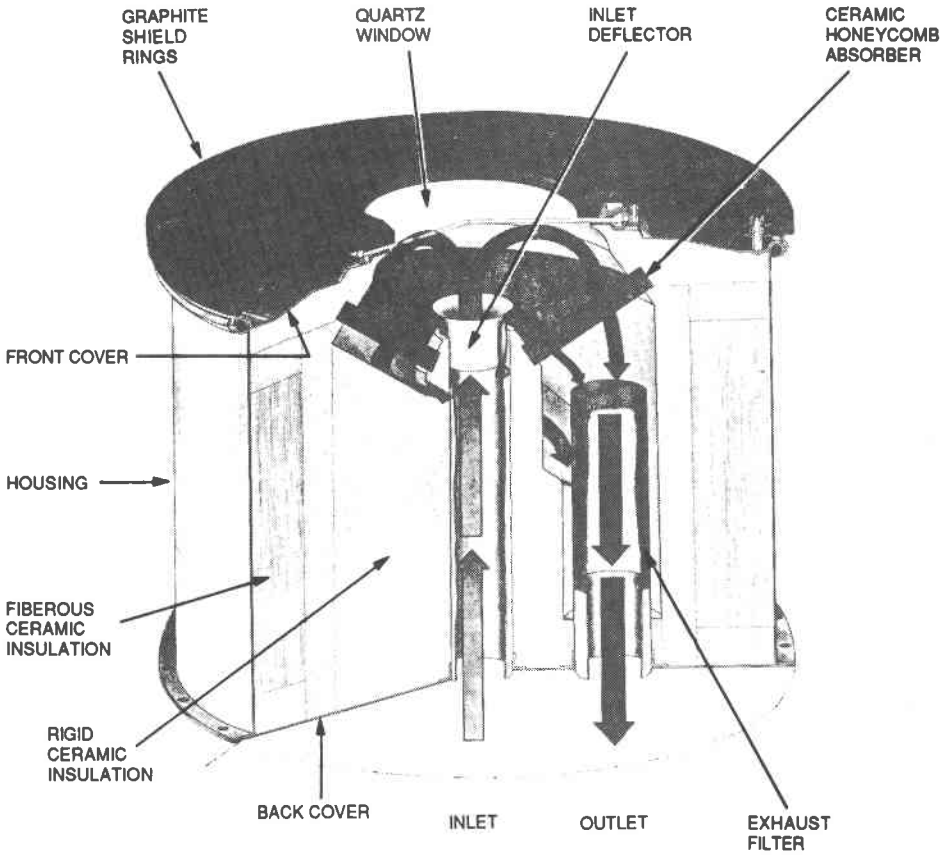

Figure 2-22. Sanders Low Pressure Brayton-Cycle Receiver (Reference 14)

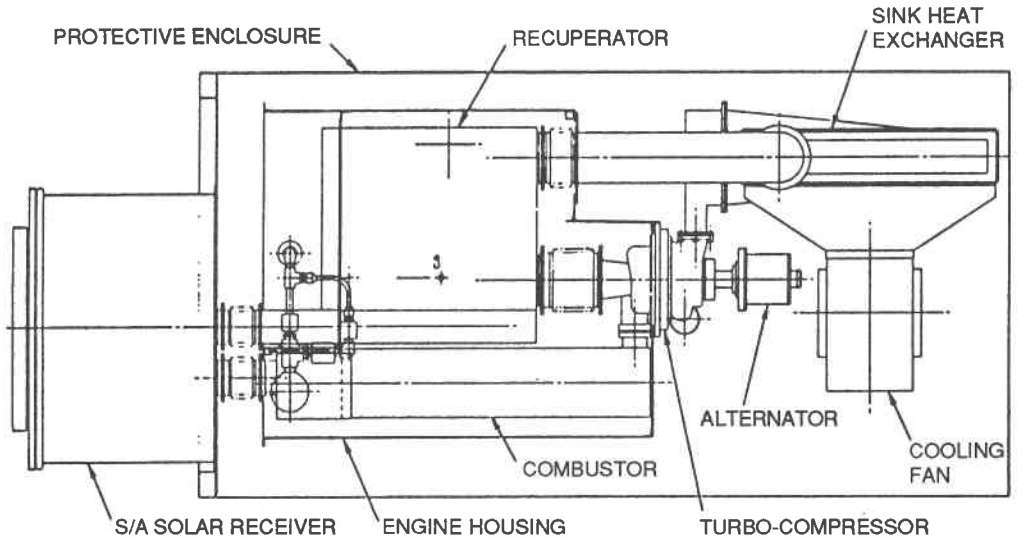

Figure 2-23. Configuration of AiResearch Brayton-Cycle Engine/Alternator with Sanders Receiver (Reference 18)

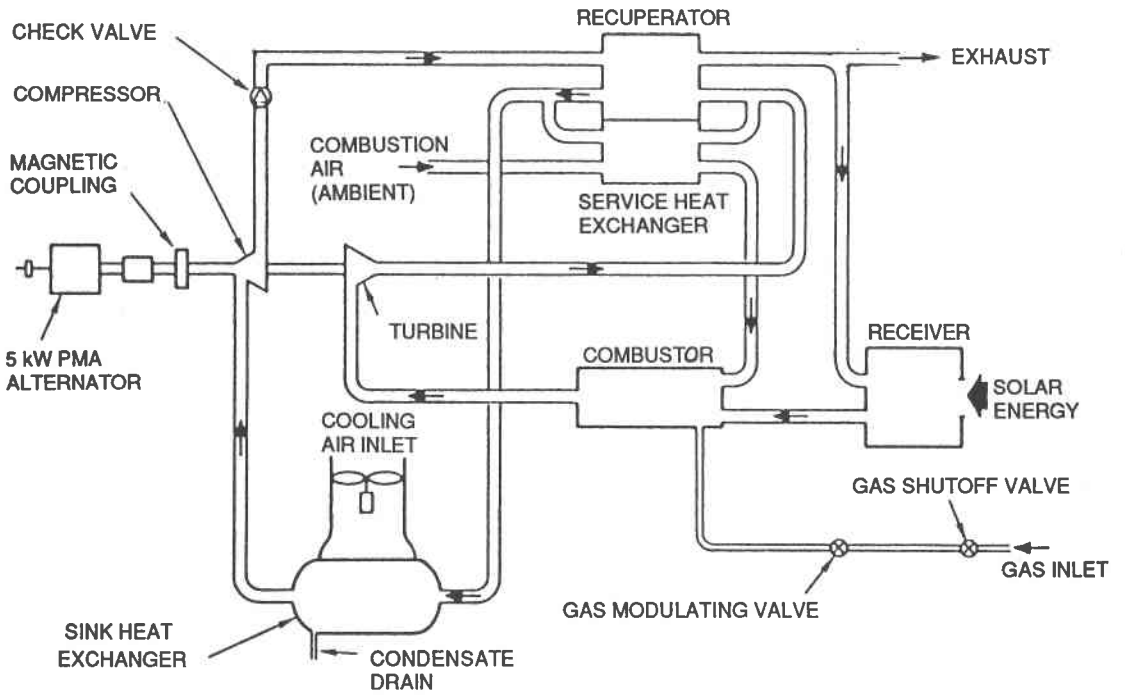

Figure 2-24. Schematic of AiResearch Brayton-Cycle Engine/Alternator with Sanders Receiver (modified from Reference 18)

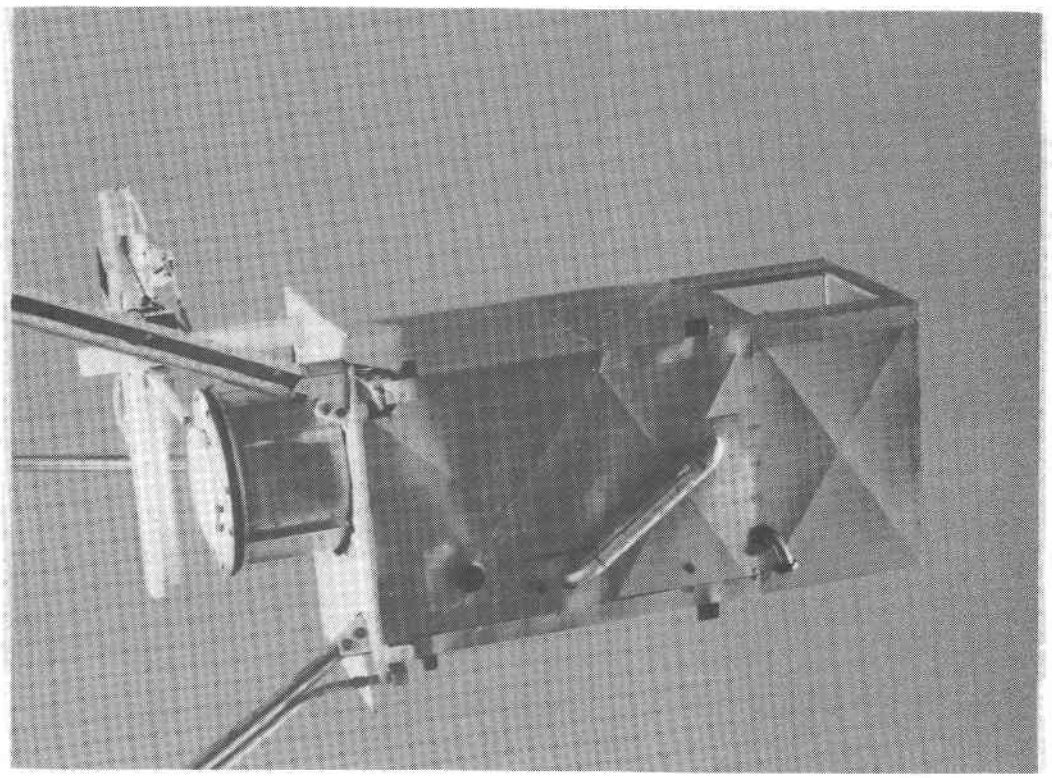

Figure 2-25. Brayton Power Conversion Assembly on LaJet Concentrator at Merrimack, New Hampshire

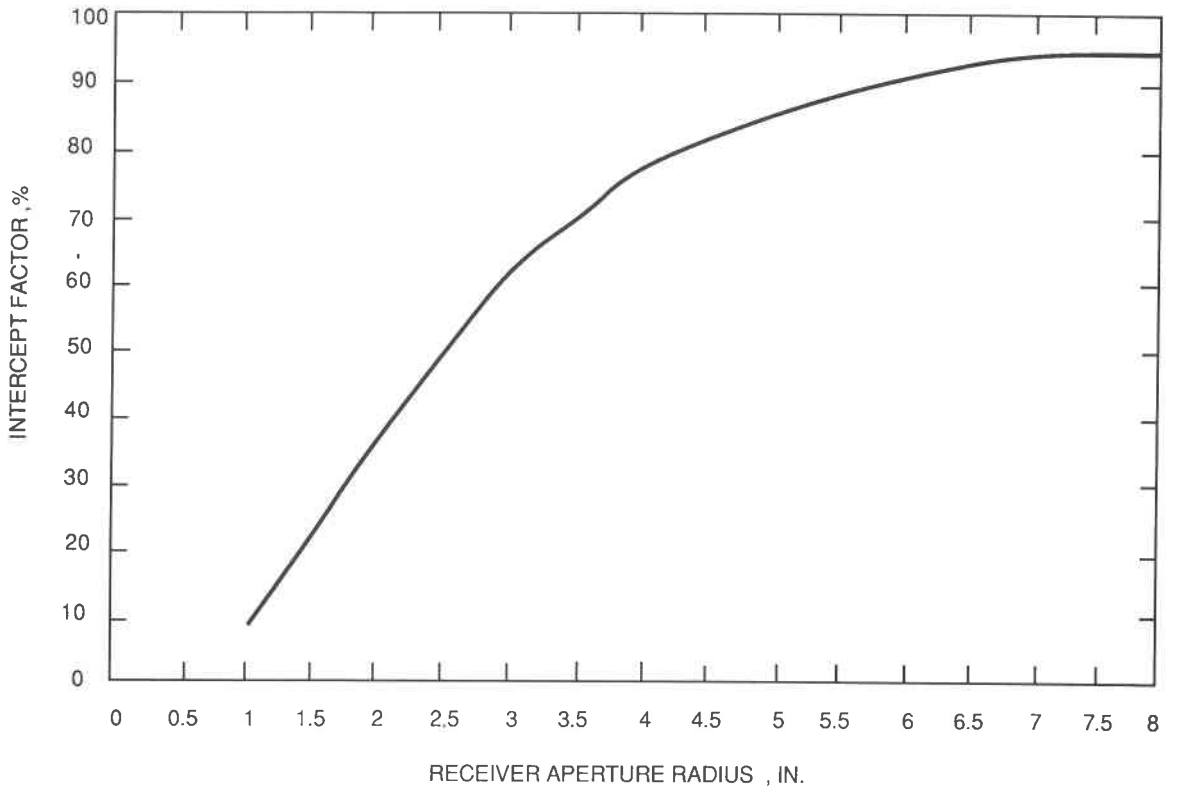

Figure 2-26. Performance of LaJet Concentrator (Uncertainty equal to ±20%) (modified from Reference 15)

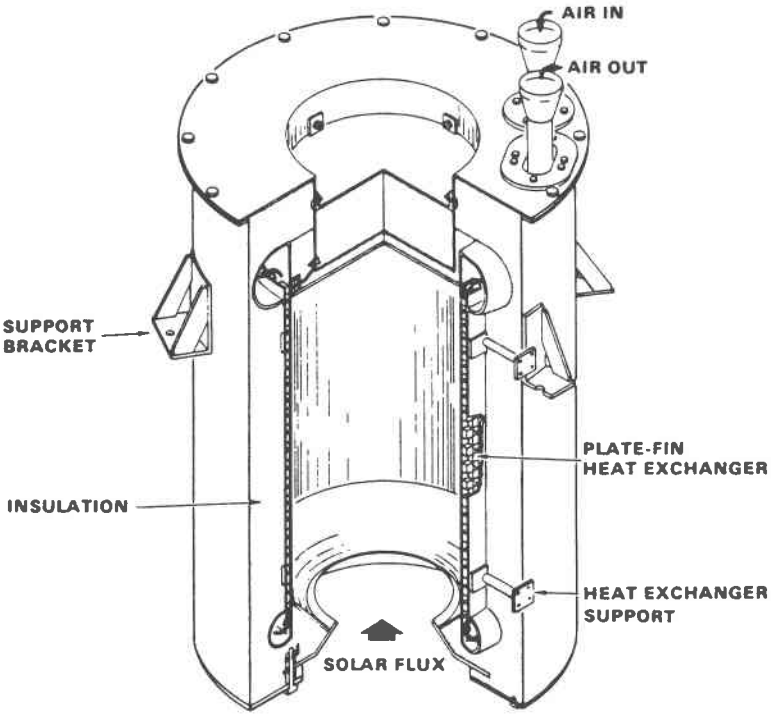

Figure 2-27. Garrett Brayton Receiver

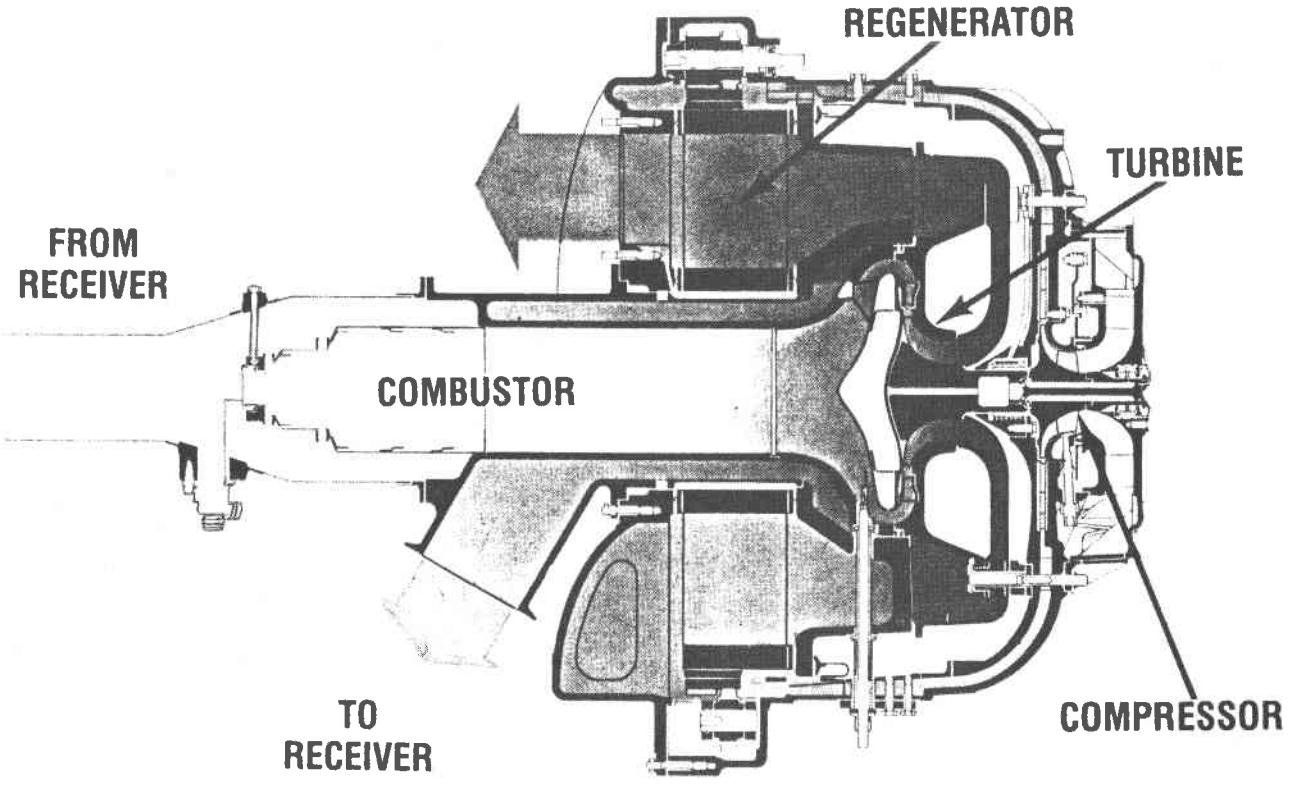

Figure 2-28. Garrett SAGT Engine

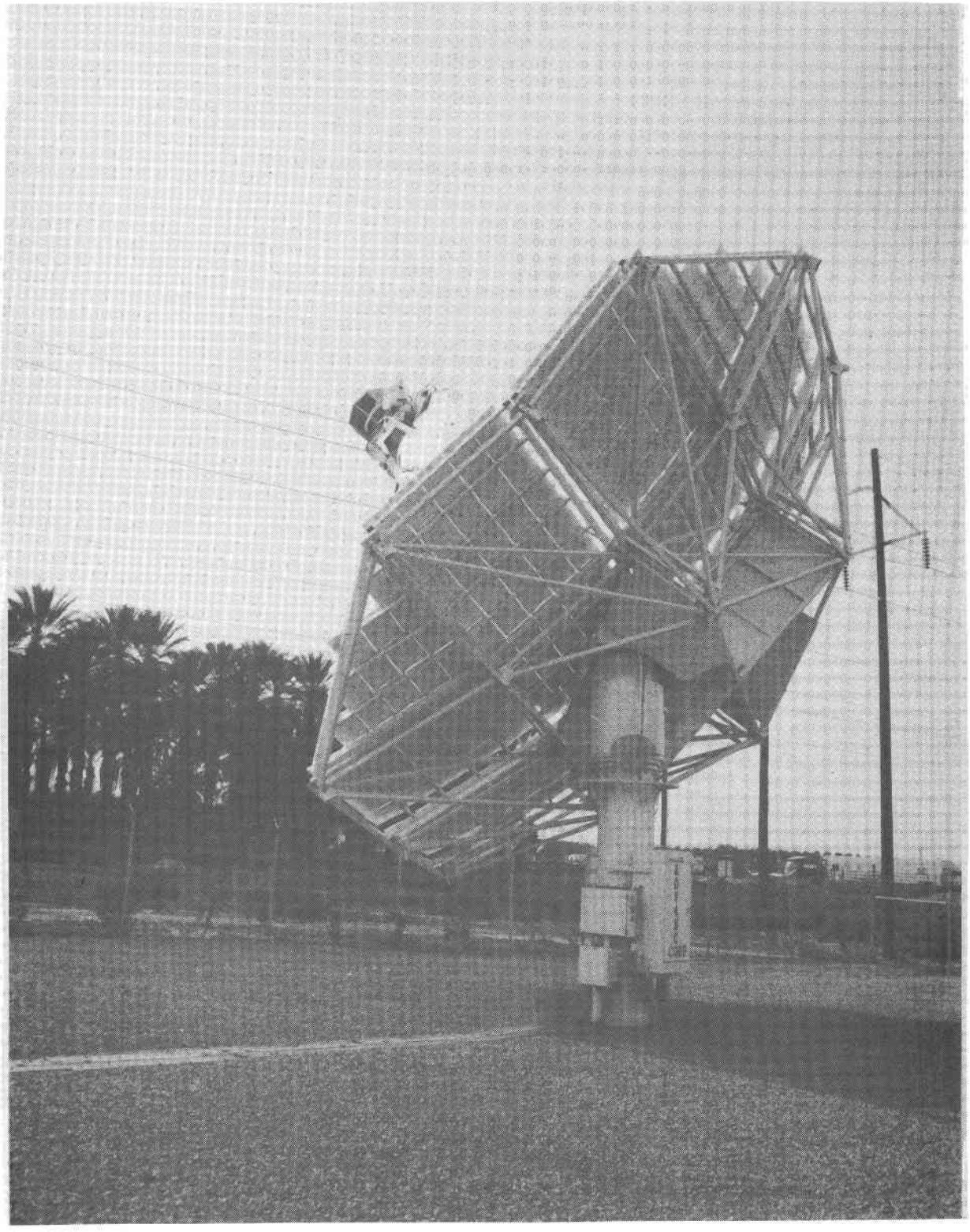

Figure 2-29. Advanco Stirling Module at Rancho Mirage, California (Rear View)

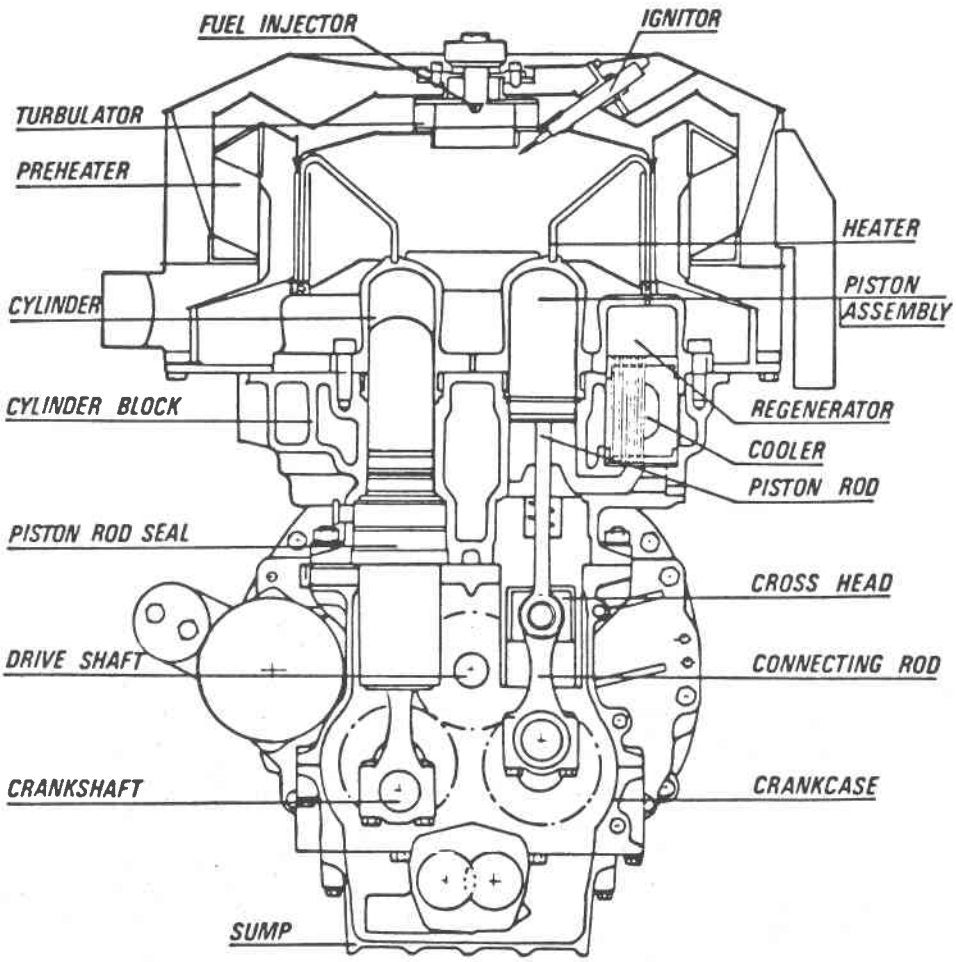

Figure 2-30. Cross Section of Fuel-Fired USAB 4-95 Stirling Engine

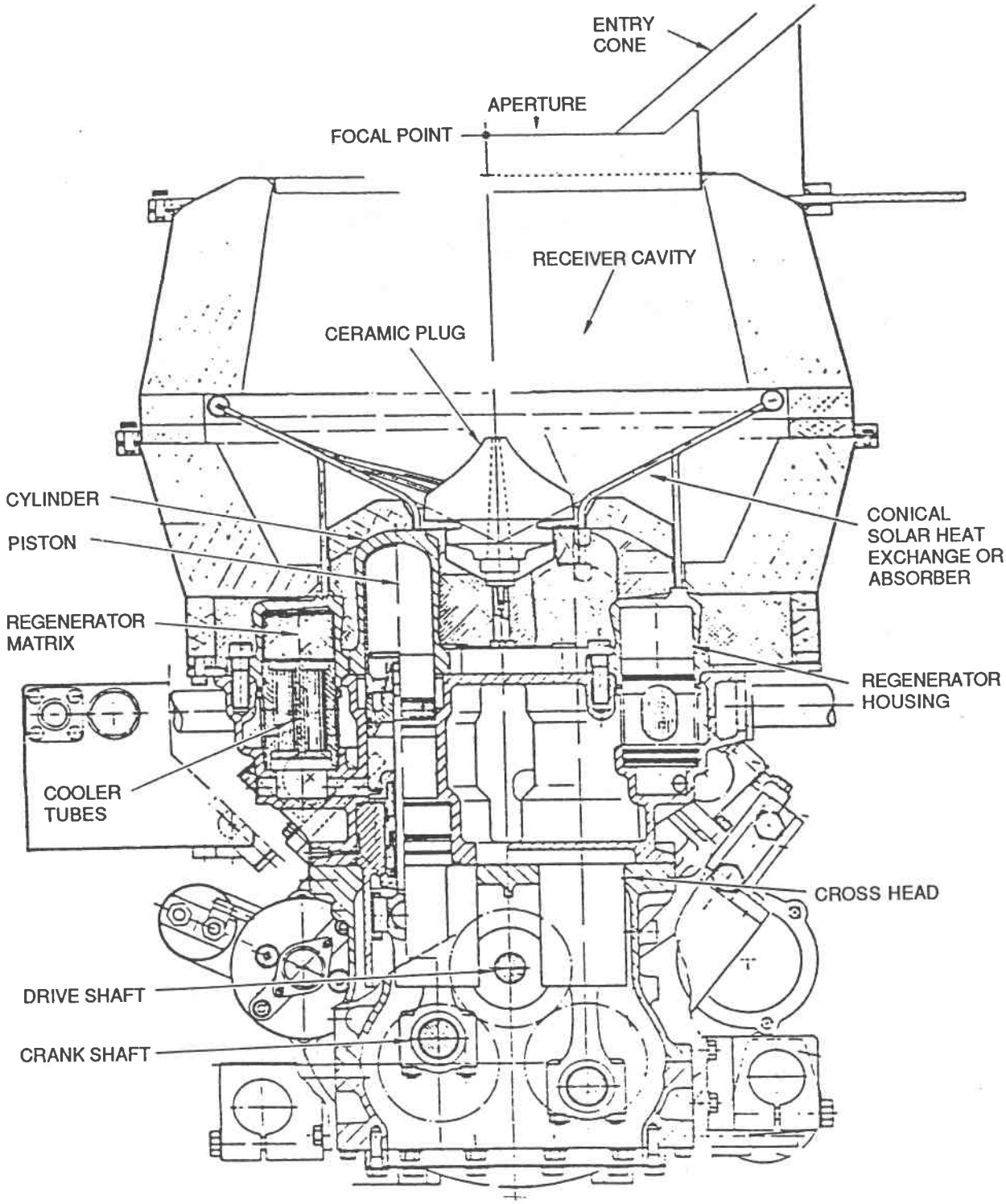

Figure 2-31. Cross Section of USAB Stirling Engine with Solar Receiver (Reference 20)

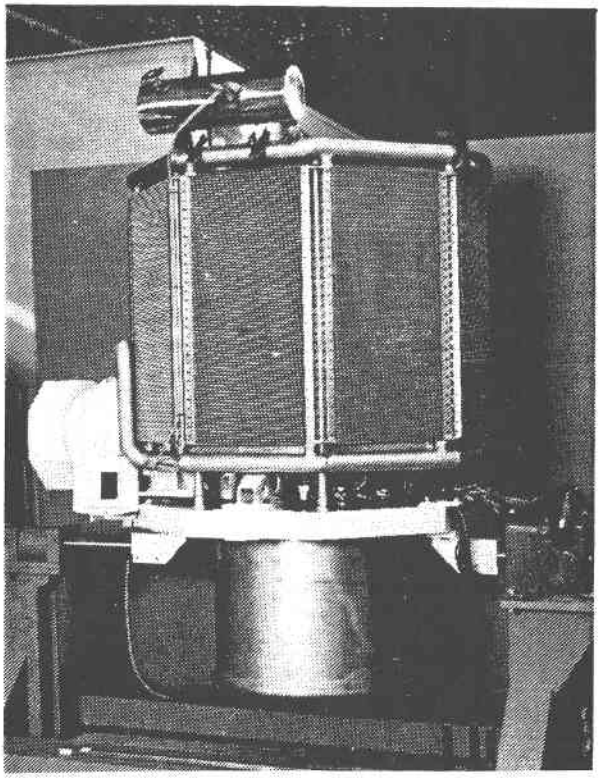

Figure 2-32. USAB Power Conversion Assembly

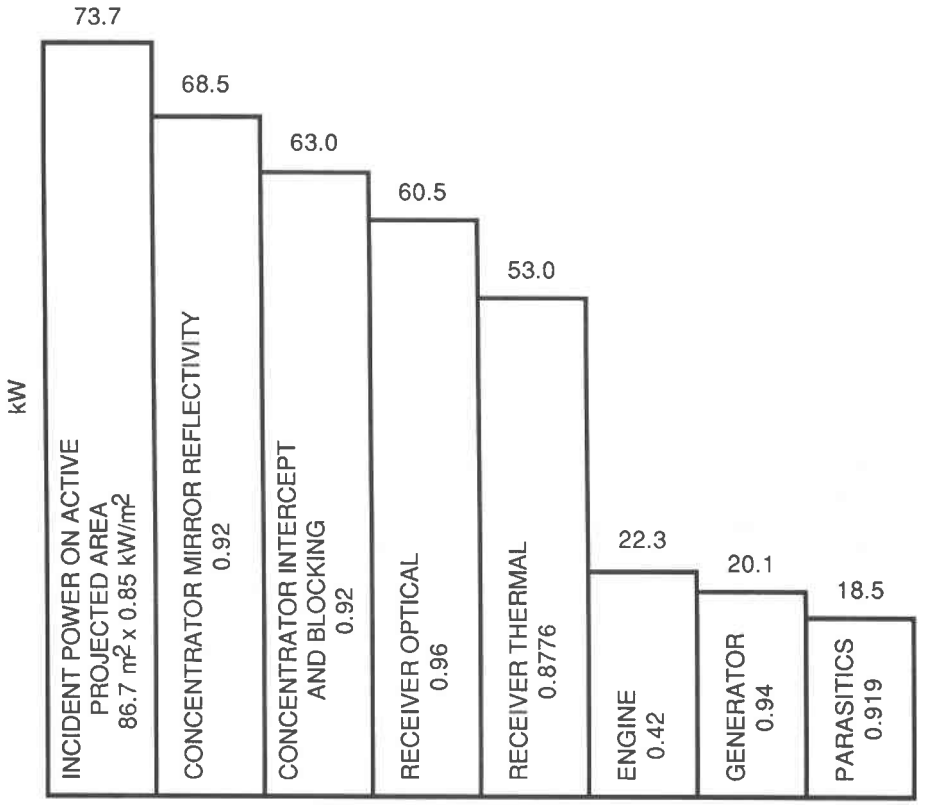

Figure 2-33. Subsytem Performance of Advanco Stirling System at 850 W/m^2 Insolation (modified from Reference 20)

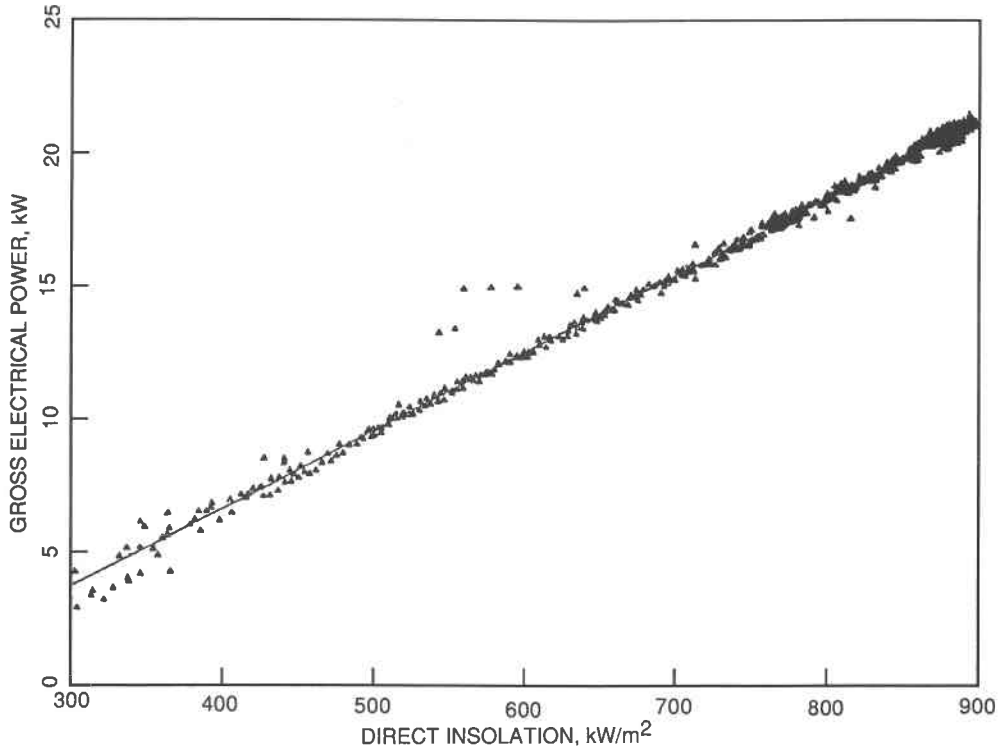

Figure 2-34. Gross Output of the Advanco Stirling Module as a Function of Direct Normal Insolation (Reference 20)

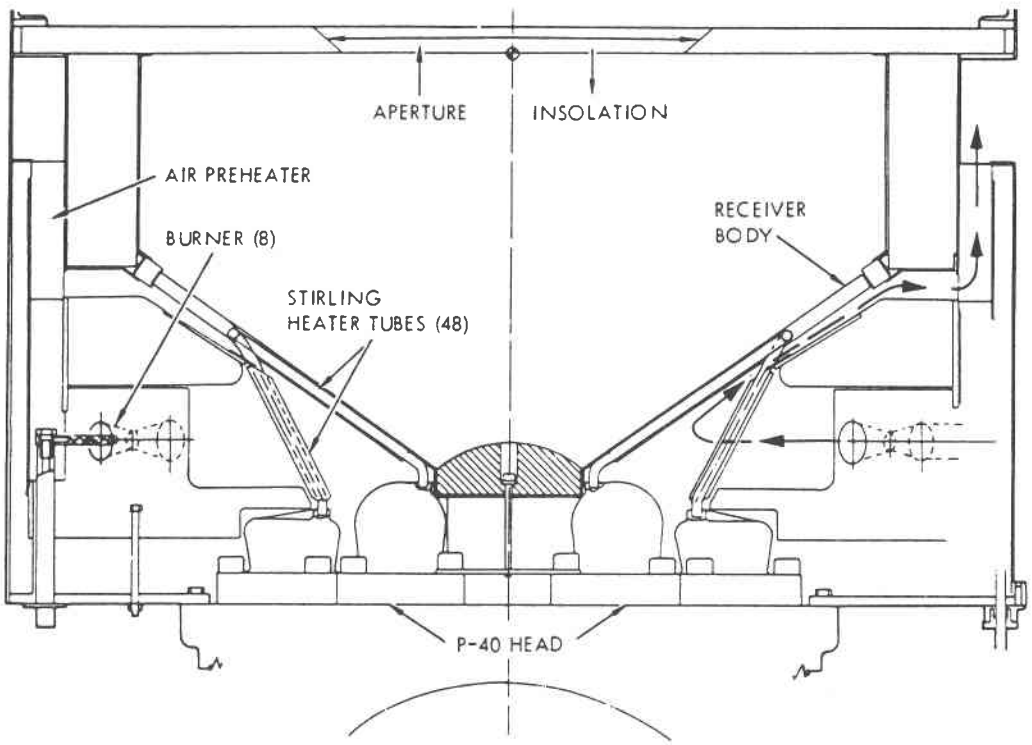

Figure 2-35. Fairchild Hybrid Stirling Solar Receiver

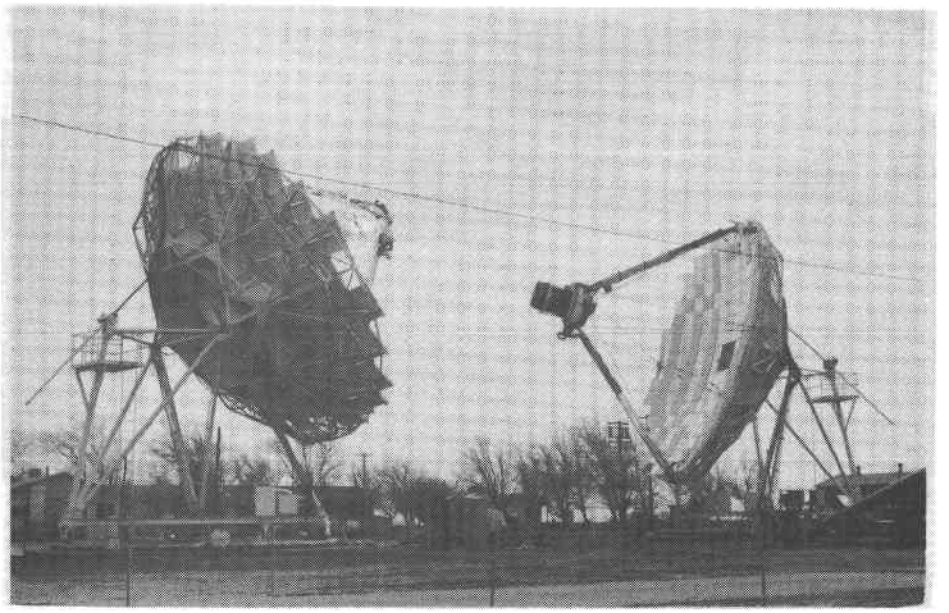

Figure 2-36. Test Bed Concentrators at the PDTS

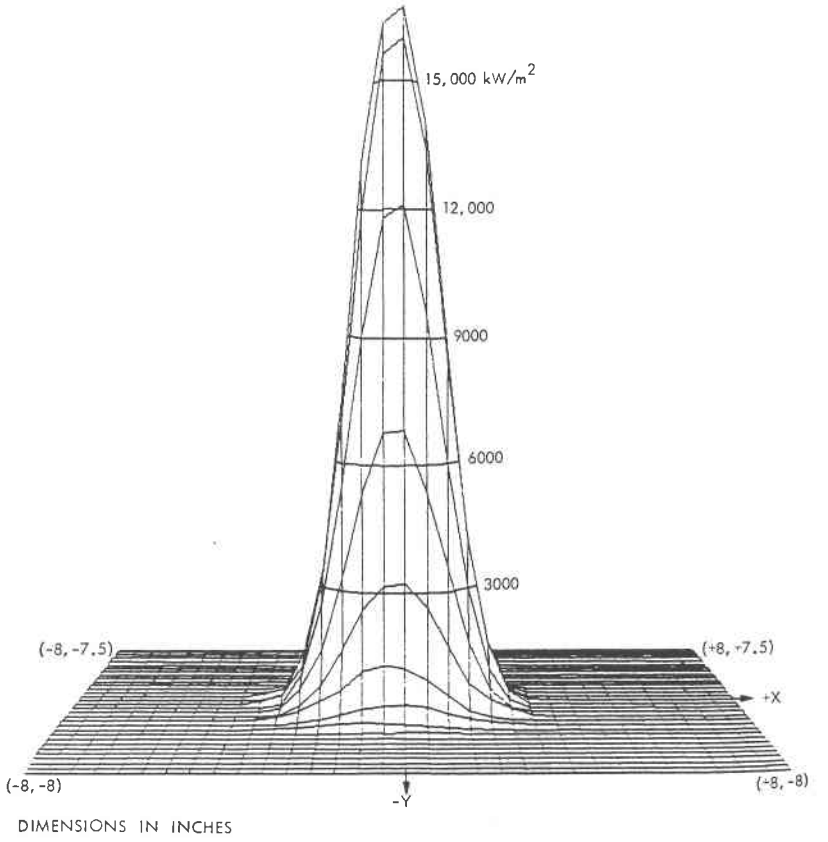

Figure 2-37. TBC Focal Plane Flux Distribution with All Facets Focused on a Point (Reference 22)

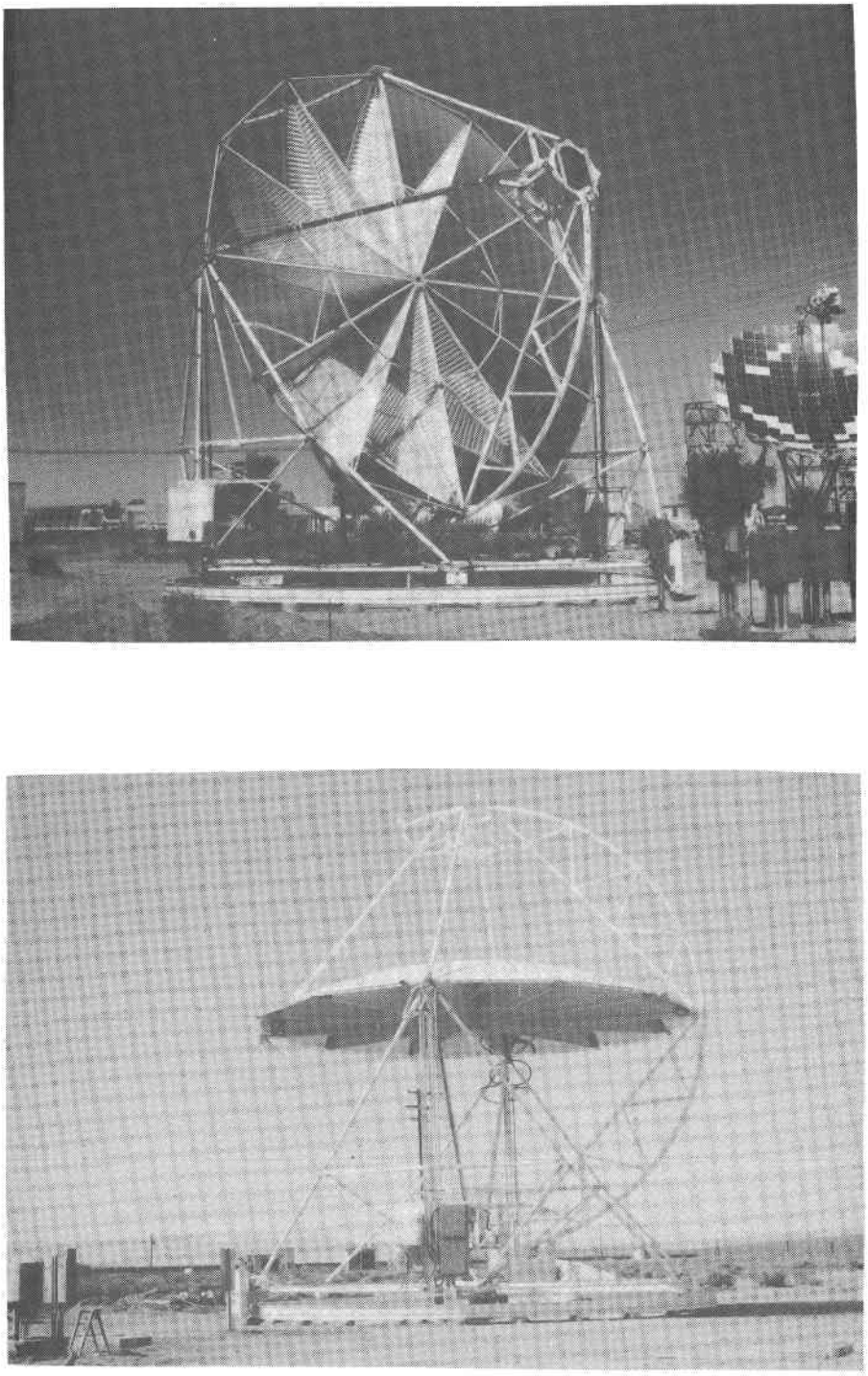

Figure 2-38. Parabolic Dish Concentrator No. 1 in Operating and Stowed Positions at the PDTS

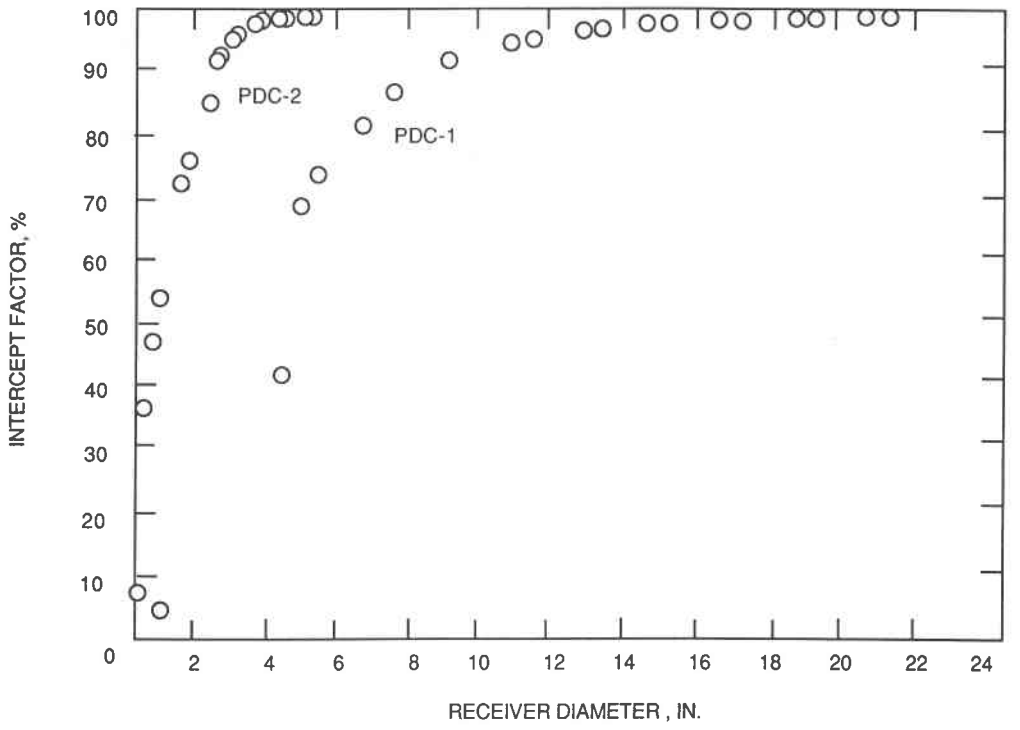

Figure 2-39. Intercept Factors for Test Panels for Parabolic Dish Concentrators Nos. 1 and 2 Measured with 0.9 mrad Source (modified from Reference 28)

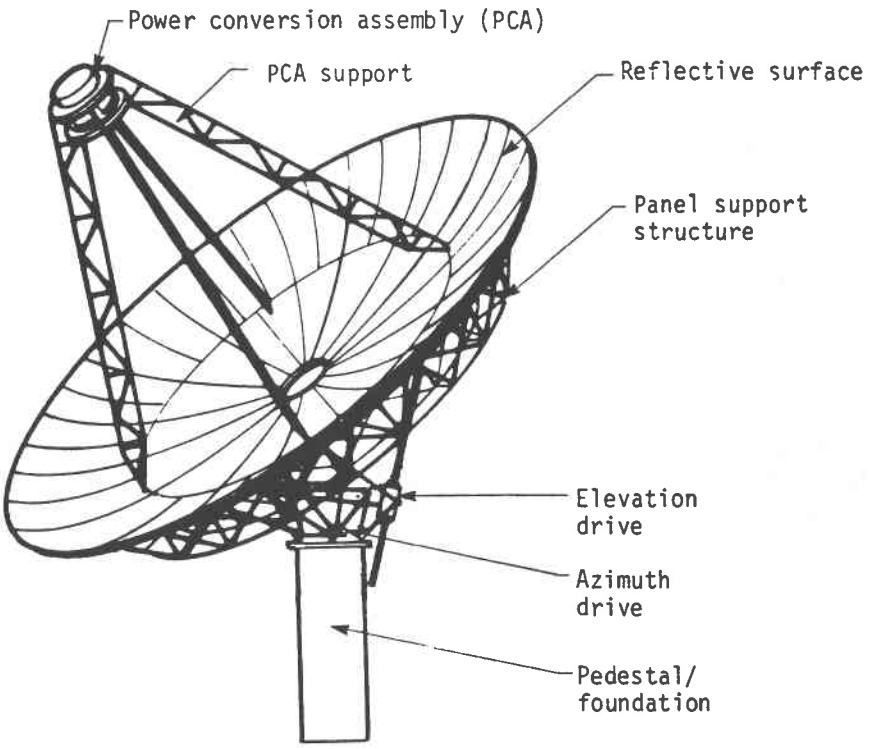

Figure 2-40. Sketch of Acurex Parabolic Dish Concentrator No. 2

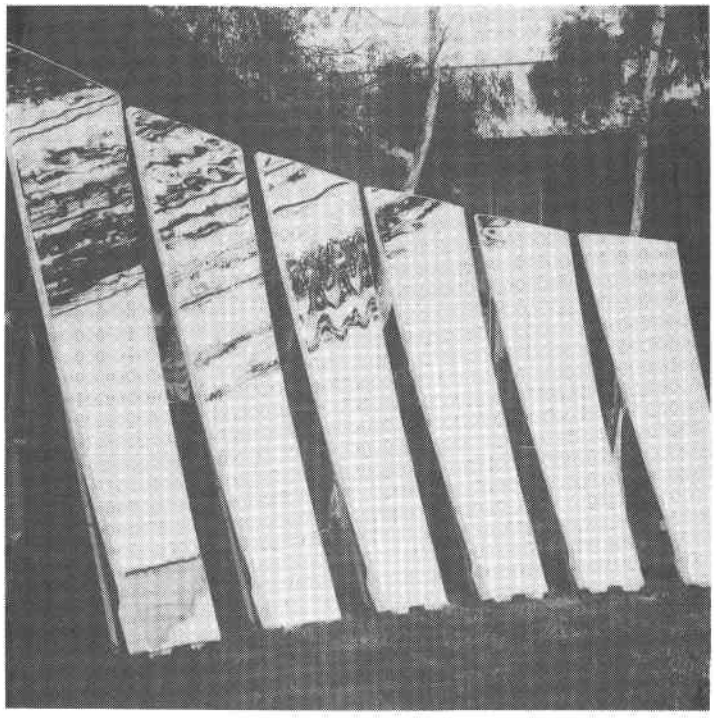

Figure 2-41. Photograph of Manufactured Cellular Glass Panels for Parabolic Dish Concentrator No. 2

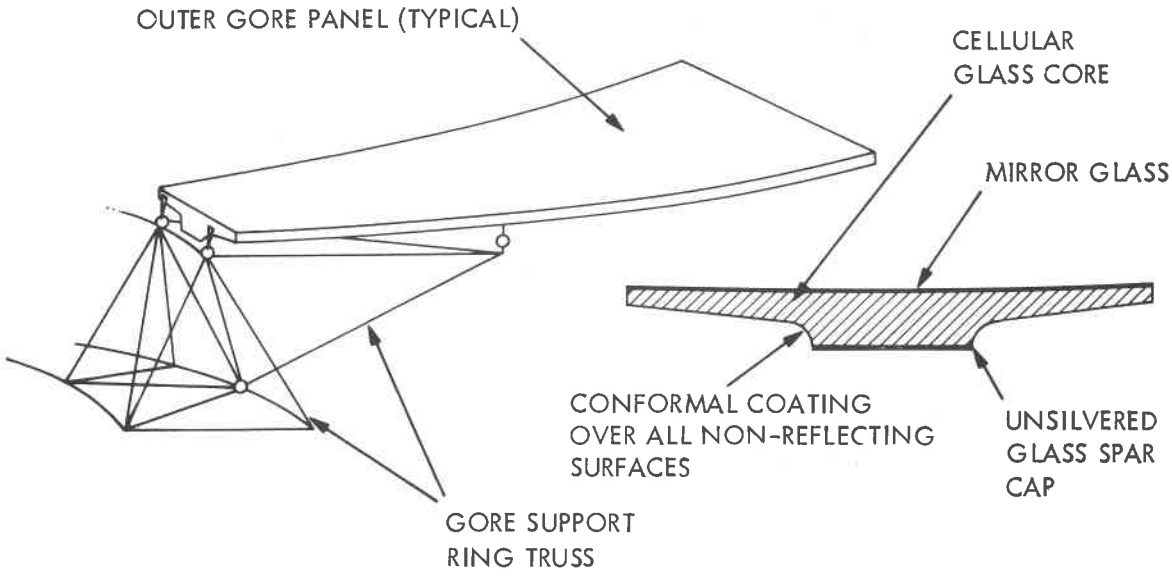

Figure 2-42. Side View and Cross Section of a Cellular Glass Panel

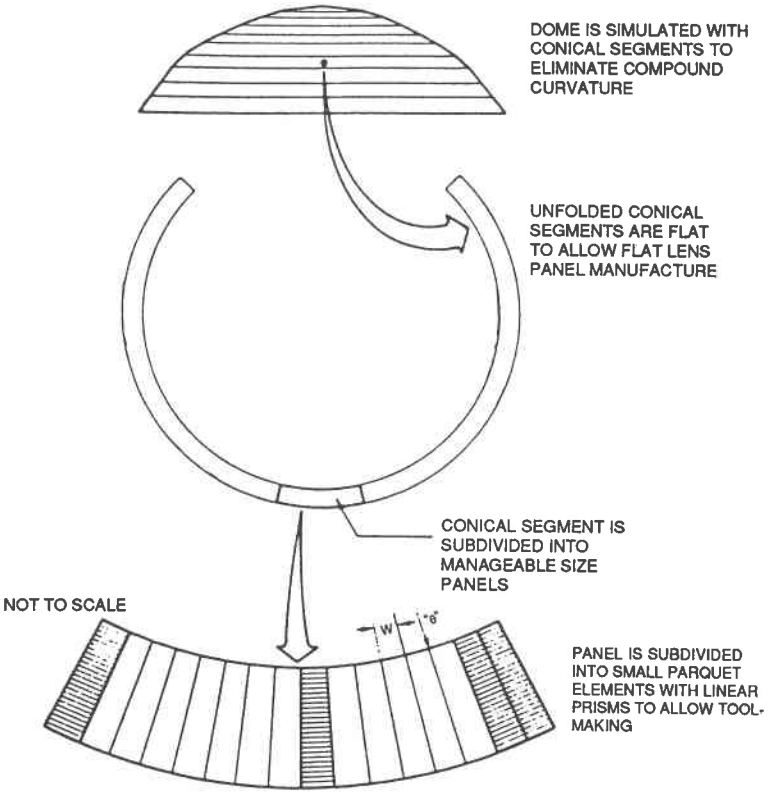

Figure 2-43. Geometry of Entech Lens Panel and Proposed Fresnel Lens (Schematic) (Reference 34)

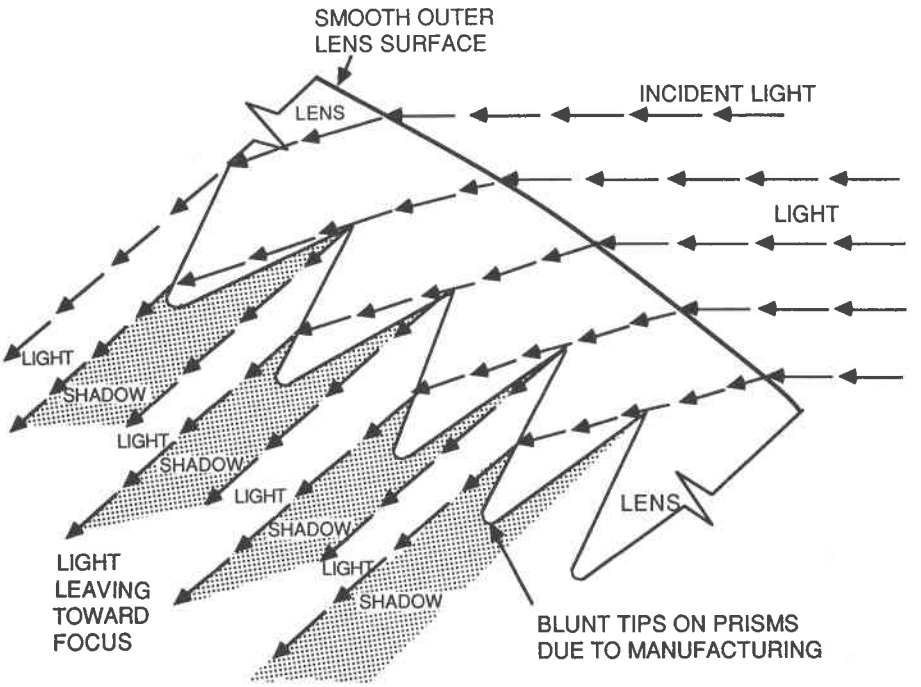

Figure 2-44. Sketch of Prismatic Element of Entech Fresnel Lens Element (Reference 34)

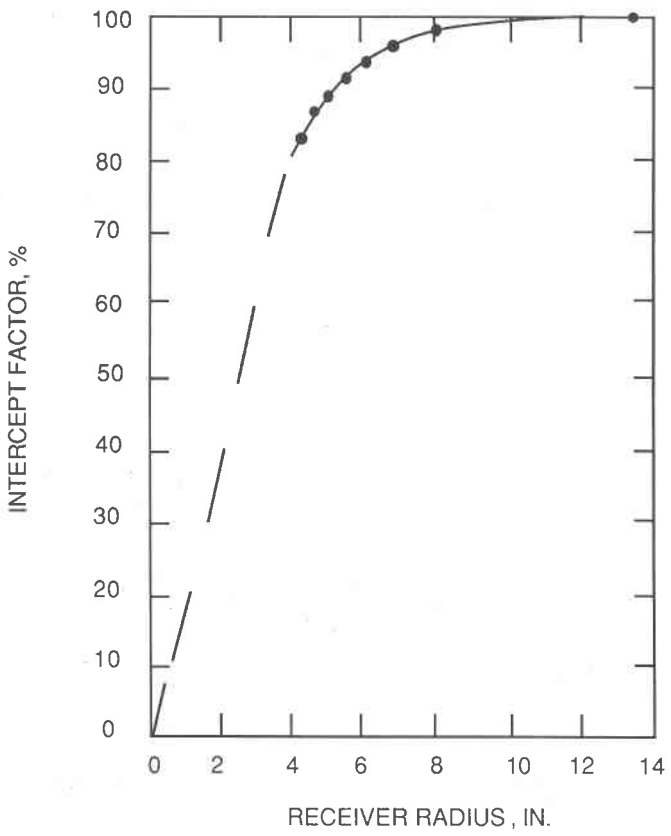

Figure 2-45. Measured Intercept Factor for Entech Fresnel Lens Test Panel (Reference 34)

Figure 2-46. University of Chicago Secondary Concentrator

SECTION III

PROJECTED SYSTEM CHARACTERISTICS

A. PLANT PERFORMANCE

1. Introduction

All of the solar thermal electric power plants considered here have the following characteristics in common:

(1) An output capability of 5 MWe that is not exceeded; any excess power generated during periods when the direct normal insolation exceeds the design value of 1 kWt/m^2 is assumed to be wasted.

(2) The plant has negligible capacity to store energy in thermal, chemical, electric, or in any other form.

(3) The plant comprises a collection of identical solar thermal electric power modules, each capable of generating approximately 23, 30, or 36 kWe, depending upon whether the type of thermodynamic engine employed operates on the Stirling, organic-Rankine, or Brayton cycle, respectively. Each module consists of a parabolic dish concentrator, a cavity receiver with open aperture, a thermodynamic engine connected to an alternator, and appropriate auxiliary equipment. The modules are clustered, and the power produced is properly conditioned and synchronized so as to be acceptable by the electric grid to which the plant is connected.

Four different plant configurations have been considered here, and the performance of each of these plants has been analyzed at four different locations within the contiguous United States. Only one configuration of the plant consisting of parabolic-dish/Stirling-engine modules and their auxiliary equipment has been analyzed; this is also true in the case of the plant consisting of parabolic-dish/Brayton modules and their auxiliary equipment. However, two configurations of the plant consisting of parabolic-dish/organic-Rankine engine modules and their auxiliary equipment have been analyzed; the modules of these two different configurations differ only in the dish-type used. Because either the Stirling or the Brayton engine operates at a high source temperature, the module of which either is a part must employ a parabolic dish of high optical quality in order to provide a beam of highly concentrated sunlight to the engine through a relatively small receiver aperture. Whereas the Stirling engine considered here operates at a heater head temperature of 721°C (1330°F) and the Brayton engine at a turbine inlet temperature of 2200°F, at full load the organic-Rankine engine operates at a turbine inlet temperature of only 399°C (750°F). At the lower source temperature utilized in the organic Rankine module, it is conceivable that a parabolic dish of lower quality than that required by a Stirling or Brayton module might be more cost-effective in spite of its probable lower optical quality; this is the reason the performances of two different plant configurations utilizing organic-Rankine engines have been evaluated.

It must be emphasized here that the Stirling-, organic-Rankine-, and Brayton-powered modules whose performances are reported are not contemporary! The parabolic-dish/Stirling module is available today, and its experimentally verified performance is presented. A prototypical parabolic dish/organic-Rankine module has been built and tested; the full-load performance of the tested module approached that of the module modeled here, but the assumed part-load performance of the module modeled is based on the projected performance of an improved organic Rankine engine. It is believed that realization of the modeled module is about 5 years away. The parabolic dish/Brayton module modeled here assumes the successful development of the advanced automotive Brayton engine. Virtually all the parts of this engine will be ceramic; the vital parts of the matching receiver must then also be constructed almost entirely of ceramic materials. While some success can be claimed in the development of both rotating and static components of the engine, it seems unlikely that the hypothetical module modeled can be successfully built and tested before 1995.

The four different locations within the contiguous United States that have been selected as sites for the performance evaluation of the four different plant configurations are Albuquerque, New Mexico (ABQ), Fresno, California (FNO), Dodge City, Kansas (DGC), and Fort Worth, Texas (DFW). At these sites, annual direct normal insolation received ranges from high to at least moderate as shown below:

Location	Annual Direct Normal Insolation, MWt/m^2
Albuquerque, New Mexico	2540
Fresno, California	2275
Dodge City, Kansas	2089
Fort Worth, Texas	1705

The data shown above and the corresponding histogram of annual direct normal insolation for Albuquerque, New Mexico are taken from Reference 39. Similar hitherto unpublished data for Fresno, California, and Dodge City, Kansas, were obtained at the California Institute of Technology/JPL by the same method as is described in the cited report. The data for annual direct normal insolation at Fort Worth, Texas, are published in Reference 40; however, in the absence of any more reliable data, the histogram employed for Fort Worth, Texas, was obtained by reducing the hours of occurrence for each increment of direct normal insolation to the corresponding quantity determined for Dodge City, Kansas, i.e., by the ratio 1706/2089. Only after close examination of data presented by Randall and Whitson in Reference 40 regarding the mean daily direct normal insolation for each month of the year over a large number of years at both Dodge City, Kansas, and Fort Worth, Texas, and

only after noting close similarities in the annual patterns of these data was this artifice of ratioing accepted as reasonable.

2. Concentrator Performance

The parabolic dishes considered in this document are only faceted approximations to a perfect paraboloid of revolution. In the most cost-effective designs thus far produced, the paraboloid has been approximated by concave reflecting facets whose radii of curvature correspond to the local radius of curvature of the ideal paraboloid in the same region.

The high-quality dishes considered are all assumed to use facets surfaced with thin sheets of second-surface-silvered, low-iron plate or float glass. The aperture area of the dish as defined herein is the net area of all the facets projected onto the aperture plane of the dish; thus, it is assumed that the facets are quite closely spaced in those regions of the dish that are not shaded by the power conversion assembly or its support struts and that no part of any facet is shaded. Already constructed dishes whose reflective surfaces are configured in approximately this way are the TBCs constructed by E-Systems and formerly located at the PDTS, the Advanco concentrator, and the more recently developed McDonnell-Douglas concentrator. The reflectance of the mirrored facets has been assumed to be 0.94 when new and clean. Because net aperture area and no shading by module components have also been assumed, the resultant design efficiency of the high-quality concentrators is also 0.94. Studies conducted at JPL have indicated that the assumption of an average degradation factor of 0.965 is reasonable if the mirrored surfaces are properly washed once a month. Other JPL studies have shown that, for an economically distributed field of modules located at any of the four sites chosen for study here, an annual shading factor of 0.97 is realistic. Therefore, the annual operating efficiency of any one of the three high-quality concentrators assumed here is estimated to be 0.88.

The prototype for the lower quality concentrator assumed in the alternate analysis of the parabolic-dish/organic-Rankine engine power plant is that produced by LaJet for use with the JPL-coordinated, Sanders-assembled-and-tested parabolic-dish/Brayton module. The typical facet employed in this concentrator consists of a shallow, circular pan perhaps 5 ft in diameter whose open face is covered with a front-surface-aluminized and overcoated polyester membrane. In operation, the concavity of the reflecting membrane is controlled by applying a partial vacuum to a small tube that projects through the center of the pan bottom. The radius of concavity is determined by the distance of the tube end from the undistorted, taut polyester membrane. The same assumptions regarding net aperture area, shading by the power conversion assembly and supporting struts, average degradation of the reflectance in continued service, and annual field shading as were made in the case of the high-quality concentrators has also been made here. Thus, a design efficiency of 0.85 and an annual efficiency of 0.79 have been estimated for this lower quality concentrator.

3. Receiver Performance

The receivers employed in the modules synthesized for this study belong to one generic type, and their performances have been estimated in one

consistent way. An open-aperture receiver with an approximately cylindrical cavity has been assumed. Furthermore, it has been assumed that the receiver heat transfer surfaces within the cavity consist of the end plate opposite the aperture and/or the cylindrical wall of the cavity. The remaining surfaces within the cavity are assumed to be approximately adiabatic. All the cavity surfaces are assumed to be nearly black and diffuse. The types and extent of insulation selected to fill the space between the cavity and the external shell of the receiver vary with the maximum source temperature required by the engine. The diameter of the aperture specified for a given receiver has been determined after due consideration of the aperture area and optical quality of the concentrator to which it is matched.

Receiver performance has been estimated in each case on the basis of calculations performed by Maynard and Birur (Reference 41). In the cases involving the parabolic-dish/Stirling and parabolic-dish/organic-Rankine modules, it has been possible to adjust the calculated values on the basis of experiments conducted on modules of these types at the PDTS. Having obtained parameters for a given receiver from the calculations of Maynard and Birur (see Reference 41) (adjusted where possible to account for experimental results), receiver performance at either full or part load was calculated as shown in Reference 42, p. 2-7. It should be noted that, because of the reduction in turbine inlet temperature with decreasing load required for optimal operation of the parabolic-dish/Brayton-engine module, the efficiency of the receiver incorporated into this module is higher at all but the lowest part loads than it is at full load!

4. Power Conversion Performance

The performances of the power conversion, power conditioning, and transport systems of the different power plant configurations differ in ways that will be explained in the following subsections. The final remaining performance parameter in the efficiency train is the plant parasitic loss. Because this loss has been expressed in this analysis as a fraction of the gross plant-produced, conditioned, and transported electrical output, the parasitic efficiency has been defined as the inverse of the quantity, one plus the parasitic loss. For the usual small, fractional parasitic loss, parasitic loss is closely approximated as simply the quantity, one minus the parasitic loss.

a. Stirling Engine Power Conversion Subsystem. The kinematic Stirling engine power conversion subsystem incorporated into each of the parabolic-dish/Stirling-engine modules that comprise the corresponding 5-MWe solar thermal electric power plant is configured as follows:

The assumed engine is a solarized version of the National Aeronautics and Space Administration (NASA) Automotive Stirling Engine (ASE) Mod 1; the basic ASE engine is now undergoing testing. The solarized version of the ASE Mod-1 engine should provide a modest improvement in performance relative to the solarized version of the USAB P-40 engine, and its components are fewer in number, more easily manufactured, and require less costly, more easily obtained raw materials than do those of the P-40 engine.

The parabolic-dish/Stirling modules tested at JPL and by Advanco have employed the USAB P-40 engine coupled to an induction generator. While this configuration is satisfactory if the amount of power to be supplied to the utility grid by arrays of such modules is small, it will probably be necessary to employ synchronous generators in the modules if as much as 5 MWe is to be supplied to the grid. This is because of the destabilizing effect on the grid and the cost of correcting the otherwise severely lagging power factor of inductively generated ac power. In the performance analysis reported here, it has been assumed that a suitable synchronous generator with an efficiency of 0.95 is coupled to the Stirling engine.

The solarized ASE Mod-1 kinematic Stirling engine has been assumed to operate at 1800 rev/min, a heater head temperature of 704°C (1330°F), and a cooler temperatures of 29.4°C (85°F). Under these conditions, the engine will generate 30 kWe at a thermodynamic efficiency of 0.39 (full-load conditions). Under the conditions given above regarding the assumed matching concentrator and receiver, a concentrator aperture area of 102 m^2 is required for the parabolic-dish/Stirling-engine module considered here.

The following tabulation presents the design performance parameters of the NASA Mod-1 ASE and matching receiver employed in the analysis here:

Receiver	
Operating Temperature, °F	1350.0
Input Power, kWt	95.9
Efficiency	0.881
Output Power, kWt	84.5
Engine	
Heater Head Gas Temperature, °F	1330.0
Rotational Speed,[a] rev/min	1800
Input Power, kWt	84.5
Efficiency	0.390
Output Power, kWs[b]	33.0

[a]In this application, the Stirling engine operates at constant rotational speed.
[b]s denotes rotating shaft power.

Figure 3-1 presents the estimated normalized efficiencies of these subsystems as functions of the normalized thermal power inputs to them under part-load conditions.

b. Organic Rankine Engine Power Conversion Subsystem. Two different receivers are required for the two different concentrator designs incorporated into the two different parabolic-dish/organic-Rankine engine modules that comprise the two different 5-MWe solar thermal electric power

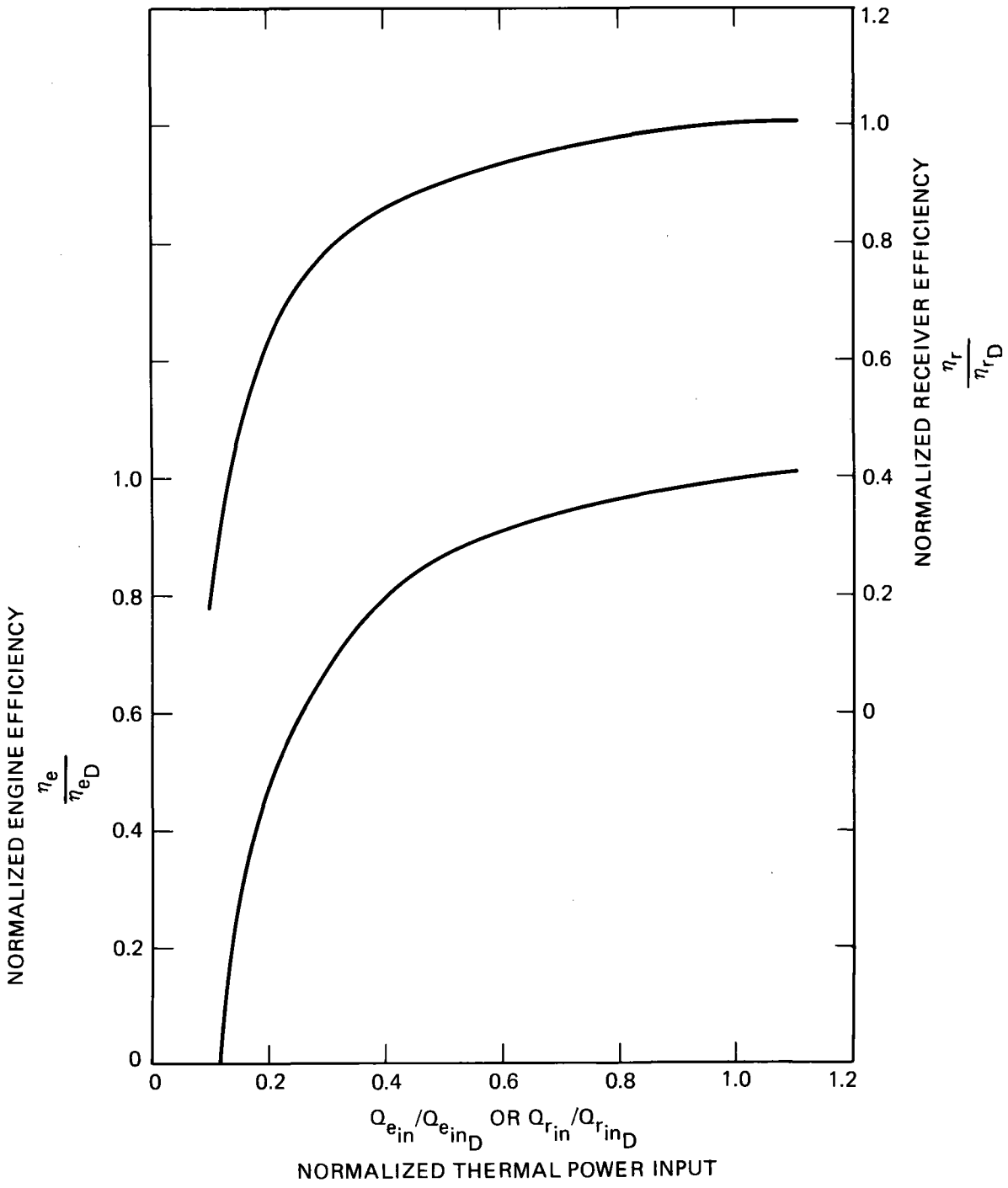

Figure 3-1. NASA Mod-1 ASE and Matching Receiver: Normalized Efficiencies of these Subsystems as Functions of the Normalized Thermal Power Input to These Components under Part-Load Conditions

plants considered; however, the organic-Rankine engine and alternator comprising the power conversion subsystem are essentially the same for these two different versions.

The organic-Rankine engine employed in these modules is that developed by Barber-Nichols and incorporated into a module designed and developed by FACC. This module was tested at the PDTS. The performance of the engine assumed in this analysis is slightly higher than that demonstrated by the prototype for two reasons. The part-load characteristics of the prototype were impaired by persistent bearing problems, and the full-load characteristics were limited by a less-than-optimum configuration of the turbine nozzle plate to the turbine wheel. It is believed that, with the correction of these two defects, the performance assumed here is realistic. Nevertheless, it is emphasized that an organic-Rankine engine with these characteristics has not yet been demonstrated.

Because the organic-Rankine engine rotational speed varies from about 40,000 to 60,000 rev/min from idle to full load, a permanent magnet alternator is mounted on the same shaft as the turbine. The output of the alternator is rectified and then converted by solid-state devices to the voltage, 60 Hz frequency, and phase required by the grid. At full load, the assumed subsystem power output and efficiency of the organic-Rankine engine power conversion subsystem are 23.3 kWe and 0.262, respectively. However, because of the extensive power conditioning and transport facilities required between the modules and the grid, the combined efficiency of these latter processes has been assumed to be only 0.95.

For the module design incorporating the high-quality concentrator, a receiver design efficiency of 0.962 has been estimated, resulting in a corresponding concentrator aperture area of 105.8 m^2. For the module design incorporating the lower quality concentrator, a receiver design efficiency of 0.936, and a concentrator aperture area of 120.4 m^2 have been estimated.

The following tabulation presents the design performance parameters of the organic-Rankine-cycle turbine engine/alternator and the two different matching receivers (each of which is matched to a different concentrator) that have been employed in the analysis here.

Second-Surface-Silvered, Float-Glass-Mirrored Concentrator:

Receiver	
Toluene Vapor Outlet Temperature, °F	750.0
Input Power, kWt	99.4
Efficiency	0.962
Output Power, kWt	95.7
Engine/Alternator[a]	
Toluene Vapor Inlet Temperature, °F	750.0
Rotational Speed, rev/min[b]	60,000
Input Power, kWt	95.7
Efficiency	0.262
Output Power, kWe	25.0

(Continued)

First-Surface-Aluminized, Mylar-Mirrored Concentrator:

Receiver	
Toluene Vapor Outlet Temperature, °F	750.0
Input Power, kWt	102.0
Efficiency	0.936
Output Power, kWt	95.7
Engine/Alternator	
All engine/alternator design data are identical for ORC power conversion units equipped with either of the two types of concentrators.	

[a]The turbine and alternator of the ORC power conversion unit are mounted on a common shaft and enclosed in one case; therefore, efficiency of the combined unit is presented here. The symbol, e, indicates electrical power out of the alternator.
[b]Under part-load conditions, rotational speed may be as low as approximately 40,000 rev/min.

Figure 3-2 presents the estimated normalized efficiences of subsystems as functions of the normalized thermal power inputs to them under part-load conditions.

c. Brayton Engine Power Conversion Subsystem. While the modules analyzed here employing the Stirling engine or organic-Rankine engine power conversion subsystems have already been demonstrated in at least prototypic form, the module employing the Brayton engine power conversion subsystem envisioned in this analysis is currently hardly more than a vision in the minds of its designers.

The Garrett Turbine Engine Co. advanced automotive gas turbine engine (NASA AGT-101) will eventually be a single-spool gas turbine engine with compressor having variable inlet guide vanes, and virtually all of its components, both stationary and rotating, are to be made of ceramic materials. If and when the limited production of such an engine becomes a reality -- and this does not seem probable until sometime after 1995 -- it will be possible to produce a solarized version of the engine that can operate at turbine inlet temperatures of at least 1149°C (2100°F) and at a corresponding full-load thermodynamic efficiency of 0.423 or more.

The vital components of a receiver capable of providing 1149°C (2100°F) air to the turbine inlet of this engine also will be made of high-temperature ceramic materials. Prototypic receivers of this type have been constructed and tested; however, the design and construction of these prototypes appear to have resulted in receiver efficiencies considerably lower than analysis indicates are possible. A receiver design efficiency of 0.772 has been estimated by the method described in earlier paragraphs of this section.

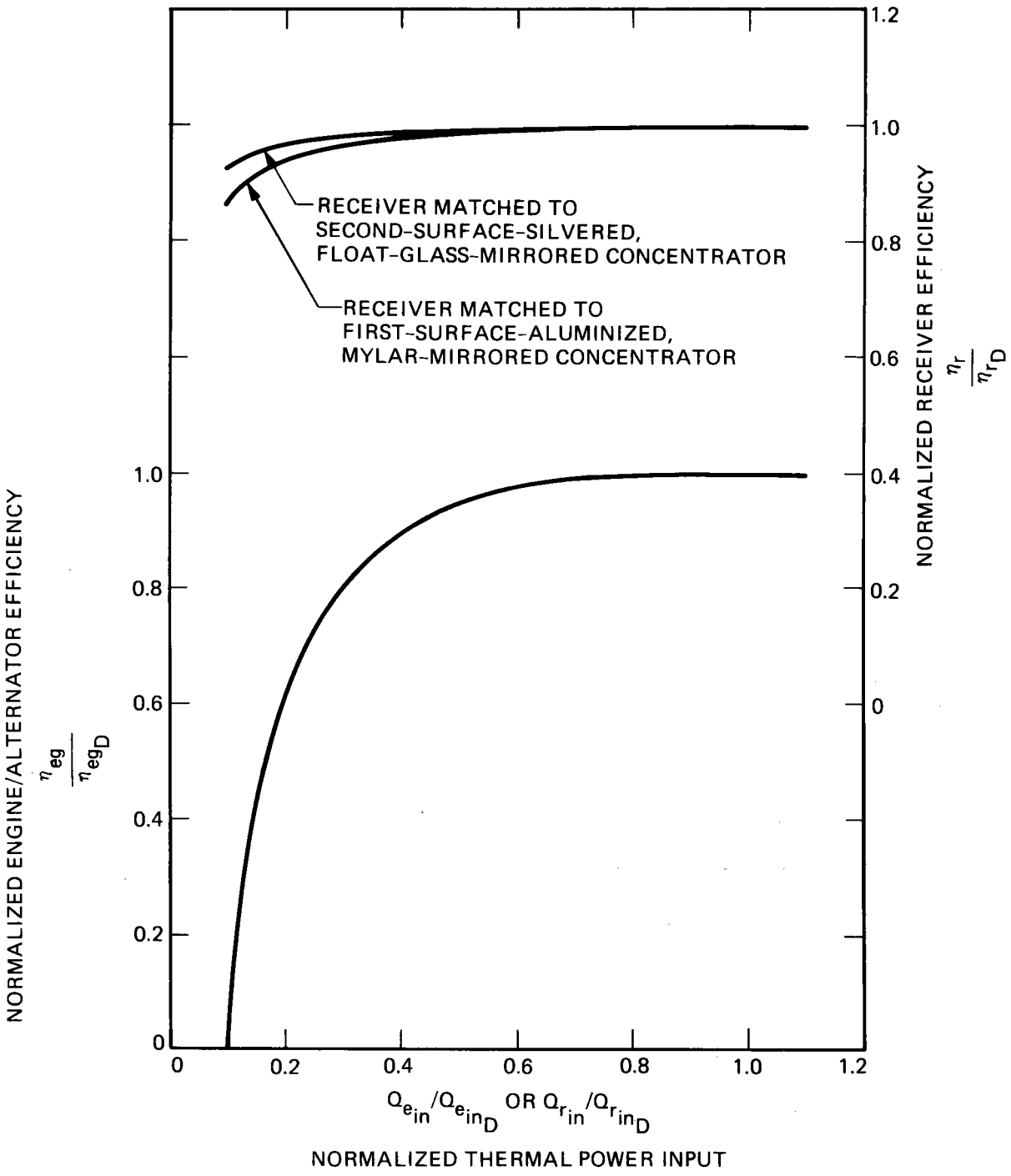

Figure 3-2. Organic-Rankine-Cycle Turbine/Engine/Alternator and Matching Receiver: Normalized Efficiencies of These Subsystems as Functions of the Normalized Thermal Power Input to These Components under Part-Load Conditions

As with the organic-Rankine engine, the optimal Brayton engine turbine rotational speed increases with increasing load and varies from perhaps as low as 50,000 rev/min at idle conditions to as high as 100,000 rev/min at full-load conditions. Unlike the analyses of the Stirling and organic-Rankine engine power conversion subsystems but in keeping with the estimated time for the realization of this Brayton engine, the source temperature of the engine has been varied from about 593°C (1100°F) at idle conditions to 1149°C (2100°F) at full-load conditions to obtain optimal engine efficiency from idle to full-load conditions.

The full-load efficiency of the solarized AGT-101 has been estimated to be 0.423 at a design output power of 40.2 kWshaft. Combined with an estimated generator efficiency of 0.95, a power conversion and transport efficiency of 0.97, and a parasitic loss of 0.02 as defined above, the design power output of the module is 36.3 kWe and the plant efficiency is 0.277.

Two especially interesting points can be made regarding the results obtained in this study of parabolic-dish/Brayton engine solar thermal electric power plant performance. Because receiver efficiency increases as receiver outlet temperature decreases and because optimal turbine inlet temperature (almost equal to receiver outlet temperature) decreases with load, (1) the annual efficiency of the receiver can exceed its design efficiency and (2) the annual efficiency of the plant can approach its design efficiency. For example, from the analysis of the 5-MWe parabolic-dish/Brayton engine solar thermal power plant operating at Albuquerque, New Mexico, the receiver annual efficiency is 0.791 and the plant annual efficiency is 0.258.

The following tabulation presents the design performance parameters of the solarized automotive Brayton-cycle turbine engine and matching receiver employed in this analysis.

Receiver	
Outlet Gas Temperature, °F	2100.0
Input Power, kWt	123.1
Efficiency	0.772
Output Power, kWt	95.1
Engine	
Inlet Gas Temperature, °F	2100.0
Rotational Speed,[a] rev/min	80,000
Input Power, kWt	95.1
Efficiency	0.423
Output Power, kWs[b]	40.2

[a]Under part-load conditions, operating temperature may decrease to as low as 1100°F, and rotational speed may drop to less than 55,000 rev/min.
[b]s denotes rotating shaft power.

Figure 3-3 presents the estimated normalized efficiencies of these subsystems and the normalized receiver outlet temperature as functions of the normalized thermal power inputs to the subsystems under part-load conditions.

5. Determination of Plant Performances and Results. The performance estimates for all four plants at all four locations have been obtained by application of the method outlined in Reference 42. The TI-59 program presented in that report was employed for the purpose.

The results obtained from this study are summarized in Table 3-1 for each location and for each type of 5-MWe plant as well as for a corresponding typical module. Figure 3-4 presents the plant performance data of Table 3-1 in graphical form.

B. INITIAL PRICE OF EQUIPMENT

The initial price of a solar thermal power plant results from the estimated price associated with five different categories of equipment. The five categories are: (1) concentrator or dish, (2) receiver, (3) power conversion, (4) balance-of-plant, and (5) indirects or overheads. The prices associated with each of these five areas are explained in subsequent subsections.

Determining the future selling price of developmental equipment is a difficult and, sometimes, very inaccurate process. Pricing the solar thermal electric power components, subsystems, and systems at JPL have involved in-house activities as well as outside vendors that specialize in cost estimating. Manufacturer estimates were also used along with data developed by other research organizations and industry cost estimating guides. The subsystems whose costs were estimated ranged from conceptual designs to completely fabricated equipment for which actual prices were known.

The following subsections present price as a function of production volume for the subsystems that make up a solar thermal power plant. The curves presented in the various figures were developed from information supplied by a variety of sources, which are cited in each paragraph. High- and low-price bounds for each subsystem are also shown and explained in these paragraphs. The high-and low bound curves are presented to give some idea of the uncertainty surrounding a particular subsystem. Naturally, subsystems that have had more development have more narrow price bounds than those subsystems that are still in earlier stages of development.

1. Parabolic Dish Prices

For the last 6 years, the price for parabolic dish concentrators has been under investigation by JPL's TPS Project. Some prototype dishes have been built, and many more designs have been costed and investigated both by JPL and other organizations. The price of dishes as a function of production volume was developed from the sources shown in Table 3-2. To place all data on a common basis, cost data that were originally presented in other than 1984

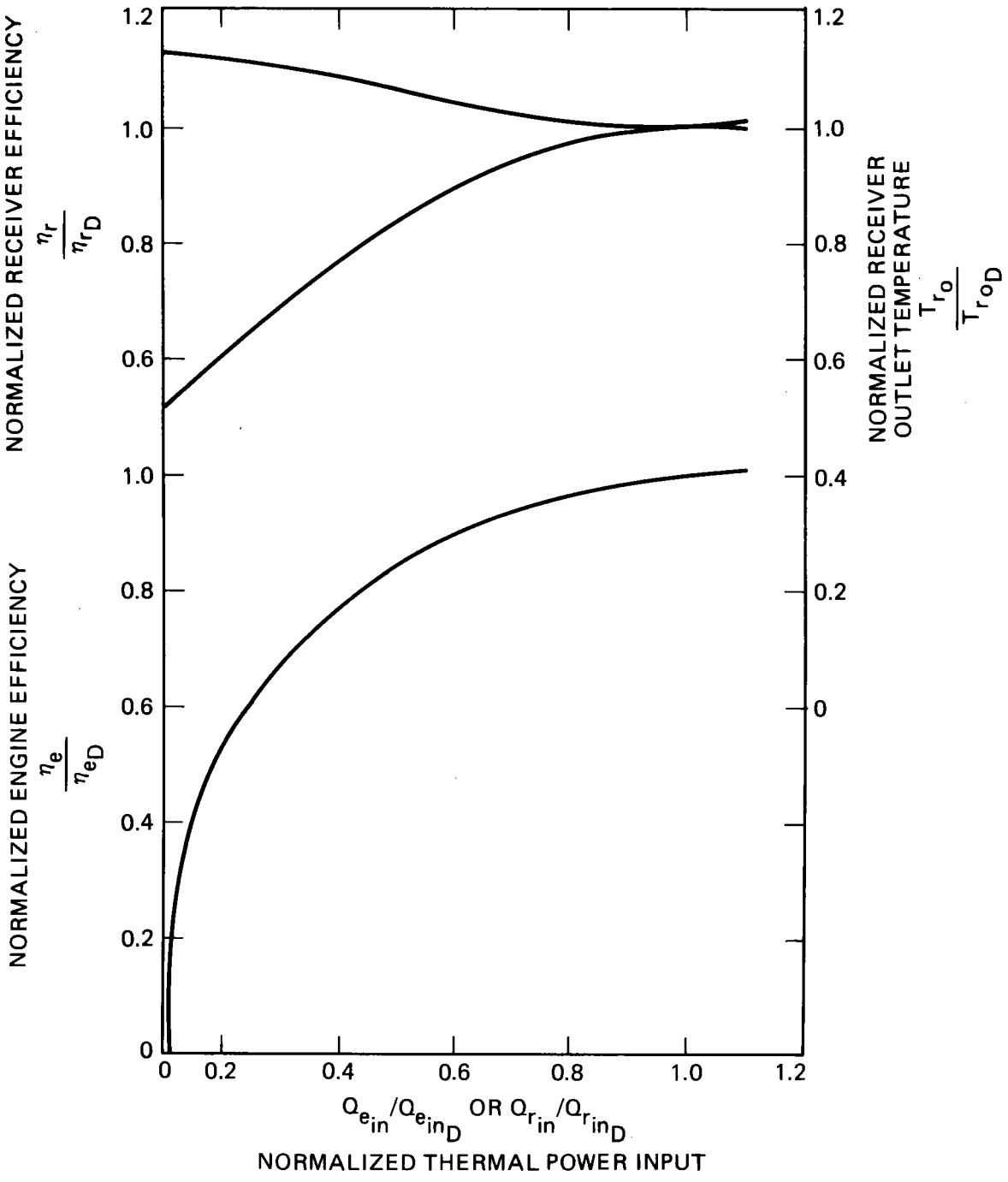

Figure 3-3. Solarized Automotive Brayton-Cycle Turbine Engine and Matching Receiver: Normalized Receiver Outlet Temperature as Functions of the Normalized Thermal Power Inputs to the Subsystems under Part-Load Conditions

Table 3-1. Analysis of Performance of Various Parabolic Dish Modules for Four Geographic Locations

		MODULE												5MW$_e$ SOLAR THERMAL POWER PLANT		
		$\sum I_{DN}$ kW$_t$h/(m^{2}y)	A_C (m^2)	η_{CD}	η_{CA}	η_{RD}	η_{RA}	TH °f	P_{ED}	η_{EGD}	η_{EGA}	P_{SD}	η_{SD}	η_{SA}	Total Concentrator Aperture m^2	Annual Energy Output MWh/y	Annual Energy Output per Unit Concentrator Area kWeh/m^{2}y
PD/S	ABQ	2540	102.0	.940	.880	.881	.834	1330	33.0	.371	.359	30.0	.294	.240	16,995	10,376	610
	FND	1175	102.0	.940	.880	.881	.817	1330	33.0	.371	.351	30.0	.294	.231	16,995	8,912	524
	DGC	1089	102.0	.940	.880	.881	.815	1330	33.0	.371	.351	30.0	.294	.229	16,995	8,150	480
	DFW*	1705	102.0	.940	.880	.881	.815	1330	33.0	.371	.351	30.0	.294	.229	16,995	6,652	391
PD/ORC (Glass)									Eng&Alt.								
	ABQ	2540	105.8	.940	.880	.962	.956	750	25.0	.262	.252	23.3	.221	.198	22,672	11,380	502
	FNO	2275	105.8	.940	.880	.962	.953	750	25.0	.262	.249	23.3	.221	.194	22,672	10,021	442
	DGC	2089	105.8	.940	.880	.962	.953	750	25.0	.262	.248	23.3	.221	.194	22,672	9,173	405
	DFW*	1705	105.8	.940	.880	.962	.953	750	25.0	.262	.248	23.3	.221	.194	22,672	7,486	330
	(Mylar)																
	ABQ	2540	120.4	.850	.792	.936	.925	750	25.0	.262	.252	23.3	.194	.172	25,796	11,257	436
	FNO	2270	120.4	.850	.792	.936	.920	750	25.0	.262	.249	23.3	.194	.169	25,796	9,898	384
	DGC	2089	120.4	.850	.791	.936	.921	750	25.0	.262	.248	23.3	.194	.168	25,796	9,057	351
	DFW*	1705	120.4	.850	.791	.936	.921	750	25.0	.262	.248	23.3	.194	.168	25,796	7,391	287
PD/B	ABQ	2540	131.0	.940	.880	.772	.791	1100 to 2200	40.2	.402	.410	36.3	.277	.258	18,058	11,830	655
	FNO	2270	131.0	.940	.880	.772	.799	"	40.2	.402	.397	36.3	.277	.252	18,058	10,368	574
	DGC	2089	131.0	.940	.880	.772	.799	"	40.2	.402	.397	36.3	.277	.252	18,058	9,522	527
	DFW*	1705	131.0	.940	.880	.772	.799	"	40.2	.402	.397	36.3	.277	.252	18,058	7,770	430

* In the absence of reliable data regarding the direct normal insolation at Fort Worth, TX, and after reviewing the available information, it was decided that the histogram for direct normal insolation pertaining to Dodge City, KS, uniformly reduced by the ratio of the total annual direct normal insolation at Fort Worth divided by that at Dodge City, should provide a reasonably accurate histogram for Fort Worth. This is the reason that η_{RA}, η_{EGA}, and η_{SA} are respectively equal at the two sites.

† The turbine and alternator of the organic-Rankine-cycle power conversion unit are mounted on a common shaft and immersed in a toluene vapor environment; thus, the efficiency of the engine and alternator together is used in this case.

+ Since a viable ceramic Brayton engine is not anticipated before the year 1995, optimal operation of this receiver-engine combination involving reduced turbine inlet temperature at reduced loads has been assumed in this study.

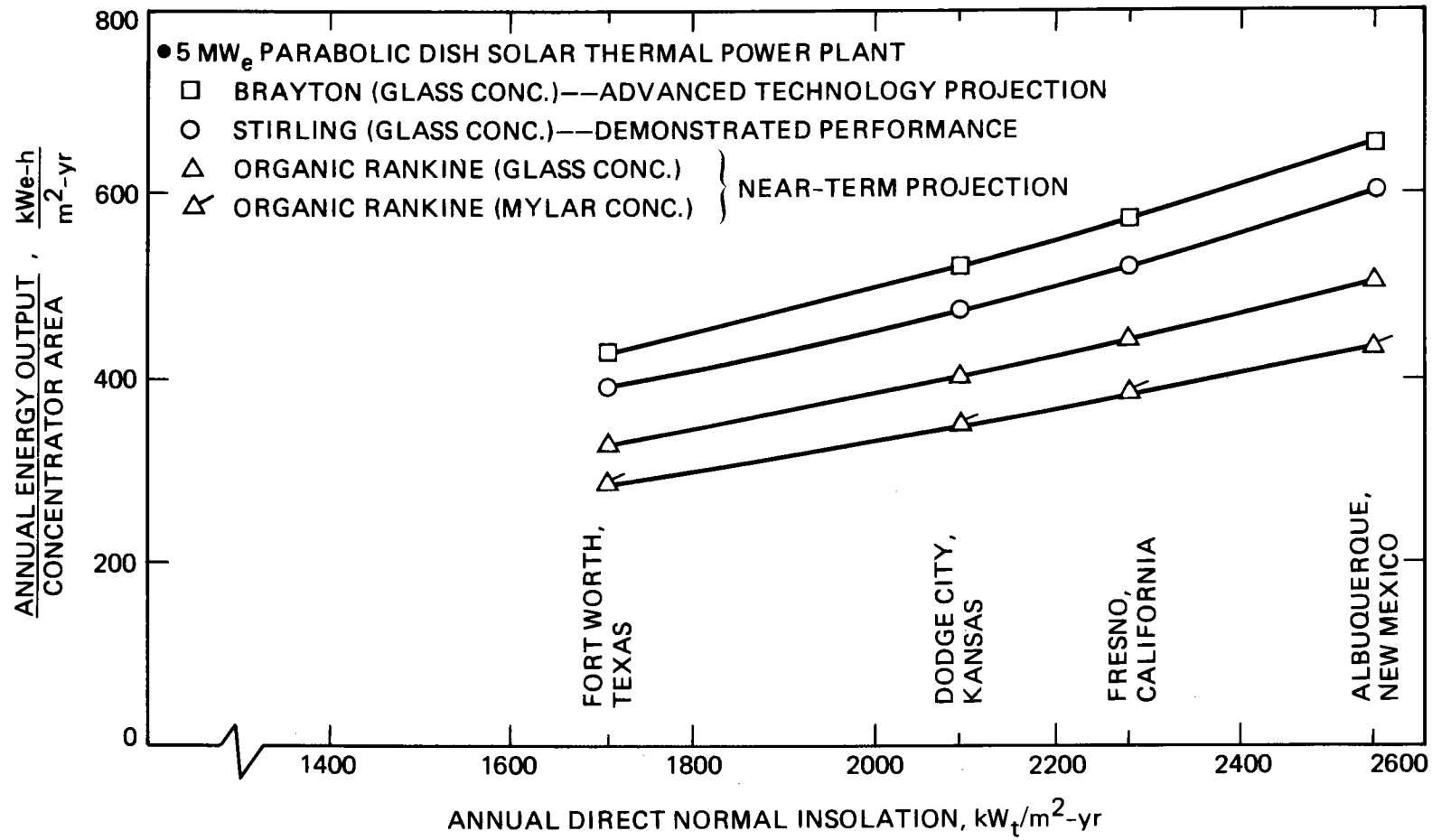

Figure 3-4. Energy Output Characteristics at Selected Sites

Table 3-2. Dish Pricing Data Sources

(1) A quotation from Power Kinetics, Inc. (PKI) to JPL on March 27, 1982, for one first-of-a-kind solar concentrator. Price included installation and start-up of the unit. Also based on a quote for a unit of the same design to Sanders Associates on April 7, 1982.

(2) The cost incurred for 115 dishes fabricated by Solar Kinetics, Inc. (SKI) for the Solar Total Energy Project at Shenandoah, Georgia, per R. Hunke of Sandia National Laboratories, Albuquerque, New Mexico. Also based on a quotation from SKI to Sanders Associates for 100 follow-on concentrators in March 1982.

(3) The cost incurred by Ford Aerospace and Communications Corporation (FACC) at Newport Beach, California, for Parabolic Dish Concentrator No. 1 (PDC-1) built under the JPL TPS Project.

(4) Final price paid by JPL for two TBCs.

(5) Survey of quoted prices for the Solares Program in 1979.

(6) Heliostat cost data from Reference 43.

dollars were escalated by the Marshall and Swift Equipment Cost Index as published monthly by Chemical Engineering Magazine. The cost data were normalized by the concentrator aperture area to provide costs on a $\$/m^2$ basis.

The data in Table 3-2 were plotted; these plots formed the basis for the three curves shown in Figure 3-5. The high-cost curve bounds all actual costs of prototype units that were built and the projected costs of all those units if they were to be mass produced. The most probable price curve reflects estimates of later prototype dish concentrators that were investigated by the JPL TPS Project. The low-bound curve reflects estimates and projections based on less certain information where detailed supporting material is not available. It is believed that this low-bound curve captures the potential low-bound for advanced and innovative future designs to achieve lower costs.

It is noted that the price basis for concentrators in Figure 3-5 and Table 3-2 do not specifically refer to mylar-type concentrators. The published data base for mylar concentrators is limited. These systems have the potential for achieving lower initial prices, but the performance is lower as indicated in Figure 3-4. Also, limited data exists regarding the life and associated maintenance costs of the mylar concentrators. For this reason, glass concentrators will be used in evaluating prices. Based on the significant performance penalties associated with using mylar concentrators, substantial reductions in the combined effect of initial price and maintenance must be achieved in order to be competitive with glass concentrators.

2. Receiver Prices

The cost estimates for receivers were generated by three JPL contractors under contract to develop receivers (References 44, 45, and 46). The estimated prices for receivers as a function of production volume are shown in Figure 3-6. The high-bound curves enclose the highest prices projected for the work referenced above. The most probable curve represents an effort by one of the contractors to actually build working receivers. The low-bound estimate represents JPL's price estimate for a second-generation receiver. This is approximately 30% below the most-probable-price curve.

The level of effort directed toward estimating the cost of receivers was not as intensive as that for concentrators because the initial price of a typical cavity receiver does not represent a substantial cost factor compared to the cost of a typical concentrator.

3. Power Conversion Prices

A significant amount of effort has been expended in attempting to establish the price of a power conversion subsystem for a parabolic dish power plant. The first efforts were reported in Reference 47. These data have been corrected to 1984 dollars by using the same inflation factor as discussed in Section III.B.1.

The price estimate for the organic-Rankine engine was developed from data supplied by Sundstrand, FACC, and Barber-Nichols. JPL reviewed the data and obtained quotations on some components to ensure consistency in the costs developed. The higher price of the organic-Rankine engine results from the heat exchangers and the high-piece count associated with the unit. The heat exchangers operate over a lower temperature difference than do those of other engines. The lower operating temperature results in a larger heat exchanger surface area and a higher resultant price. Figure 3-7 shows the prices of all three engine cycles (Brayton, Stirling, and Rankine) as functions of annual production rate.

The price associated with any alternators to be used with the engines was investigated, and results were reported in Reference 57. These data are used here, updated to 1984 dollars by using the inflation factor specified in Section B.1. above.

4. Balance-of-Plant Prices and Indirect Costs

The balance-of-plant prices and indirect costs were developed at JPL with the help of several organizations, some of which were electric utilities. The results of this cooperative effort are detailed in Reference 48. Because the latter report resulted from the combined efforts of many different organizations, data from it are quoted in this document without change, except to correct to 1984 dollars (see Table 3-3).

Table 3-3. Balance-of-Plant Prices and Indirect Costs on a Per-Module Basis (Based on a 30-kWe Module)

Land and its acquisition, $	683
Surveying, $	466
Grading, $	509
Temporary facilities, $	509
Substations, $	596
Power conditioning, $	444
Controls, $	1973
Cabling, $	683
Miscellaneous, $	715
Architectural and engineering fees, %	10
Construction management and contingencies, %	10
Spare parts, %	5
Shipping costs, %	1.5

Table 3-3 shows the prices associated with balance-of-plant and indirect-cost categories for a single power module. To place all data on a common basis, these prices have been corrected to 1984 dollars by applying the Marshall and Swift Equipment Cost Index as published monthly by Chemical Engineering Magazine.

C. MAINTENANCE COST ESTIMATE ASSOCIATED WITH A SOLAR THERMAL PARABOLIC DISH PLANT

The following sections discuss the development of cost estimates for the maintenance associated with the major subsystems of a solar powered power plant. First, the maintenance costs associated with the dish and receiver are presented; this presentation is followed by a section on the balance-of-power equipment. Each of the three engines that have been investigated by the TPS Project is evaluated in a corresponding section detailing how the maintenance cost associated with each of them was developed. All of the developed operations and maintenance (O&M) costs have high and low bounds associated with them. These upper and lower bounds, along with a discussion as to how the O&M cost varies with production volume of the subsystem, are then presented.

1. Maintenance Cost Associated with the Solar Concentrator

The maintenance cost associated with the dish was determined by dividing the dish cost into three parts and then determining the maintenance cost associated with these parts. Based on previous work at JPL, it was

determined that about one third of the dish cost is associated with its structure, which consists of structural members and requires minimal maintenance. An annual maintenance cost equal to 2% of the initial cost for this portion of the dish was assumed to be adequate to cover maintenance work such as washing and painting.

The remaining cost of the dish was found to be equally divided between the reflective surface and the drive and control mechanisms, which include motors, sensors, and controls. Advanced designs and mass production should reduce the overall production cost of the reflector but probably will not significantly affect the cost of the mechanism. The cost of the mechanism is not much reduced by production volume because many of its components are already in mass production. The current data indicate that the viable life of a glass dish's reflective surface is probably about 15 years. A preliminary study has indicated that because of the higher initial cost yet higher performance of glass reflectors, plastic-film reflectors having a 2-yr useful life are about equally cost effective as glass reflectors having a 15-yr useful life. The 15-yr life of the glass reflector represents an annual maintenance cost of approximately 6.7%/yr.

The last portion of the dish subsystem is composed of the drive and control mechanisms. Current and advanced designs seek to avoid unique or unnecessarily complex mechanical designs because they have proved to be less cost effective and less reliable than the more conventional, simpler designs. The maintenance cost associated with these mechanisms has been based on industry-standard estimates for machines with average complexity and amounts to 6%/yr of their initial cost.

The maintenance costs associated with a solar concentrator are summarized in Table 3-4. As shown in the table, 4.9% has been used to calculate the maintenance costs associated with the dish concentrator for an assumed production volume of 25,000 units/yr.

a. High- and Low-Bound Estimates. Maintenance cost estimates are usually less well known than initial equipment costs and, therefore, have a greater uncertainty range associated with them. Because of our lack of proven data, the relative high- and low-bounds of solar collector cost were assumed to be the same as the uncertainty range previously established in analyzing Stirling engine O&M costs. This range is from one-half to twice the nominal value and leads to a low annual cost of 2.25% of the initial price and a high annual cost of 9% for the solar concentrator.

b. Maintenance Cost as a Function of Production Volume. The effect of production volume affects only the maintenance cost associated with the components of the dish that are unique to solar concentrators. As previously discussed, current cost-effective designs minimize the number of solar-unique components to avoid the adverse effects that such components have on the reliability, availability, and maintainability, as well as the initial cost of the dish. Therefore, in the studies presented, the reflector portion of the maintenance cost has been adjusted in a straightforward manner. A

Table 3-4. Solar Concentrator Maintenance Costs at a Production Volume of 25,000 Units/Year as a Percentage of Initial Price

Item	Initial Cost, %	Maintenance Cost Per Year, %	Maintenance as Fraction of Total Initial Cost, %
Reflector	33	6.7	2.2
Structure	33	2	0.7
Mechanisms	33	6	2.0
Total			4.9

maintenance cost for the reflector based on a fixed percentage of the initial price has been used. Because the initial price is a function of production rate, the maintenance cost will also vary with production rate.

2. Maintenance Cost Associated with Solar Receivers

The solar receiver's maintenance cost is based upon the particular configuration of the receiver. The receiver associated with the Stirling engine is treated as a part of the Stirling engine because it is the heater head of the engine that constitutes the principal cost of the dish/Stirling receiver. The receiver maintenance costs associated with the Brayton and organic-Rankine-cycle engines are based upon industrial data for heat exchangers. Receivers used with both the Brayton and the organic-Rankine-cycle engines operate at moderate to high temperatures and pressures; therefore, an annual maintenance cost of 8% of the initial price of these receivers has been used in estimating their O&M costs.

a. High- and Low-Bound Estimates. The high- and the low-bound estimates associated with the solar receiver were developed in the same manner as those for the dish. This results in a high-bound maintenance cost of 16%/yr and a low-bound cost of 4%/yr of the initial receiver cost.

b. Maintenance Cost as a Function of Production Volume. The maintenance cost of the receiver as a function of production rate has been calculated in a straightforward manner. A maintenance cost based on a fixed percent of the initial price has been used as the annual maintenance cost of the receiver. Thus, as the assumed production rate is increased, the cost of maintenance falls with the decreasing cost of each receiver.

3. Maintenance Cost Associated with the Balance-of-Plant Equipment

The maintenance costs associated with the balance-of-plant were developed in a fashion similar to that employed in estimating the receiver and dish maintenance costs described above. The balance-of-plant is divided into its constituent parts, and then the maintenance cost associated with each part is evaluated. Data gathered from several industrial cost-estimating books led to the assumption of the following maintenance cost estimates:

(1) General facilities, simple or undemanding operating conditions: 1.5 to 3%.

(2) Moderately complex or average operating conditions: 4 to 7%.

(3) Highly complex or severe high-temperature or high-pressure operating conditions: 8 to 10% and higher.

Using the above guidelines, Table 3-5 summarizes the maintenance cost factors assumed for various balance-of-plant items.

a. High- and Low-Bound Estimates. Similar to the receiver and dish upper and lower bounds, the balance-of-plant upper and lower bounds will be:

$159/module/yr (-50%) and $636/module/yr (+100%)

b. Maintenance Cost as a Function of Production Volume. The balance-of-plant equipment consists of components and subsystems that are already in existence and in production. The maintenance associated with this category of equipment should fall within the upper and lower bounds described above, but should not be affected by the production rate of solar thermal plants. Therefore, no variation of the maintenance cost as a function of production volume is assumed.

4. Organic-Rankine-Cycle Engine Maintenance Cost Estimate

The working fluid used in the Organic-Rankine-cycle engine degrades over a period of time. The rate of this degradation is dependent upon a variety of factors such as temperature, incompatible containment materials, the presence of oxygen, and impurities that are either in the fluid at the beginning of operation or the result of fluid breakdown.

Once each year the engine's fluid will be checked and analyzed to determine if the fluid is breaking down. During this inspection, the noncondensible gases that have built up in the system will be removed. This type of maintenance will help delay any overhaul until about 15,000 h of operating time has been accumulated on the engine.

The costs associated with this annual inspection are based on cost estimation procedures as exemplified in Table 3-6 for the organic Rankine.

Table 3-5. Maintenance Cost Factors for Balance-of-Plant Items Per Module

Item	Initial Price, $	Maintenance, %	Maintenance, $/yr
Land	683	0	0
Surveying	466	0	0
Grading	509	0	0
Temporary facilities	509	0	0
Substation	596	6	36
Power conditioning	444	8	36
Controls	1973	10	197
Cabling	683	3	20
Miscellaneous	715	4	29
Total	6578		318

Table 3-6. Inspection Calculations for Organic-Rankine Engines

Move equipment to dish, min	15
Setup, min	15
Hook up equipment, min	10
Pull vacuum, min	15
Check out and test system, min	15
Break down setup, min	15
Total Time, h	1.42
Field efficiency, %	75
Personnel (1 foreman/6 workers), workforce	2.33
Burdened labor rate, $/h	36.5
Burdened equipment rate, $/h	25.0
Total Cost, $/engine/yr	208

It is expected that the heat exchangers and fans of the engine will be durable enough to last for 15,000 h of operation without any maintenance. This assumption is based upon the durability of large heat exchangers used on utility-type steam Rankine engines. The assumed overhaul procedure involves exchanging ("swapping out") the engine at the module and then performing the overhaul in a maintenance facility. The overhaul would consist mainly of replacing the heat exchanger and waste-heat cooling fan. The costs associated with this are shown in Table 3-7.

At 30,000 h, a major overhaul will be performed on the engine. This is consistent with current utility practice in the case of large steam turbine generator sets. It is assumed that, given sufficient development, these small engines will be able to achieve the durability of the larger engines.

The costs associated with a major overhaul are composed of the costs associated with the minor overhaul plus the costs associated with replacing the regenerator, pumps, and valves (Table 3-8).

The calculation of the equivalent annual maintenance expense for the engine is shown in Table 3-9. Note that minor or major overhauls are performed. Much is known about the maintenance associated with large-utility steam turbines and, as a check, the cost developed in Table 3-9 was compared to those estimates developed by General Electric for large steam turbine plants. The General Electric-estimated costs are $13.7 to 16/kW/yr and $2/MW/operating hour. Correcting for inflation, the corresponding estimated maintenance cost is $667 to 741/year/engine. This cost estimate is lower than the detailed cost estimate developed in preceding paragraphs. However, one should remember that the engines under consideration here are mounted on solar concentrators, that they have all of the components and subsystems of the larger engines, and that it takes 2000 of these small engines to equal one 40-MWe steam turbine, a moderate size by utility standards. The additional complexity of an organic working fluid and a hermetic seal also add to the increased $/kW cost of the engine.

a. High- and Low-Bound Estimates. The low bound for the organic Rankine-cycle engine is set at the lower cost determined for large utility steam turbines, i.e., $667/engine/yr. This is believed to be the lowest maintenance cost that can be anticipated for a Rankine engine because many years and much effort have been invested in reducing the O&M costs of utility steam turbines to this level.

The high-bound cost is based on the established fact that O&M estimates for new machinery can vary as much as a factor of two. Thus, a high-bound cost estimate for organic-Rankine-cycle O&M of $2418/yr/engine has been specified here.

Table 3-7. Cost of Engine Exchange and Minor Overhaul for Organic Rankine Cycle (Based on a Production Rate of 25,000 Units/Year)

Exchange of the engine (Labor), $	367.00
Overhaul:[a]	
Handling, min	15
Fixturing, min	15
Drain and strip, min	05
Remove heat exchanger and fan, min	20
Inspect and clean engine, min	20
Install new heat exchanger, min	30
Seal and test, min	30
Install fan, min	10
Purge system, min	10
Fill and test, min	10
Pull vacuum, min	20
Check out auxiliaries, min	10
Test engine, min	30
Paperwork, min	15
Total Time, h	4
Factory efficiency, %	85
Personnel, workforce	2.33
Burdened labor rate, $/h	36.5
Labor cost for overhaul, $	400
Total Labor Cost, $	767
Fan, $	200
Heat exchanger, $	3029
Total Parts Cost, $	3229

[a]This cost is incurred every other 15,000-h period because a major overhaul occurs at 30,000-h increments.

Table 3-8. Costs Associated with Major Overhaul for Organic Rankine-Cycle

Items not included in minor overhaul:	
Remove regenerator, min	15
Remove pumps, min	10
Remove valves, min	10
Remove seals, min	10
Install regenerator, min	30
Install valve, min	20
Install feed pump, min	15
Install sump pump, min	15
Install seals, min	15
Total, min	95
Factory efficiency, %	85
Personnel, workforce	2.33
Burdened rate, $/h	36.5
Labor cost, $	233
Parts cost, $	1204
Items included in minor overhaul (See Table 3-7):	
Labor cost, $	767
Parts cost, $	3229
Total Labor Cost, $ (233 + 767)	1000
Total Parts Cost, $ (1204 + 3229)	4433

b. Maintenance Cost as a Function of Production Volume. To analyze the cost effectiveness of the organic-Rankine- cycle engine at different production rates, it was necessary to determine the maintenance cost at different production rates. This was accomplished by assuming that only the parts-cost portion of the overall maintenance cost was effected by the production volume. The cost-versus-production-rate curve for the organic-Rankine-cycle engine was used to obtain the multiplying factor by which the parts costs were adjusted. The results of this effort are shown in Table 3-10.

Table 3-9. Cash Flow Per Engine Associated with ORC Maintenance Costs for the Organic-Rankine-Cycle Engine at a Production Rate of 25,000 Units/Year

Year	Hours	Annual Maintenance, $	Minor Parts, $	Overhaul Labor, $	Major Parts, $	Overhaul Labor, $
1	3500	208	0	0	0	0
2	7000	208	0	0	0	0
3	10500	208	0	0	0	0
4	14000	208	0	0	0	0
5	17500	0	3229	767	0	0
6	21000	208	0	0	0	0
7	24500	208	0	0	0	0
8	28000	208	0	0	0	0
9	31500	0	0	0	4433	1000
Total		1456	3229	767	4433	1000

(1456 + 3229 + 767 + 4433 + 1000)/31500 x 3500 = 1209/engine/yr

Table 3-10. Organic-Rankine-Cycle Maintenance Cost as a Function of Production Volume

Production Quantity	Maintenance Parts Cost, $/Engine/yr	Maintenance Labor Cost, $/Engine/yr	Total Cost, $/Engine/yr
1,000	2419	358	2777
3,000	1664	358	2022
10,000	1102	358	1460
25,000	851	358	1209
100,000	696	358	1054

5. Gas Turbine (Brayton) Maintenance Cost Estimate

The gas turbine engines that are being considered for use in solar thermal power plants use air-foil bearings and have no combustors. In conventional fossil-fueled gas turbine engines, conventional bearings and combustors are the major sources of maintenance costs. The maintenance costs developed here for solarized gas-turbine engines reflect these differences. The annual maintenance associated with this engine will involve an annual inspection of the unit and replacement of one spin-on air filter that is associated with the air-foil bearing subsystem. The costs associated with this maintenance are shown in Table 3-11.

The minor overhaul for the Brayton engine is similar to that associated with the organic-Rankine-cycle engine. The waste heat exchanger and fan will be replaced after 15,000 h of operation. Three major differences exist between maintenance costs associated with the Brayton engine as compared with the organic-Rankine-cycle engine: (1) the turbine is not hermetically sealed, (2) the waste heat exchanger is much smaller and can be handled manually, and (3) the waste heat exchanger is less costly than the condenser on the organic Rankine-cycle. Table 3-12 assumes that the waste heat exchanger and fan are replaced without having to remove the engine.

The major overhaul (Table 3-13) of the gas turbine will involve removing the engine (actually exchanging engines at the module), replacing the regenerator, general inspection and cleaning, and replacing the parts that would have been replaced in a minor overhaul (Table 3-13). The total annual cost (Table 3-14) for maintaining the gas turbine is determined on a cash flow basis. The solarized gas turbine engine maintenance cost is $397/engine/yr.

Table 3-11. Brayton Annual Inspection Costs

Move equipment to dish, min	15
Setup, min	15
Replace filter and inspect, min	5
Break down setup, min	15
Total, min	50
Field efficiency, %	75
Personnel, workforce	2.33
Burdened labor rate, $/h	36.5
Burdened equipment rate, $/engine/yr	25
Total Cost, $/engine/yr	122

Table 3-12. Minor Overhaul Costs for the Brayton[a]

Move equipment to dish, min	15
Setup, min	15
Remove old parts, min	30
Install new parts, min	30
Check out auxiliaries, min	10
Check out engine, min	30
Paperwork, min	15
Break down the setup, min	15
Total Time, h	2.66
Field efficiency, %	75
Personnel, workforce	2.33
Burdened labor rate, $/h	36.5
Burdened equipment rate, $/h	25.0
Labor cost, $	390
Parts cost, $	350

[a] Because a major overhaul occurs at every 30,000-h interval, the above minor overhaul occurs every other 15,000-h interval.

The General Electric study cited before in the organic-Rankine cycle portion of this study also contained maintenance data on gas turbines. The fixed portion of the O&M was $1/kW/yr and the variable portion was $2/MW/operating hours/year. These data were corrected for inflation by using the Marshall and Swift Equipment Cost Index (1.61 multiplier), which resulted in an annual cost of $258/engine/yr. The developed O&M cost of the gas turbine is 54% higher than that which would be calculated using the General Electric data; however, one must remember that the gas turbine used in the solar-powered system is extremely small compared to a utility-size gas turbine and that reduced size has the effect of driving up the $/kWe maintenance cost. Conversely, the solarized gas turbine does not employ the two most maintenance-intensive subsystems the General Electric turbine, the lubrication subsystem and the fuel supply/combustor subsystem. The O&M cost estimates developed above, therefore, are considered to be reasonably accurate.

a. High- and Low-Bound Estimates. As in the case of the organic-Rankine-cycle engine, the lowest possible annual maintenance cost that could be achieved by the solarized Brayton engine is judged to be that associated with the large General Electric industrial gas turbines, i.e., $258/engine/yr.

Table 3-13. Major Overhaul Costs for Brayton

Exchange of engines (labor), $	367
Handling, min	15
Fixturing, min	15
Remove heat exchanger and fan, min	30
Remove regenerator, min	45
Install new regenerator, min	45
Install new heat exchanger and fan, min	30
Checkout auxiliaries, min	10
Checkout engine, min	30
Paperwork, min	15
Total Time, h	3.9
Factory efficiency, %	85
Personnel, workforce	2.33
Burdened labor rate, $/h	36.5
Labor cost, $	390
Total Labor Cost, $	757
Fan and heat exchanger, $	350
Regenerator,$	875
Total Parts Cost, $	1225

The high-bound estimate is also based upon the same factor of two that was employed in the organic-Rankine cycle estimate. This factor yields a high-bound cost of $794/engine/yr.

b. Maintenance Cost as a Function of Production Volume. Using the same method explained in the organic-Rankine cycle section of this report, maintenance cost was estimated as a function of production volume for the Brayton engine. The results of this effort are shown in Table 3-15.

Table 3-14. Cash Flow Per Engine Associated with Brayton Maintenance Costs

Year	Hours	Annual Maintenance, $	Minor Overhaul Parts, $	Minor Overhaul Labor, $	Major Overhaul Parts, $	Major Overhaul Labor, $
1	3500	122	0	0	0	0
2	7000	122	0	0	0	0
3	10500	122	0	0	0	0
4	14000	122	0	0	0	0
5	17500	0	350	390	0	0
6	21000	122	0	0	0	0
7	24500	122	0	0	0	0
8	28000	122	0	0	0	0
9	31500	0	0	0	757	1225
Totals		854	350	390	757	1225

(854 + 350 + 390 + 757 + 1225)/31500 x 3500 = 397/engine/yr

Table 3-15. Brayton Maintenance Cost Per Engine as a Function of Production Volume

Production Quantity per Year	Maintenance Parts Cost per Year, $	Maintenance Labor Cost per Year, $	Total Cost per Year, $
1,000	300	274	574
3,000	230	274	504
10,000	161	274	435
25,000	123	274	397
100,000	92	274	366

6. Stirling Engine Maintenance Cost Estimate

The Stirling engine's maintenance cost estimate has been a subject of intense discussion. A review board was established at JPL to review the data that were available and to determine O&M cost estimates that could be justified from an assessment of the data. The result of this review is summarized below. The procedures, the dollars-per-hour cost for personnel, crew size, and equipment costs, used in this analysis have been estimated on the same basis as that employed in determining the same items for the gas turbine and organic-Rankine engines.

The cost estimates shown below are baseline high- and low-bounds as determined by the review committee.

a. Cost to Exchange Engines. When the Stirling engine is opened to the environment, the repair will be done in a shop because the engine contains precision parts fitted to close tolerances, high-pressure hydrogen, and an oil pan that must be removed to gain access to some of the parts. This type of work cannot be done in dirty and inefficient field conditions. The most cost-effective method of performing this work is to exchange engines at the module and perform the disassembly, repair, and reassembly in a shop environment. The cost of exchanging engines, regardless of the type of engine, is shown in Table 3-16.

b. Ring and Seal Replacement. The JPL review committee reviewed all the data regarding replacement of the rings and seals (Table 3-17) and determined that "the engine operating period before a failure forces shutdown for servicing is projected to be 1000-h mean time between failures (MTBF)." The cost for this replacement is shown in Table 3-17.

c. Engine Overhaul. The goal of the Stirling automotive engine program is to achieve a lifetime of 3500 h for the engine. The solar application of the engine is at a higher average power loading than the automotive application and operates over longer periods of time. The automotive application will entail a greater number of start/stop cycles. It has been assumed that the Stirling engine used here will need a major overhaul only at 4000 h. This overhaul will involve the replacing of the heater head in the receiver and the replacing of the regenerator cores in the engine, along with repair or replacement of items such as bearings, hoses, hydrogen compressor, and gaskets. The cost associated with this overhaul is shown in Table 3-18.

d. Engine Replacement. Like all engines, the Stirling engine cannot be repeatedly disassembled, repaired, and reassembled and never need replacement. The review committee determined that the lifetime of a mature Stirling solar engine might be 8000 h. By this time, the engine has gone through six ring and seal change outs and one major rebuild. This is a factor of 2.3 times the design life of the automotive engine without taking into account the fact that the average operating power of the solar application is higher than that of the automotive application (approximately 75% higher).

Table 3-16. Cost of Exchanging a Stirling Engine[a]

Move equipment to dish, min	15
Set up equipment, min	15
Remove assembly, min	30
Install new assembly, min	30
Check out assembly, min	30
Breakdown and clean up, min	15
Total Time, h	2.5
Personnel (1 foreman/6 workers), workforce	2.33
Field efficiency, %	75
Burdened labor rate, $/h	36.5
Combined equipment rate, $/h	25
Total Cost to Exchange Engine Assemblies, $	367

[a] The above estimate assumes that the dish can be positioned so as to lower the engine to a location allowing removal without the need for a specialized vehicle.

Based on input from one research firm, the expected selling price of the Stirling engine package is $5050 at a production rate of 25,000 engines/year. To this, the installation cost of $367 (see exchange of engines as described above) must be added to arrive at the total installed cost of $5417.

e. Cash Flow. The cash flow associated with the above detailed maintenance costs is presented in Table 3-19, along with the prorated costs for 1 year of operation in a solar plant (3500 h/yr).

f. High- and Low-Bound Estimates. The JPL review board also investigated the effects of not achieving or exceeding the 1000-h MTBF used in the above analysis. The high-bound cost is based upon a 350-h MTBF for replacement of rings and seals whereas the lower cost assumes that: (1) the regenerator and heater head lasts 8000 h, (2) the cost of the hydrogen seals and piston rings is $26/engine, (3) an engine exchange cost is $168, and (4) there are no major engine overhauls.

Table 3-17. Cost to Replace Rings and Seals for Stirling Engine

Exchange engine at the module (labor), $	367
Handling, min	15
Fixturing, min	15
Drain and strip, min	05
Remove seals and rings, min	10
Install new parts, min	10
Fill and pressure check, min	05
Check out engine (operate), min	30
Paperwork, min	15
Total time, h	1.7
Factory efficiency, %	85
Personnel, workforce	2.33
Burdened labor rate, $/h	36.5
Total labor cost, $	537
Four sets of rings, $	80
Four high-pressure hydrogen seals, $	200
Oil, $	5
Hydrogen, $	5
Gaskets + misc. parts, $	30
Total parts cost, $	320

The effects of these two sets of assumptions result in a low-bound cost of $3500/engine/yr and a high-bound cost of $12,000/engine/yr. Both the low- and high-bound costs were rounded off to the nearest $500.

g. Maintenance Cost as a Function of Production Volume. The variation of the maintenance cost with production volume for the Stirling engine was calculated in the same manner as for the other two engines. The result of this effort is shown in Table 3-20.

Table 3-18. Cost of Stirling Engine Overhaul

Cost to change out rings and seals (see Table 3-17):	
Labor, $	537
Parts, $	320
Additional time required to overhaul engine and auxiliaries, h	4
Factory efficiency, %	85
Personnel, workforce	2.33
Burdened labor rate, $/h	36.5
Labor cost, $	400
Total labor cost, $	937
Heater head cost, $	2004
Regenerator core cost, $	200
Total parts cost, $	2524

7. Summary of Maintenance Costs

Figures 3-8 through 3-10 depict the maintenance costs for each component. Graphs comparing initial price and maintenance costs for the three complete systems using the three different engines are shown and discussed in III.D below.

D. TOTAL PLANT COSTS

The total plant costs were developed using the previously presented cost data of Section 111.B, the maintenance data presented in Section III.C, and the physical plant descriptions presented in Section III.A and summarized in Table 3-21.

The cost of each plant was determined at annual production rates of 100, 1K, 10K, 25K, 50K, and 100K units per year, both for the initial price of a 5-MWe plant and also for the annual maintenance associated with each plant. The cost associated with each subsystem (dish, receiver, engine) was calculated and then combined with the balance-of-plant cost associated with

Table 3-19. Cash Flow Per Engine Associated with Stirling Maintenance Costs at a Production Rate of 25,000 Engines/Year

	Rings and Seals		Overhaul		Engine Replacement	
Hours of Operation	Parts, $	Labor, $	Parts, $	Labor, $	Parts, $	Labor, $
1000	320	537	0	0	0	0
2000	320	537	0	0	0	0
3000	320	537	0	0	0	0
4000	0	0	2524	937	0	0
5000	320	537	0	0	0	0
6000	320	537	0	0	0	0
7000	320	537	0	0	0	0
8000	0	0	0	0	5054	367
Total	1920	3222	2524	937	5054	367

(1920 + 3222 + 2524 + 937 + 5054 + 367)/8000 x 3500 = 6135/engine/yr

Table 3-20. Stirling Maintenance Cost as a Function of Production Volume

Production Quantity per Year	Maintenance Parts Cost per Year, $	Maintenance Labor Cost per Year, $	Total Cost per Year, $
1,000	12922	1980	14902
3,000	9465	1980	11445
10,000	6156	1980	8136
25,000	4155	1980	6135
100,000	2202	1980	4182

Table 3-21. Summary of 5-MWe Plant Characteristics

System	Dish Size, m^2	No. of Modules
Organic Rankine	105.8	214
Stirling	102	167
Brayton	131	138

the number of modules that made up the plant. This direct equipment cost was then multiplied by the factor for indirect costs to arrive at the final cost of the overall plant.

Finally, the overall plant cost for each system at each production rate was then divided by the nominal plant rating of 5 MWe (5000 kWe) to yield the $/kWe cost that has been plotted in Figure 3-11.

The maintenance costs, associated with the curves in Figure 3-11, were developed in a similar manner. First, the maintenance cost associated with a particular module at a particular production rate (cost) was calculated. The corresponding maintenance cost associated with the dish, receiver, engine, and balance-of-plant cost was calculated and then added to obtain the overall plant maintenance cost. The overall plant maintenance cost, on a $/yr basis for a plant size of 5 MWe, is given in Figure 3-12.

Caution is necessary before using the above costs in any market analysis. The data presented do not reflect the cumulative units sold but, rather, the annual expected cost assuming the market to be infinite and that a particular production rate would be maintained for 5 yr. Table 3-22 shows one scenario by which a production rate of 25,000 modules/yr could be achieved and the corresponding cumulative total that is associated with this production rate.

As one can see from Table 3-22, the total cumulative installed power associated with a 25,000-unit/yr production rate can be quite substantial. The above scenario, and all of the costing presented up to this point assumes that, in order to be able to afford the cost-cutting production machinery corresponding to the 25,000-unit/yr analysis, the above production occurs in one massive plant. The plant needed for this production rate would be about the same size and about as complex as a new automobile production plant.

The data developed do not include competition. Markets that can sustain 25,000 units/yr will attract several companies to the market place and, therefore, the unit-per-year production rate in any one plant will be lower or the market will have to be substantially greater than that projected in Table 3-22.

Table 3-22. Annual Production Rate versus Cumulative Units Produced (Assuming 29 kW/module)

Year	Annual Production Rate	Cumulative Total Produced	Total Power in MWe
1982	1	1	0.029
1983	3	4	0.116
1984	7	22	0.319
1985	14	25	0.725
1986	28	53	1.537
1987	56	109	3.161
1988	112	221	6.4
1989	250	471	13.6
1990	500	971	28.1
1991	1,000	1,971	57.1
1992	5,000	6,971	202.1
1993	10,000	16,971	492.1
1994	15,000	31,971	927.1
1995	20,000	51,971	1,507.1
1996	25,000	76,971	2,232
1997	25,000	101,971	2,957
1998	25,000	126,971	3,682
1999	25,000	151,971	4,407
2000	25,000	176,971	5,132

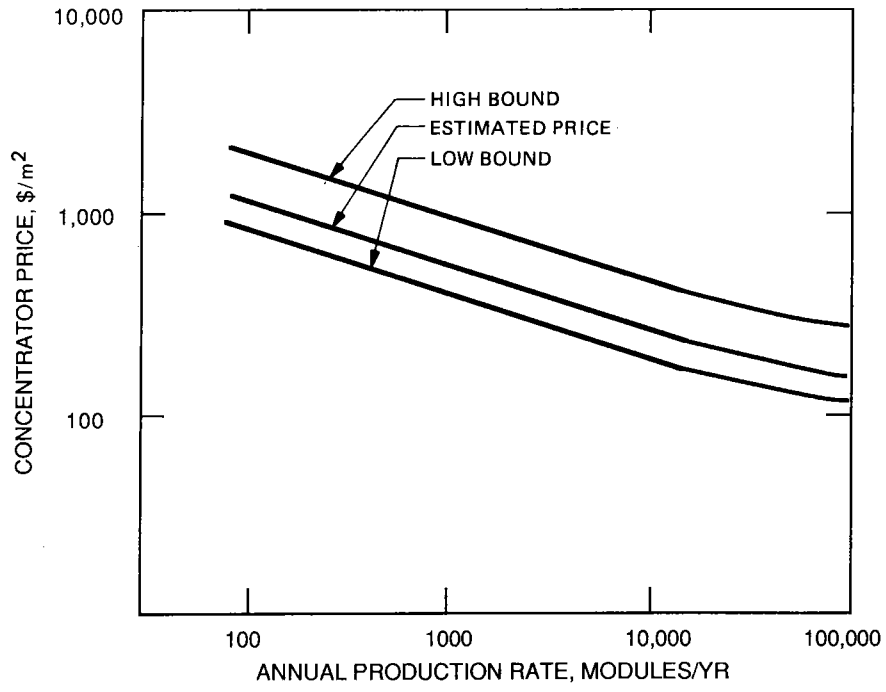

Figure 3-5. Parabolic Dish Concentrator Price as a Function of Production Volume (1984 Dollars)

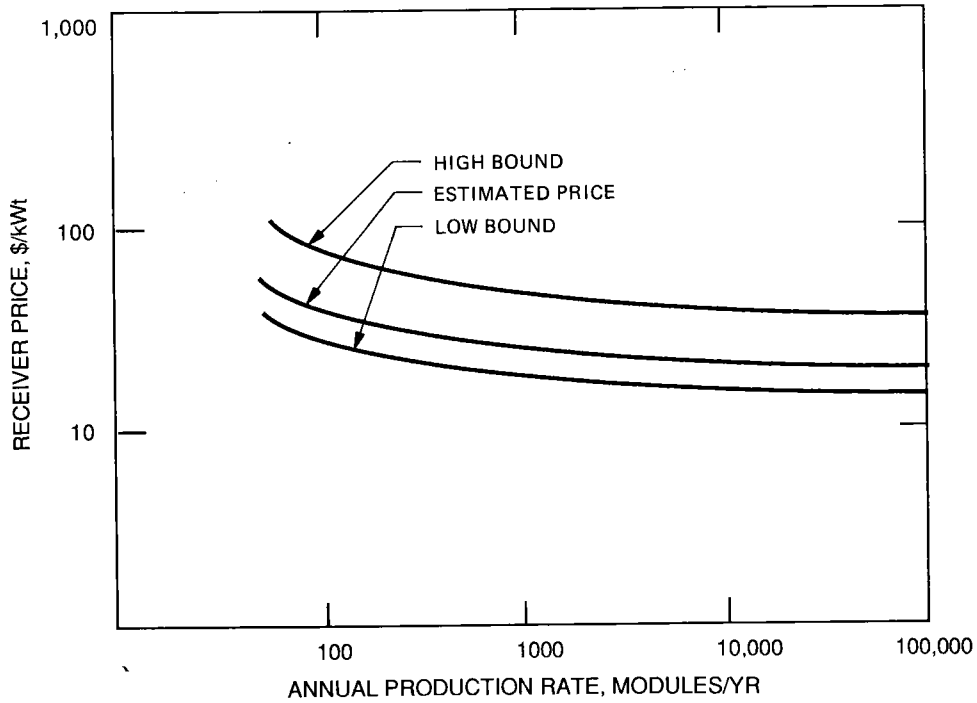

Figure 3-6. Receiver Price as a Function of Production Volume (1984 Dollars)

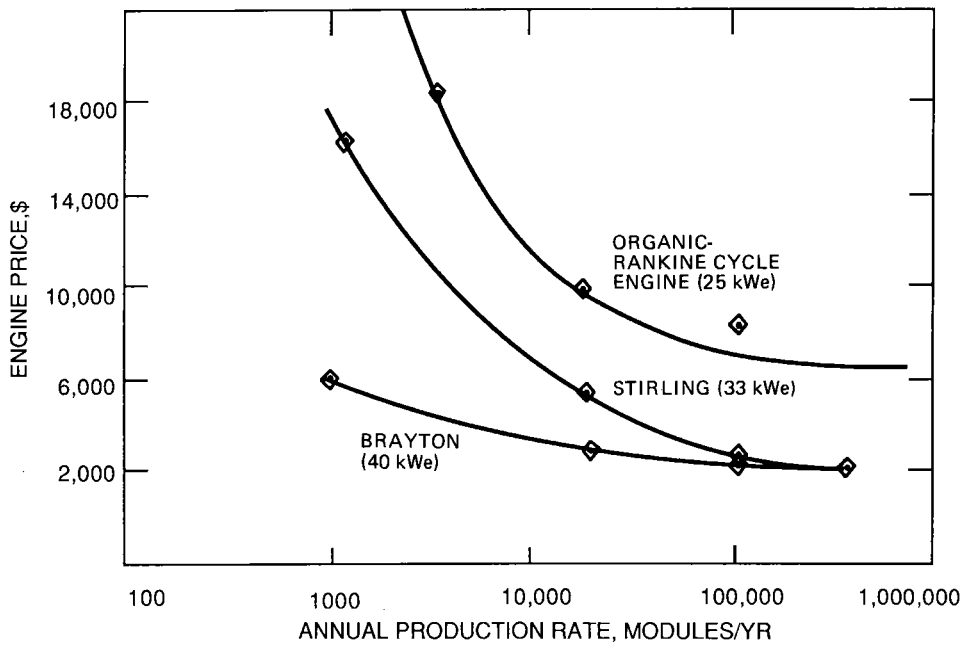

Figure 3-7. Price of Engines as a Function of Annual Production Rate (1984 Dollars)

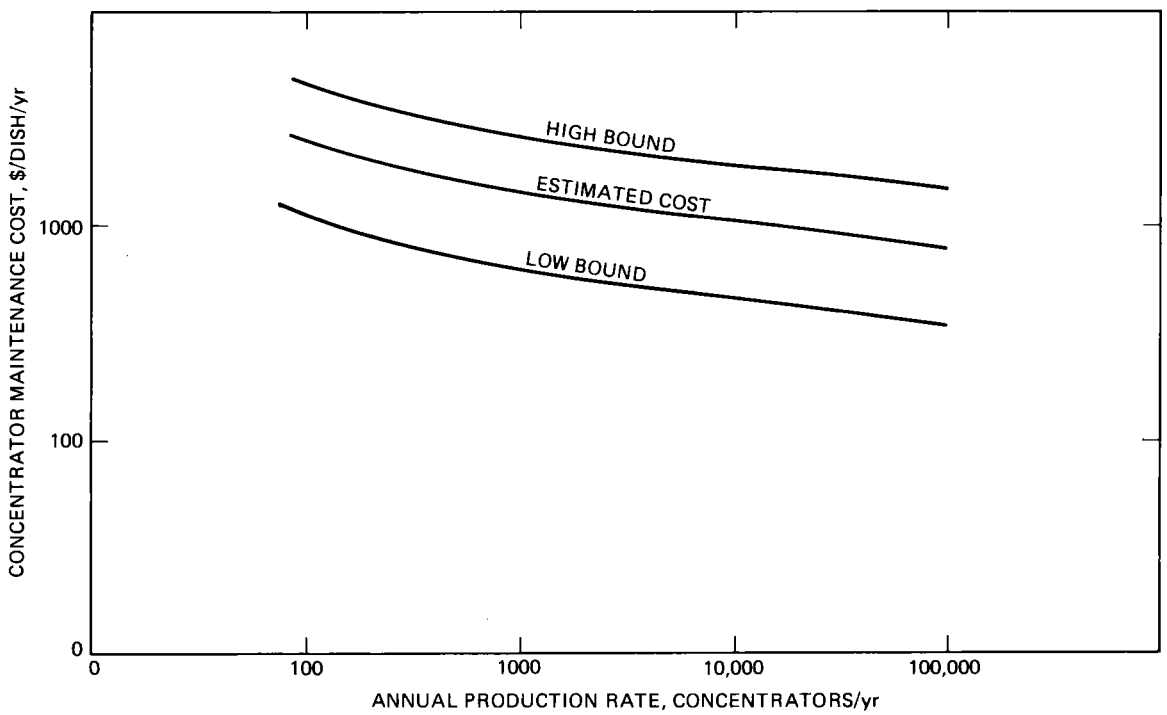

Figure 3-8. Maintenance Cost for Parabolic Dish Concentrators

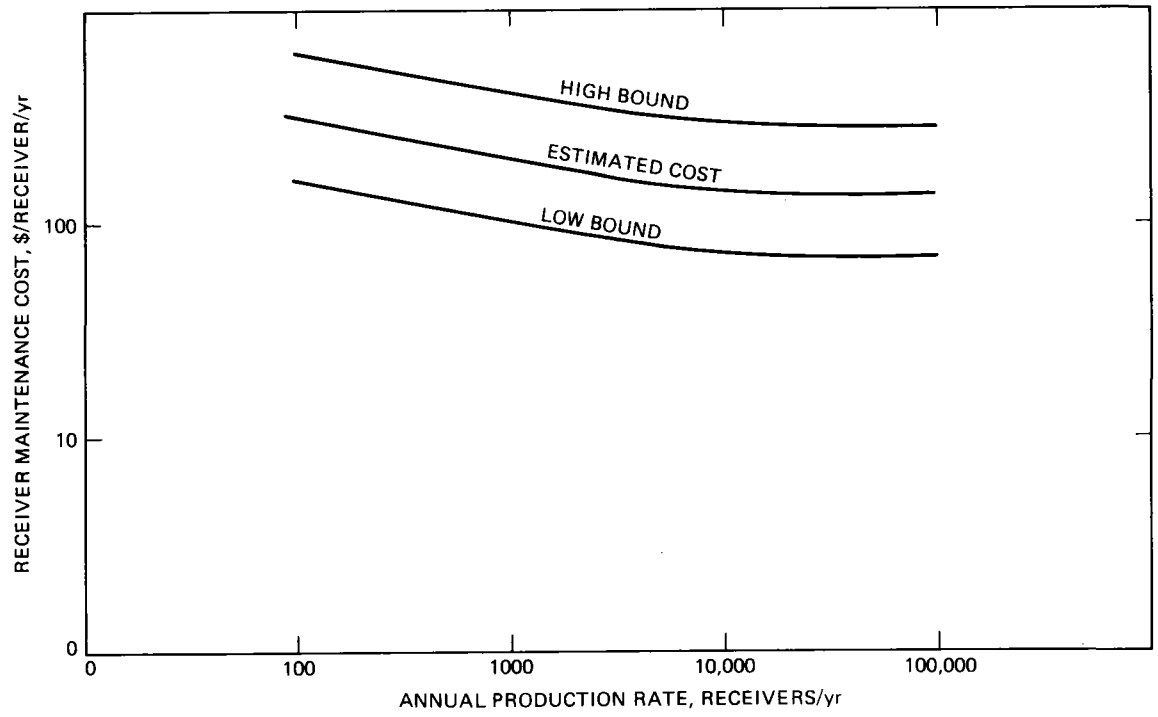

Figure 3-9. Maintenance Costs for Solar Thermal Receivers

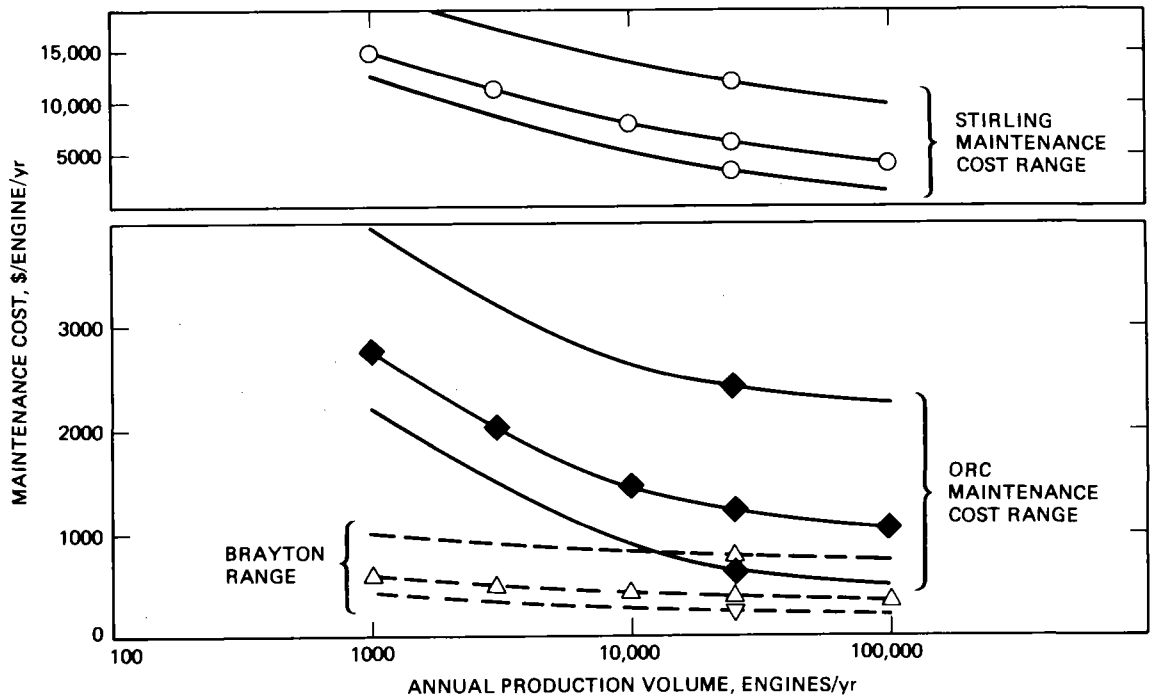

Figure 3-10. Maintenance Costs for Three Heat Engines

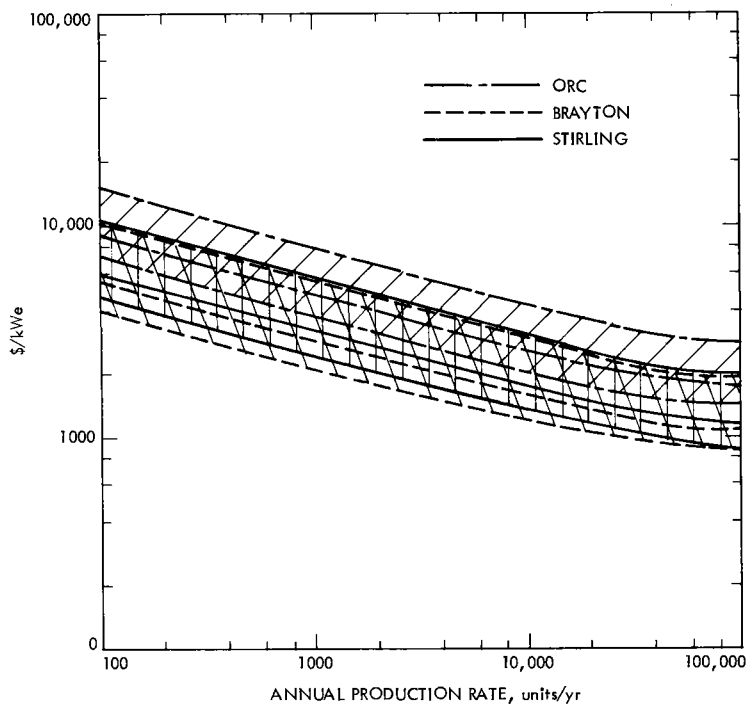

Figure 3-11. Initial Plant Price versus Annual Production Rate for Brayton-, Stirling-, and Organic-Rankine-Type Modules (1984 Dollars)

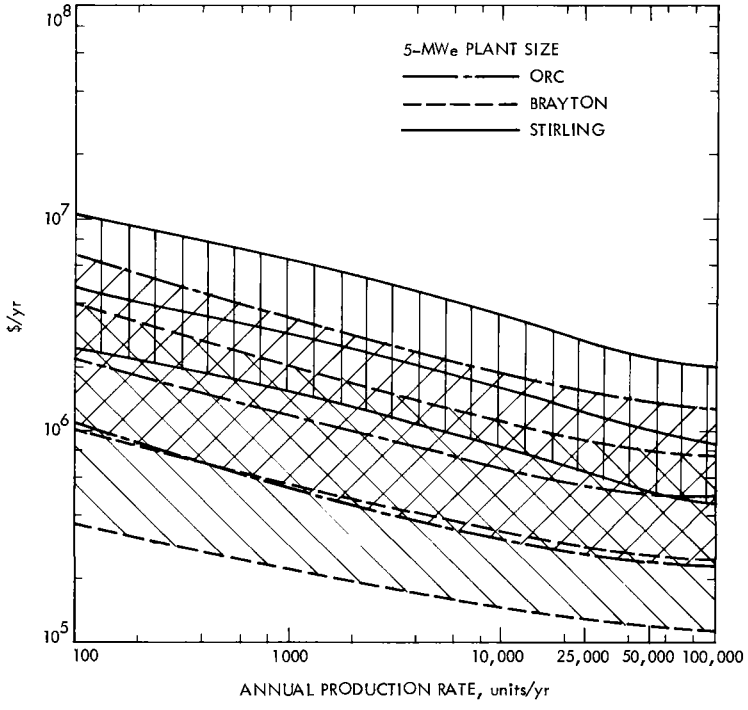

Figure 3-12. Overall Plant Maintenance Cost versus Annual Production Rate for Brayton-, Stirling-, and Organic-Rankine-Type Modules (1984 Dollars)

SECTION IV

MARKET POTENTIAL

This section contains estimates of the potential market size for parabolic dish systems in different market sectors. Breakeven costs, along with supporting assumptions, are determined for each market sector. To penetrate a market sector, it is necessary that the energy produced by dish systems costs no more than the total value of the energy they displace. In turn, the production level for determining dish system cost is constrained by market size (based on a combination of sectors). This breakeven cost criterion is a necessary but not sufficient condition for market penetration because it does not consider competition between parabolic dish systems and other innovative energy options that could possibly capture part or all of the markets. Because of the difficulty involved in estimating the future cost and operating characteristics of other developing energy technologies, inter-technology competition has not been included in this analysis. Instead, conventional technologies with projected 1990 characteristics are assumed to represent the best available alternative to dish systems in the early 1990s. If this assumption is inaccurate, the parabolic dish market potential will be smaller than estimated here.

This section is organized so that the data base regarding markets is presented along with the assumptions used in estimating the overall market size. Then, the value analysis methodology used to determine the breakeven costs for the identified market sectors is explained. Finally, the potential size of the markets for dish systems is determined by comparing breakeven costs with dish system costs as a function of production volume (as determined in the previous section). Emphasis is placed on delineating sensitivities to key assumptions, including fossil-fuel price escalations and the projected level of technology advancement achieved in the parabolic dish development program.

A. IDENTIFIED MARKETS

The market for solar thermal parabolic dish systems in electric utility applications can be divided into two broad categories: isolated loads and grid-connected applications. Isolated loads include non-grid connected applications currently using oil-fired, electricity-generating capacity. Examples of isolated loads include islands, agricultural irrigation, military applications, and stripper wells (which use electric and thermal energy). Grid-connected applications include parabolic dish installations in electric utilities that are connected to the electrical grid. To account for differences in financing arrangements and tax impacts, grid-connected applications can be further distinguished by ownership type. More specifically, this analysis will consider investor-owned utilities, municipal

utilities (equivalent for these purposes to Federal and rural electric utilities), and third-party ownership.[7]

Table 4-1 presents total market capacity estimates for both isolated loads and grid-connected utilities in the 1990s. Solar thermal parabolic dish systems will be one of many technologies competing to capture a share of this market. The capacity of economically justified parabolic dish installations in 1990 depends on the expected parabolic dish production costs (parabolic dish supply side) and the projected value of parabolic dish systems to electric utilities as determined by the cost of the energy they displace (parabolic dish demand side). The parabolic dish supply side was discussed in Section III. The parabolic dish demand side will be discussed here, then demand and supply will be compared.

B. METHODOLOGY

A methodology was devised to estimate the expected demand for parabolic dish systems (i.e., the economic market potential). The methodology uses a computer simulation model to compute the value of fuel and O&M expenses displaced by parabolic dish systems of different capacities. More specifically, energy outputs were estimated for different-sized parabolic dish power plants. Then, a probabilistic capacity dispatching model was used to determine the fuel and O&M costs for a utility installing parabolic dish systems ranging in size from 0 to 30 percent of peak-energy demand. The value of the avoided fuel and O&M costs is determined by comparing the fuel and O&M costs in the baseline no-solar case with the costs observed after installing different parabolic dish system capacities. The avoided fuel and O&M expenses are used to determine the total value of parabolic dish systems to different owners.

Purchase decisions, however, are based on changes in the total value of parabolic dish systems as parabolic dish capacity increases. Changes in the total value, referred to as incremental values, indicate the economic benefits attributable to expanding parabolic dish capacity. As long as the incremental value of parabolic dish exceeds its cost, utilities have an incentive to purchase additional parabolic dish capacity.

The incremental value of dish systems is calculated by determining the change in total value between successive parabolic dish capacity levels and normalizing by the change in system capacity. The utility simulation model is used to estimate the value of additional parabolic dish capacity to the electric utility owners, given descriptions of the utility's generating capacity and load patterns, scenarios for future energy costs, cost-induced changes in generating capacity and load patterns over time, insolation levels, and the financial parameters related to the utility's investment decision

[7]Third-party ownership includes systems purchased by private investors who then sell electricity to the grid. Third-party investors had received special Federal tax benefits, augmented in some cases by state tax incentives. However, these tax incentives were terminated in the mid-1980s (see Section F).

Table 4-1. Estimated 1990 U.S. Generating Capacity

Application	Estimated Generating Capacity, MWe
Grid-Connected[a]	700,000
Isolated Load	
Island[b]	5,600
Agricultural Irrigation[c]	2,200
Military[d]	300
Stripper Wells[e]	100

[a]In the early 1990s, solar thermal electric applications in grid-connected utilities will be limited to specific utilities characterized by good insolation, high dependence on oil or natural gas, and a close correspondence between peak demand for electricity and peak insolation. This market will be further divided between photovoltaics, solar thermal central receivers, and other alternative technologies. Source: Reference 49.

[b]Includes Hawaii, Puerto Rico, and the Virgin Islands. Source: Reference 49.

[c]Source: Reference 50.

[d]Source: Reference 51.

[e]Source: Reference 52.

criteria (Reference 53). The methodology described here was applied by making the assumptions described below in Section IV.C.

C. ASSUMPTIONS

On the demand side, insolation levels, fuel price projections, utility system characteristics, and the financial parameters represent the primary assumptions used to estimate the value of parabolic dish systems.

1. Insolation Levels

This analysis concentrates on 16 states in the southern and south-western portion of the United States. Individual states were grouped into three insolation regions, corresponding to above-average (Region A), average- (Region B), and below-average (Region C) insolation levels relative to the norm of the states considered. SOLMET data were used to represent the insolation levels in these three regions. Albuquerque, New Mexico, insolation was used to represent the above-average insolation region, Fresno, California, for the average insolation region, and Dodge City, Kansas, for the below-average case (Table 4-2). For each state, parabolic dish systems are expected to penetrate electric utility applications earlier in the higher

Table 4-2. Regional Variations: Insolation Levels and States Considered (Grouped by Insolation Level)

Region	SOLMET Insolation Data[a]	States[b]
A High Insolation $I \leq 7.0$[c]	Albuquerque, New Mexico	California Arizona New Mexico Nevada
b Medium Insolation $6.0 \leq I < 7.0$[c]	Fresno, California	Utah Colorado Texas
C Low Insolation $I < 6.0$[c]	Dodge City, Kansas	Kansas Oklahoma Missouri Arkansas Louisiana Hawaii Mississippi Alabama Florida

[a]Selection based on availability and quality of data as well as consistency with relevant insolation levels for the states in each region.

[b]Groupings based on highest insolation level for which a significant land area exists.

[c]Insolation values measure average direct normal insolation and are expressed in $kWh/m^2/day$.

isolation areas of the state. Parabolic dish systems can be connected to existing power lines if high insolation areas do not correspond with electricity demand centers. Therefore, states were assigned to insolation groups based on the highest insolation level for which a significant land area exists. Representative insolation data for each region were selected based on: (1) the availability and quality of the data, and (2) the correspondence between the insolation level of the representative sites and the relevant areas of the states included within the grouping in question.

2. Fuel-Price Projections Under Uncertainty

As with insolation levels, fuel prices vary across geographic regions. There is also uncertainty regarding future trends in fuel prices. Many possible events affect both absolute and relative energy costs [e.g., an oil embargo, the collapse of Organization of Petroleum Exporting Countries (OPEC), a nuclear disaster, a technical breakthrough in a competitive energy technology, a war in the Middle East, etc.] Each individual event, or combination of events, would cause a different scenario for the future state of the energy sector. Point estimates of future fuel costs are of little practical use because they obscure the underlying uncertainty characterizing these estimates. A range of region-specific fuel costs was considered to reflect geographic variations and future uncertainty (Table 4-3). The scenarios were selected to encompass the likely range of outcomes.

These fuel-price scenarios are based on Energy Information Administration (EIA) average national fuel-price projections made in 1983 (Reference 54). Data Resources, Inc. (DRI) regional fuel-price data were used to regionalize EIA's average national forecasts (Reference 55). Three fuel-price escalation rates were assumed for the post-1990 period: real annual fuel-price escalation rates of 4, 2, and 0 percent, corresponding to the high, medium, and low fuel-price scenarios, respectively. These fuel-price escalation rates reflected a dramatic decrease in the actual rates experienced during the 1970s, while they represent a slight increase over the rates witnessed during the 1960s.

These fuel-price scenarios do not correspond to specific scenarios of future events; they merely represent a range of possible values. If energy prices are below these values, a market for parabolic dish systems in the 1990s seems highly unlikely. Therefore, these fuel price scenarios should not be considered to represent projections of the future. Instead, they represent a range of values where parabolic dish systems may penetrate the energy market. Estimating the likelihood that the energy sector will track one scenario or another is a subjective assessment that varies dramatically over time. For example, the medium-to-high fuel-price scenario was generally accepted as most likely following the 1978 to 1979 Iranian oil embargo; conversely, the low oil-price scenario currently seems high considering the oil glut that began early in 1982. Because of their subjective nature, no probabilities were attached to any of these fuel-price scenarios.

Table 4-3. Fuel-Price Assumptions (1990 Fuel Prices in 1984 $/Btu x 10^6)

Fuel-Price Scenario[a]	Region[b]	Fuel Type				
		Nuclear[c]	Coal	Natural Gas	Residual	Distillate
Low	California	1.45	2.32	4.88	5.52	7.63
	West	1.45	1.57	d	5.88	8.13
	Texas	1.45	2.12	4.02	d	6.12
	Southcentral	1.45	2.06	4.24	d	9.15
Medium	California	1.45	2.32	5.34	6.30	9.39
	West	1.45	1.57	d	6.72	10.01
	Texas	1.45	2.12	4.40	d	7.53
	Southcentral	1.45	2.06	4.63	d	11.27
High	California	1.45	2.32	5.82	7.44	11.59
	West	1.45	1.57	d	7.93	12.35
	Texas	1.45	2.12	4.80	d	9.30
	Southcentral	1.45	2.06	5.05	d	13.91

[a]Low, medium, and high fuel-price scenarios based on projected world oil prices of $30/barrel, $39/barrel, and $48/barrel, respectively (1990 prices in 1984 dollars). Post-1990 price escalation rates are 0, 2, and 4 percent for the low, medium, and high scenarios, respectively.

[b]West region includes Arizona, New Mexico, and Nevada. Southcentral region inclues Utah, Colorado, Kansas, Oklahoma, Missouri, Arkansas, Louisiana, Hawaii, Mississippi, Alabama, and Florida. To calculate regional prices, regional scale factors were estimated by comparing DRI regional costs to DRI national averages. DRI regions were weighted by the electric generating capacity for the states included. EIA average prices were multiplied by the regional scale factors to obtain the prices reported here.

[c]EIA does not report nuclear fuel prices. Prices reported here are DRI national average prices. No regional data available.

[d]Fuel type not used in this region.

Source: References 54 and 55.

3. Utility Characteristics

The Electric Power Research Institute (EPRI) has modeled various synthetic utilities, providing hourly load data, generation capacity mixtures, and information regarding the technical operation and maintenance characteristics for these hypothetical utilities (Reference 56). The data for each synthetic utility represent average values for a particular region in the United States, thus providing a consistent set of data covering all aspects of utility power generation and energy demand. The states grouped in regions B and C are represented by the EPRI southcentral synthetic utility. The states grouped in region A are represented by the EPRI western synthetic utility. However, there have been two modifications. First, the hydroelectric capacity in EPRI's west utility has been changed to coal to more accurately represent the western states considered in this analysis. Second, the synthetic utilities used to represent California and Texas have been modified to reflect the much higher than average reliance on oil and natural gas in these states. As modified, the synthetic utilities represent the average characteristics of the relevant regions but not any specific utility.

The 1990 generation mixes for the regional synthetic utilities used in this analysis are shown in Table 4-4. During the period between 1990 and 2019, peak electricity demand was assumed to grow at an annual rate of 3 percent and to have a constant load profile.[8] With the exception of nuclear power plants, a screening curve methodology was used to determine the "optimal" generation mix in 2019, given the projected demand for electricity and the expected relative fuel, O&M, and capital costs in the year 2019, the last year of the study.[9] The growth of nuclear capacity was constrained to a maximum of 6 percent per year. Generating capacity was adjusted in equal increments every 5 years to ensure a smooth transition from the baseline 1990 generation mix to the "optimal" 2019 system. Because of the influence of fuel prices and parabolic dish penetration on the optimal generating mix, there are different capacity mixtures in 2019 for each region, fuel-price scenario, and parabolic dish penetration level. With the exception of California and Texas, the generation mix showed an aggressive transition to coal-fired capacity.

[8]Peak electricity demand growth will depend on the fuel-price scenario, with growth rates decreasing as fuel prices increase. However, little data is available regarding this relationship. Furthermore, the effect of higher fuel prices will be partially mitigated by the more rapid transition to coal in the higher fuel-price scenarios. As a result, a 3 percent escalation rate was assumed for all fuel-price scenarios.

[9]Screening curves consider both annualized capital costs as well as variable fuel and O&M costs to determine the capacity mix that minimizes the total cost of satisfying a given demand for electricity.

Table 4-4. Base Case 1990 Utility Generating Capacity (MWe)[a]

Fuel Type	Region			
	California[b]	West[c]	Texas[d]	Southcentral[e]
Nuclear	1800	1800	1200	1200
Coal	1800	6100	3000	5000
Natural Gas	5100	f	7600	5600
Residual Oil	3000	3800	f	f
Distillate Oil	700	700	600	600

[a]1990 capacity mix is constant across fuel-price scenarios.

[b]Based on EPRI's western synthetic utility modified to reflect the higher than average natural gas and residual oil capacity in California.

[c]Based on EPRI's western synthetic utility with hydroelectric capacity converted to coal. The western region includes: Arizona, New Mexico, and Nevada.

[d]Based on EPRI's southcentral synthetic utility modified to reflect the higher-than-average natural gas capacity in Texas.

[e]Based on EPRI's southcentral synthetic utility. The southcentral region includes Utah, Colorado, Kansas, Oklahoma, Missouri, Arkansas, Louisiana, Hawaii, Mississippi, Alabama, and Florida.

[f]Fuel type not used by EPRI's synthetic utility in this region.

Source: Reference 56.

4. Financial Parameters

This analysis considers the financial parameters of municipal and investor-owned utilities. Municipal utilities can generally obtain more favorable capital financing, making them particularly attractive for early parabolic dish installations. The financial parameters used in this analysis correspond to the parameters adopted by the Solar Thermal Cost Goals Committee in 1980/81 (Reference 57), updated to reflect the Tax Equity and Fiscal Responsibility Act of 1982 (TEFRA). These parameters are listed in Table 4-5. Financial parameters for third-party ownership are also presented, assuming that the Federal incentives in TEFRA are extended but that state incentives are eliminated. The Federal incentives have since been terminated. However, for the sake of analysis, they are retained here. As will be discussed later, without these incentives third-party investors would not represent a viable funding alternative.

Table 4-5. Financial Parameters

Parameters	Municipal Utility	Investor-Owned Utility	Third-Party Ownership
System Life, yr	30	30	30
Depreciation Life, yr	--	15	5
Depreciation Method	--	ACRS[a]	ACRS[a]
Effective Tax Rate, %	--	48	52
Investment Tax Credit, %	--	10	10
Energy Tax Credit, %	--	0	15
Other Taxes and Insurances as Fraction of Capital Investment, %	1.25	2	2
General Inflation Rate, %	6	6	6
Discount Rate (Real), %	2	3.6	15
O&M Escalation Rate (Real), %	1	1	1
Return on Equity (Real), %	--	5.6	15
Return on Debt (Real), %	2	3	7
Debt Fraction, %	100	50	50

[a]The 1981 Accelerated Cash Recovery System (ACRS) as modified by the Tax Equity and Fiscal Responsibility Act of 1982.

5. Inter-Technology Competition

The value of dish systems depends on the cost of the best alternative to parabolic dish systems. Estimating the future demand for these systems requires explicit or implicit assumptions regarding the relative costs of all alternative energy sources, both those currently in use and those expected to become available during the time period being considered. Many demand analyses, including this one, assume that parabolic dish systems displace current technologies. This is equivalent to assuming that all other energy-related R&D projects fail to produce technologies that can compete economically in the markets served by parabolic dishes. If this, in fact, turns out to be an inaccurate prediction, the parabolic dish demand curves estimated here will overstate the true demand. Competition between parabolic

dish and similar innovative energy technologies is an important element of demand-curve analysis. Because of the difficulty involved in estimating the future outcome of alternative R&D projects, this analysis does not consider inter-technological competition. Conventional technologies with projected 1990 characteristics are assumed to represent the best available alternatives to parabolic dish during the time frame considered in this analysis. This assumption becomes less realistic for the high fuel-price scenario. When oil prices are high, oil is less likely to represent the best available alternative.

6. 1990 Installations

This analysis estimates the demand for parabolic dishes at a particular point in time, namely 1990. Implicit in these demand projections are assumptions regarding parabolic dish installations both before and after the time being examined. Many studies including this analysis, estimate the demand for dish systems in a future year assuming that no installations have been made prior to that year. Any change in this assumption results in a shift of the demand curve for the year in question. Prior installations reduce the demand for parabolic dish. Future demand characteristics and installation decisions can also influence parabolic dish purchases. The impacts of dynamic considerations were not included in this analysis. The demand curves estimated here represent the total parabolic dish market demand projected to be economically viable by 1990, not the actual purchases of parabolic dish capacity in that year.

For reference, the major assumptions used in this analysis are summarized in Table 4-6.

D. 1990 PARABOLIC DISH DEMAND

Considering the utility characteristics, insolation data, and future fuel-price projections described above, a utility simulation was used to estimate the fuel and O&M costs displaced by parabolic dish systems of differing capacities (referred to as fuel and O&M credits). The fuel and O&M credits were converted to after-tax values by incorporating the financial parameters described in Table 4-5.[10] In these calculations, annual parabolic dish O&M costs were assumed to equal 5% of the initial capital cost. A 5% O&M fraction is consistent with the medium-cost case for the ORC engine, according to Figures 3-11 and 3-12. The assumptions in the high, medium, and low-cost cases for the initial plant costs are consistent with the assumptions for the high-, medium-, and low-cost cases for the annual O&M costs, respectively. Therefore, the O&M fractions for the ORC medium-cost case can be calculated by comparing the initial cost and annual O&M costs, expressed in $/kWe, for the medium-cost case. For example, at a production volume of

[10]The parabolic dish after-tax values were calculated using a methodology developed at JPL. However, this methodology is similar to several other frequently cited valuation procedures. For a detailed description see Reference 53, in particular Appendix B.

Table 4-6. Summary of Assumptions Used in Analysis

	Assumption	Comments
(1)	Parabolic dish systems	None.
(2)	No storage	Forces dish systems to compete with coal.
(3)	Investor, municipal utility, and third-party ownership	None.
(4)	Aggressive transition to coal	In all states except California and Texas, utilities are assumed to be installing coal plants in preference to oil/nuclear plants. Thus, parabolic dishes must compete with the lower-priced coal in the future.
(5)	Southwest, southcentral, and southeastern regions only	Average characteristics of utilities in these regions were used.
(6)	1990 installation	Calculation is simplified by assuming all parabolic dish plants installed in the early 1990s are installed in a single year, 1990. This overstates actual 1990 installations, but ignores post-1990 increases in demand.
(7)	Electric Power Research Institute (EPRI) utility data	Gives lower conventional generating cost estimates than other sources; captures expected improvements in conventional technology; poor correlation between power demand and insolation.
(8)	SOLMET insolation data	Three levels: High (Albuquerque, NM), medium (Fresno, CA), and low (Dodge City, KS).
(9)	1984 dollars	None.
(10)	Energy Information Administration fuel prices regionalized according to Data Resources, Inc., regional price data	Sources: References 54 and 55.
(11)	Electricity demand escalation rate	3%/yr, constant across fuel-price scenarios
(12)	No inter-technology competition with alternative energy sources	May overstate the potential market share capture by parabolic dishes

10,000 units/yr, the initial plant cost is approximately $2600/kWe (see Figure 3-11). At that production volume, the annual O&M cost is approximately $650,000 per year for a 5-MWe system (see Figure 3-12). This is equivalent to $130/yr/kWe, which is 5% of the initial plant cost. This fraction is relatively stable as the production volume changes. It increases to 9% in the high-cost case and decreases to 3% in the low-cost case. The ORC engine was selected as representative of an attractive 1990 technology because the O&M costs of the Stirling engine appear high and the Brayton is a later technology. In addition, market penetration will be difficult if the O&M fraction exceeds 10%. Therefore, 5% was used to indicate the potential market. If O&M significantly exceeds this value, the solar thermal parabolic dish market will be negligible.

Finally, to describe the utilities' purchase decisions, incremental after-tax values per kWe were calculated by determining the change in total after-tax values between successive parabolic dish capacity levels and dividing by the change in a system capacity. These incremental values (also referred to as breakeven values) represent points on the demand curves for parabolic dishes, assuming no inter-technological competition from other alternative energy technologies.

The breakeven values for solar thermal parabolic dish systems installed in California are shown in Table 4-7 for a variety of alternative ownerships and utility types. These figures represent the breakeven values for the first parabolic dish systems installed. Early solar thermal installations will replace the most valuable alternative fuels and least efficient conventional capacity. As parabolic dish penetration increases, less valuable fuels will be displaced, and the value of additional parabolic dish capacity will decrease.

Figure 4-1 illustrates the incremental value of solar thermal parabolic dish capacity in grid-connected utility applications, in the southwestern and southcentral United States, under three fuel-price assumptions. Again, annual parabolic dish O&M costs are assumed to equal 5 percent of the initial system cost. This figure demonstrates the sensitivity of the value of solar thermal parabolic dish capacity to the installed capacity. According to Figure 4-1, utilities would pay approximately $1250/kWe for the first 500 MWe of parabolic dish capacity in the medium-oil-price scenario. After 5000 MWe have been installed, however, the value of an additional unit of parabolic dish capacity would fall to $950/kWe.

E. 1990 PARABOLIC DISH ECONOMIC MARKET POTENTIAL

Once a range of values has been estimated for both parabolic dish production costs and demand, the estimates can be combined to examine the 1990 economic market potential.[11] The demand curves (Figure 4-1) give the

[11]This analysis assumes that parabolic dish production costs are independent of future oil prices. Actually, parabolic dish prices will probably tend to increase as oil prices increase, and this would tend to reduce the market potential. It is expected that this will be a second-order effect.

Table 4-7. Incremental Values for Early Parabolic Dish Installations in California[a]

Market	Fuel-Type Displaced	Fuel Prices[b]	Municipal Utility	Investor-Owned Utility	Ownership Third-Party
Isolated Loads[c]	Oil	Medium	1350	1000	1075
		Low-High	925-2125	700-1550	825-1450
Grid-Connected Applications[d]	Mixture (Oil, Coal, Nuclear)	Medium	1275	950	1025
		Low-High	875-2100	650-1500	800-1375

[a]This table provides the incremental values, in $/kWe, for 1990 installations expressed in 1984 $. These figures represent the breakeven values for the first parabolic dish systems installed.

[b]Medium fuel-price scenario corresponds to the EIA medium scenario of $39/barrel (1990 price in 1984 $). Low and high scenarios correspond to a range of $30/barrel to $48/barrel, respectively (1990 price in 1984 $). Post-1990 annual rates of escalation -- 0, 2, and 4% for low, medium, and high scenarios, respectively.

[c]Market limited to non-grid connected applications currently using oil-fired capacity only.

[d]Based on parabolic dish penetration equivalent to 1% of peak demand (equal to approximately 400 MWe) in California in 1990.

relationship between market price ($/kWe) and cumulative parabolic dish capacity. On the other hand, the cost curves (reproduced in Figure 4-2) give the relationship between market price and annual production rates. Therefore, these curves are not directly comparable. However, keeping in mind the differences in units, the 1990 economic market potential can be discussed with reference to Figures 4-1 and 4-2.[12]

[12]The cost and demand curves could be expressed in comparable terms by assuming a production scenario for the Solar Thermal Technology industry. However, the results of the analysis would depend on the accuracy of the production scenario. To avoid this, the demand and cost curves will be expressed in different units. However, allowing for a gradual build-up of production capacity, a plant should produce approximately seven times its annual production capacity over a 10-year period, as a rough rule of thumb.

Figure 4-1 and Table 4-7 indicate that parabolic dish systems cannot expect to penetrate the electric utility market, even in the high fuel-price scenario, until prices fall to approximately $2000/kWe. Prices would have to reach approximately $1500/kWe to $1000/kWe to have parabolic dish utility market penetration in the medium and low fuel-price scenarios, respectively. At these prices, market penetration would be moderate, probably less than 500 MWe total. To reach a market potential of 10,000 MWe, prices would have to fall to the $1000/kWe to $600/kWe range.

Figure 4-2, on the other hand, indicates that a substantial annual production would be required to achieve the prices consistent with a moderate market penetration. Using optimistic cost estimates for the Organic-Rankine-cycle system, the production volume would have to exceed 10,000 units/yr (approximately 250 to 300 MWe/yr) before system prices would fall to $2000/kWe. To give a rough approximation to cumulative production capacity, assume investors require a 10-yr expected production period before establishing a production facility. Allowing for a gradual build-up in production, a 10,000-unit/yr plant would produce approximately 70,000 units over 10 years (approximately 1,750 to 2100 MWe).[13]

Less-optimistic organic Rankine-cycle cost estimates indicate that prices will not fall to this level even if the production volume reaches 100,000 units/yr. Production costs are slightly lower for Stirling-cycle parabolic dish systems, but higher O&M costs are likely to more than offset the upfront cost advantage. Finally, production costs for the Brayton-cycle parabolic disk system are the lowest of the options considered. They could achieve $2000/kWe prices for production volumes ranging between 1,200 and 60,000 units/yr (approximately 30 to 1500 MWe/yr). However, these systems are not expected to be on the market until the mid-1990s.

Comparing Figures 4-1 and 4-2 indicates that the market for parabolic dish electric systems in the early 1990s is likely to be small and volume production is unlikely. More specifically, parabolic dish installations will be limited to a few specific applications where unique conditions make parabolic dish systems particularly attractive. These favorable applications are not captured in the type of aggregrate analysis presented here. The potential market for parabolic dish systems in electric-utility applications appears more promising as parabolic dish technologies mature and their prices fall. Under the most favorable conditions (high fuel prices and low parabolic dish system prices), parabolic dish systems could potentially start to penetrate the electric utility market when the Brayton-cycle parabolic dish system becomes commercially available.

[13]To reach $2000/kWe, a single plant must achieve an annual production rate of 10,000 units. In competitive markets, production will probably be divided among several firms. Thus, total market production would have to be larger than 10,000 units/yr to support a 10,000-unit/yr production rate in a single firm. Furthermore, the market potential estimated in Figure 4-1 will be split among various alternative energy technologies (e.g., wind, photovoltaics, etc.). On the other hand, the market for alternative energy technologies is likely to grow over time. Figure 4-1 does not consider market growth beyond 1990.

Figures 4-1 and 4-2 illustrate that the 1990 parabolic dish market size is sensitive to both parabolic dish system costs and future fuel prices. A decrease in parabolic dish system costs would shift the cost curves downward, while an increase in future fuel prices would shift the demand curves upward. Either of these developments would increase the parabolic dish economic market potential. Furthermore, because of the demand curves' shapes, a small change in either curve could have a large impact on the 1990 parabolic dish market.

1. The Transition from Oil to Coal

At least two additional factors have a significant impact on the market potential of parabolic dishes: the high incidence of coal displacement observed in this analysis and parabolic dish O&M costs. The high incidence of coal displacement results from two influences: the high percentage of coal-fired capacity in the utilities' generation mix, and the poor correspondence between peak insolation and peak electricity demand in the EPRI electricity demand data. Because an aggressive transition toward coal is assumed in this analysis, oil and natural gas are used primarily as peak-load fuels. With the exception of California and Texas, base- and intermediate-load demands are satisfied by coal and nuclear capacity. As a result, parabolic dish will displace oil and natural gas only to the extent that solar energy is available during periods of peak demand. Unfortunately, peak electricity demand in the EPRI synthetic utilities for the western and southcentral United States normally occurs during hours of the day that have poor insolation. With this capacity mix and electricity demand pattern, parabolic dishes without storage is forced to compete with coal-fired capacity.

As Figure 4-3 illustrates, coal represents 60 percent of the fuel displaced for the first 1 percent penetration in the low fuel-price scenario. The coal displacement increases as both parabolic dish penetration and projected fuel prices increase. For reference, Figure 4-4 shows the relationship between the 1990 value per electric kilowatts of parabolic dish capacity and the percentage of coal displacement for a municipal utility in the western region. The curves would be lower for investor-owned utilities and in the southcentral region.

2. Operation and Maintenance Costs

Another critical factor in estimating the 1990 parabolic dish market is parabolic dish O&M costs. This anaylsis assumes that the initial annual O&M costs will equal 5 percent of the parabolic dish system's capital costs and grow at a 1 percent real annual escalation rate. Future O&M costs are highly uncertain at this time, and small variations can have a large impact on parabolic dish incremental values. Figures 4-5 shows the impact that changes in parabolic dish O&M costs have on incremental parabolic dish values in the medium fuel-price scenario. For all fuel-price scenarios, if O&M costs are reduced to 2 percent of capital costs, incremental values increase by 35 percent. If O&M costs increase to 8 percent of capital costs, incremental values decrease by 20 percent. Finally, if O&M costs increase to 10 percent of capital costs, incremental values decrease by 30 percent. O&M costs are uncertain and can have a significant effect on the 1990 parabolic dish economic market potential.

3. Dynamic Considerations

As discussed earlier, total economic market potential for dish systems at a particular time is likely to exceed the actual level of dish systems purchases and installations. Consumers may be constrained by capital market imperfections or inaccurate information, while suppliers in growing industries frequently face bottlenecks to establishing the required industry infrastructure, especially in industries experiencing a relatively rapid rate of technological change. For these and other reasons, actual purchases of dish systems will be less than the total projected demand for that period. Cumulative installations during the 1990s, however, will approach the total capacity for which parabolic dish is cost-competitive. This suggests the use of a dynamic approach to projecting future parabolic dish deployment decisions. Because a dynamic formulation is beyond the scope of this analysis, static estimates of total potential demand have been used.

Furthermore, these demand curves represent the price utilities would be willing to pay for parabolic dish systems if growing demand requires the utility to increase generating capacity. In other words, the demand curves in Figures 4-1 and 4-2 really represent utilities that must add new generating capacity and are deciding whether to add parabolic dish or some other type of capacity.[14]

Alternatively, parabolic dish systems can be installed to displace conventional fuel even when additional capacity is not required. This application becomes more attractive as fuel prices rise. However, in fuel-displacing applications, utilities have a viable delay option. They can choose to delay parabolic dish installations an additional year. To depict accurately the utilities' decisions to install parabolic dish capacity in fuel-saving applications, the value of parabolic dish capacity should be estimated by assuming constant, real fuel prices (0 percent real escalation rate). The demand curves calculated here reflect the value of parabolic dish systems in capacity-expanding applications, but overstate their value in fuel-saving applications.

F. THIRD-PARTY INVESTORS AND EARLY PARABOLIC DISH MARKETS

In actuality, initial parabolic dish installations during the early 1990s will occur in applications where parabolic dish has a relatively high value and can rely on beneficial financial arrangements. Utility simulation using average regional characteristics cannot accurately reflect these favorable circumstances. Early applications include those utilities that

[14]Strictly speaking, parabolic dish systems that displace conventional generating capacity can claim a capacity credit for the reduced expenditure on conventional capacity. However, because of the poor correlation between peak insolation and peak energy demand in the EPRI synthetic utility data, the capacity credit was less than 5 percent of the value of parabolic dish installations. For simplicity, the capacity credit has not been included in these calculations.

continue to use a significant quantity of oil and natural gas, utilities that have a close correspondence between peak electricity demand and peak isolation, and remote sites and non-grid-connected applications (island utilities, stripper oil wells, agricultural irrigation, etc.). Until recently, third-party investors were expected to offer an attractive funding source for early parabolic dish installations.

Third-party investors generally face higher debt and equity costs than public utilities because public utility investments are normally perceived as being more secure. However, in the early 1980s, third-party investors received various Federal income tax incentives. More specifically, the Federal tax incentives, embodied in the Economic Recovery Tax Act of 1981 (ERTA), included accelerated depreciation and a 15 percent business energy tax credit. Many states also offered a mixture of additional state tax deductions, including accelerated depreciation and tax credits. In many cases, the state and Federal tax benefits more than offset the higher debt and equity costs, making third-party investors an apparent funding source for early parabolic dish installations.

The initial optimism for third-party financing has since been tempered. The Tax Equity and Fiscal Responsibility Act of 1982 (TEFRA) reduced the Federal tax incentives. Furthermore, Federal and most state incentives were terminated during the mid-1980s. Without these state and Federal tax benefits, higher debt and equity costs will make third-party investments in parabolic dish systems highly unlikely. For example, the third-party ownership financial parameters embodied in Table 4-6 assume that 1990 parabolic dish installations capture the Federal tax incentives embodied in TEFRA but no State tax incentives. Under these assumptions, municipal utilities are a more attractive funding source than third-party investors for all fuel-price scenarios. The value of parabolic dish installations is higher for third-party owners than it is for investor-owned utilities in the low and medium fuel-price scenarios, but not in the high fuel-price scenario.

Without state and Federal tax benefits, third-party investors are not expected to provide a viable funding alternative (with the possible exception of individuals or companies that have a vested interest in establishing a parabolic dish industry). Furthermore, maintaining the Federal tax incentives alone would not stimulate significant interest from third-party investors. More liberal tax benefits would be required to create a market with third-party investors.

G. DISCUSSION

This analysis has estimated the 1990 market potential for cost-competitive parabolic dish installations in electric-utility applications under a range of future fuel-price scenarios and parabolic dish system costs. This analysis concludes that the market potential can be expected to vary widely depending both on the parabolic dish system costs and on the relevant fuel-price scenario. As with most R&D projects, future parabolic dish costs are quite uncertain, as reflected by the range of plausible parabolic dish system costs. In the parabolic dish R&D program, however, this uncertainty is compounded by the extreme variability in expectations regarding future fuel prices.

Over the last 15 years, world oil prices have been influenced by the OPEC cartel. After the 1978-79 Iranian oil embargo, fuel prices were generally expected to fall within the medium or high fuel-price scenario. Since the oil glut early in 1982, prices have fallen below the low oil-price scenario. Because fuel-price expectations vary greatly, affecting the anticipated market for parabolic dish, there is a greater-than-average uncertainty regarding parabolic dish R&D. (Figure 4-6 illustrates the wide variations in fuel price projections over time.) To private industry, parabolic dish R&D represents a risky investment; private parabolic dish R&D initiatives are unlikely in the absence of Federal participation.

The Federal government, however, has a variety of concerns, including minimizing the impact of energy market imperfections, protecting the economy from disruptive influences of rapidly escalating fuel prices, and limiting the environmental consequences of oil, coal, and nuclear facilities. Because of the energy market imperfections introduced by the OPEC cartel, private industry is unlikely to independently finance parabolic dish R&D. Expenditures on parabolic dish R&D could result in significant energy cost savings, limit the impact of potentially dramatic oil-price increases, and reduce environmental degradation associated with conventional energy technologies. Federal participation in parabolic dish R&D would help capture these significant national benefits.

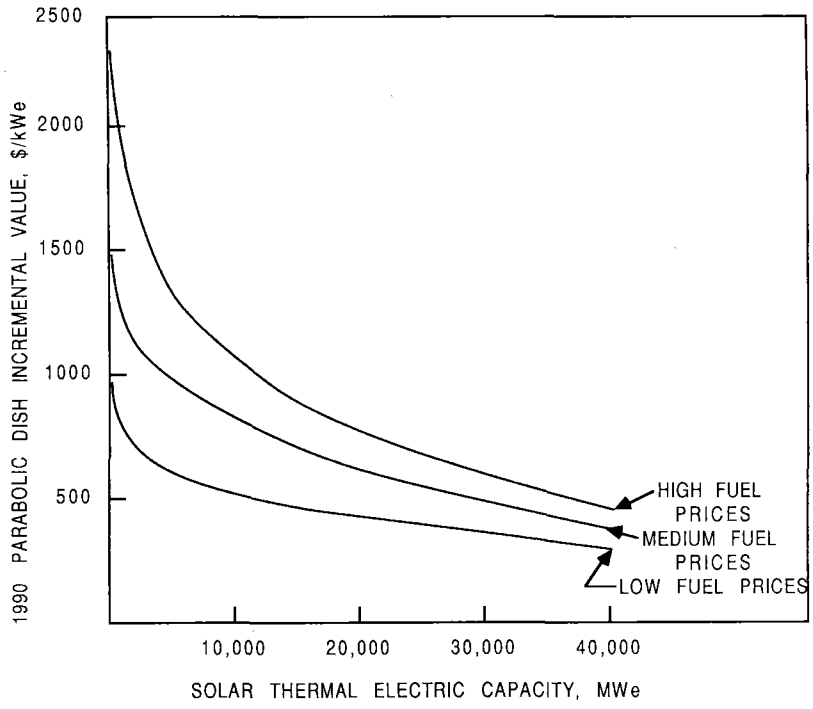

Figure 4-1. 1990 Market Potential for Cost-Competitive Solar Thermal Parabolic Dish Systems in Grid-Connected Applications

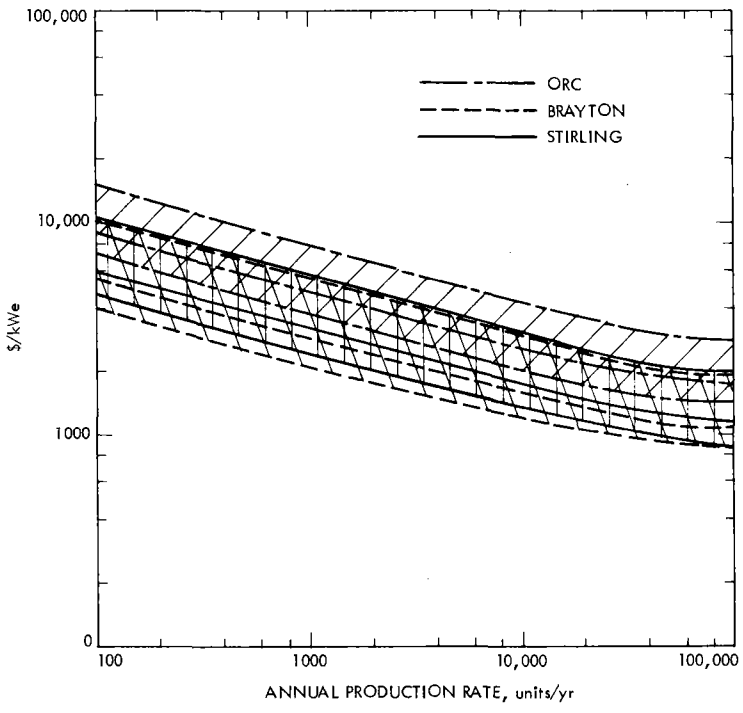

Figure 4-2. Initial Plant Price versus Annual Production Rate for Brayton-, Stirling-, and Organic-Rankine-Type Modules (1984 Dollars)

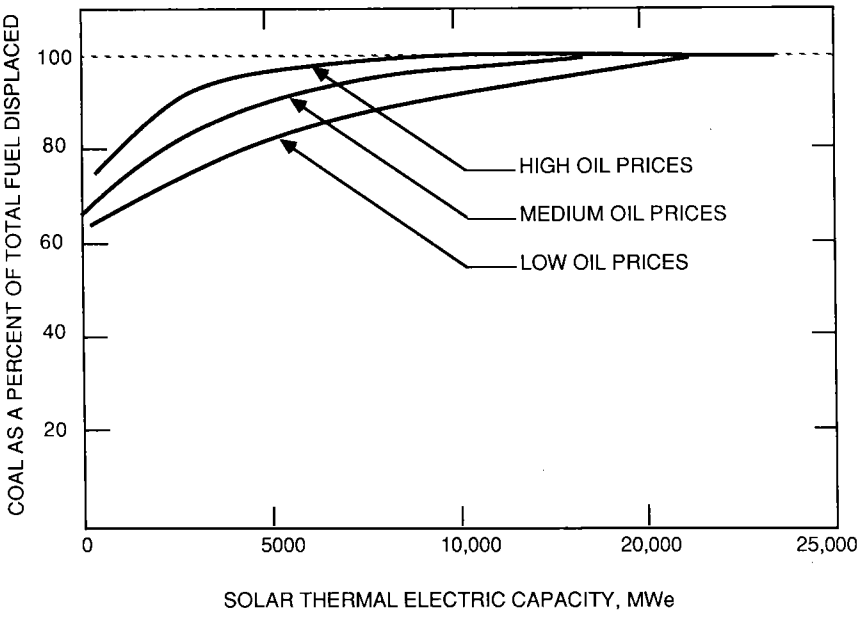

Figure 4-3. 1990 Solar Thermal Electric Capacity and Life-Cycle Coal Displacement

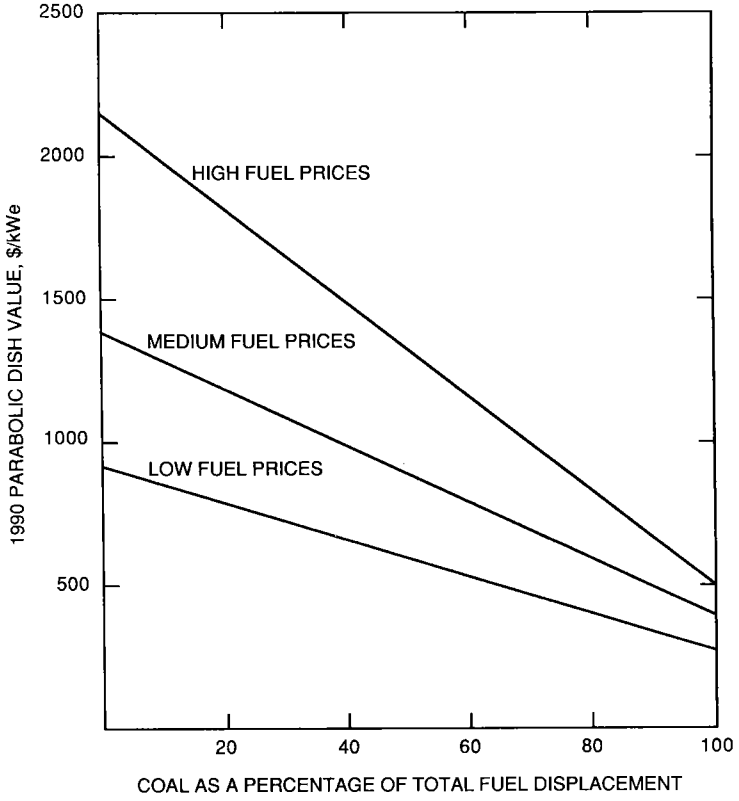

Figure 4-4. Parabolic Dish Value and the Percentage of Coal Displacement (Investor-Owned Utility; Two Fuels: Oil and Coal; Albuquerque Insolation; No Storage; Capacity Factor = 25%)

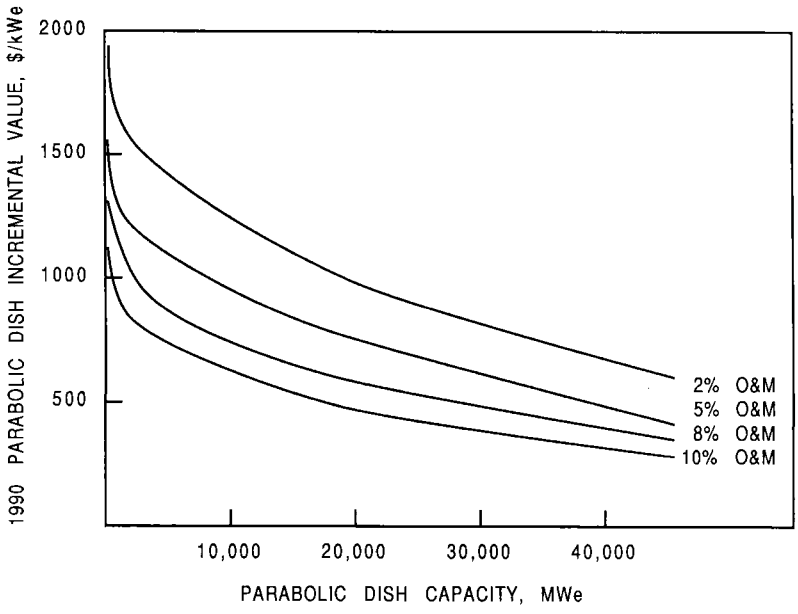

Figure 4-5. 1990 Parabolic Dish Incremental Value: O&M Sensitivity for Medium Fuel Price Scenario (O&M Expressed as a Percentage of Initial Capital Cost)

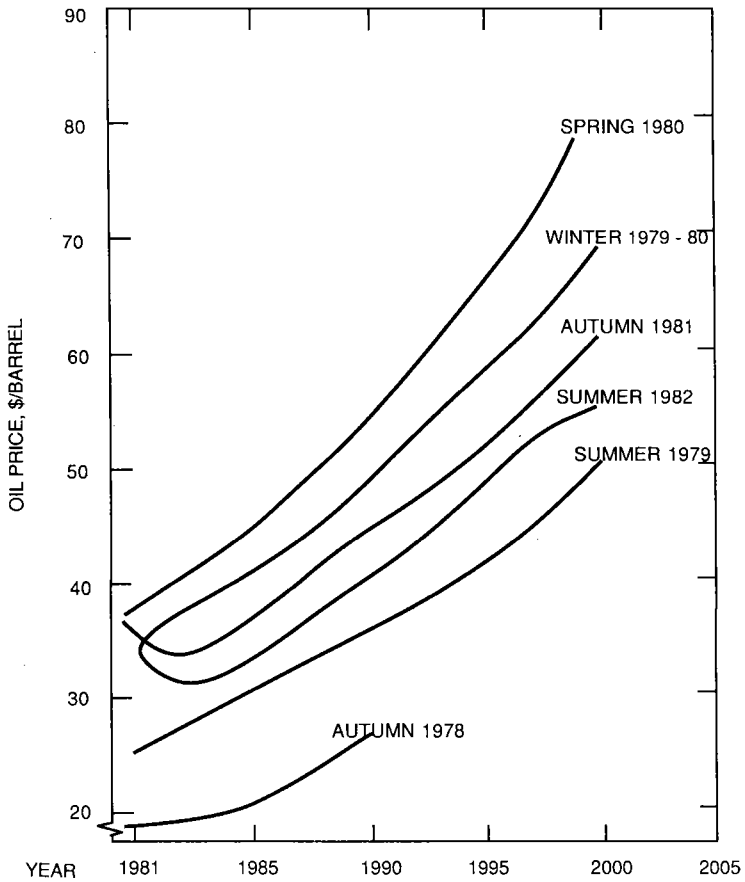

Figure 4-6. Baseline Imports Crude Oil Price Forecasts (from Various Volumes of Reference 55)

SECTION V

CONCLUSIONS

The following conclusions are drawn from this study:

(1) If fuel price escalation occurs at rates near the upper bound of the range used in this study, evolutionary engineering development of the modules currently being tested can achieve the breakeven costs needed to penetrate markets.

(2) If fuel price escalation occurs at nominal or intermediate values within the range, technology advancements beyond evolutionary engineering development of current modules are required to achieve breakeven costs.

SECTION VI

REFERENCES

1. Kiceniuk, T., Development of an Organic Rankine-Cycle Power Module for a Small Community Solar Thermal Power Experiment, JPL Production 85-3, DOE-JPL-1060-80, Jet Propulsion Laboratory, Pasadena, California, January 15, 1985.

2. Dennison, E.W., and Thostesen, T.O., Development and Test of Parabolic Dish Test Concentrator No. 1, JPL Publication 85-4, DOE/JPL-1060-81, Jet Propulsion Laboratory, Pasadena, California, December 15, 1984.

3. Boda, F.P., "Test Results for the Small Community Solar Power System," Proc. Fourth Parabolic Dish Solar Thermal Power Program Review, JPL Publication 83-2, DOE/JPL-1060-58, pp. 95 to 108, Jet Propulsion Laboratory, Pasadena, California, February 1, 1983.

4. Osborn, D.B., Haskins, H.J., Conway, W.A., and Wen, L.C., "Design and Test of a Solar Receiver for an Organic Rankine Cycle Engine," Solar Engineering, pp. 449 to 457, 1982.

5. Johnson, H., and Penney, T., Qualification Test Report, Power Conversion Subsystem for Small Community Thermal Power Experiment, Report to Ford Aerospace and Communications Corporation, by Barber-Nichols Engineering, Arvada, Colorado, November 1981.

6. Fulton, D.G., "Control System Development for the Small Community Solar Power System," Proc. Fourth Parabolic Dish Solar Thermal Power Program Review, JPL Publication 83-2, DOE/JPL-1060-58, pp. 83 to 94, Jet Propulsion Laboratory, Pasadena, California, February 1, 1983.

7. Nesmith, B., Bearing Development Program for a 25-kWe Solar-Powered Organic Rankine-Cycle Engine, JPL Publication 85-81, DOE/JPL-1060-92, Jet Propulsion Laboratory, Pasadena, California, September 15, 1985.

8. Patzold, J.D., "Omnium-G Concentrator Test Results," Proc. First Semi-Annual Distributed Receiver Systems Program Review, JPL Publication 80-10, DOE/JPL-1060-33, pp. 125 to 131, Jet Propulsion Laboratory, Pasadena, California, April 15, 1980.

9. Selcuk, M.K., Parabolic Dish Test Site: History and Operating Experience, JPL Publication 85-18, DOE-JPL-1060-84, pp. 2-70 to 2-93, Jet Propulsion Laboratory, Pasadena, California, February 15, 1985.

10. Thermal System Engineering Experiment, Final Report, K05-01-82-FR, Report to Jet Propulsion Laboratory, Applied Concepts Corporation, Woodstock, Virginia, October 29, 1982.

11. Hauger, J.S., and Pond, S.L., Capitol Concrete Solar Industrial Process Heat Experiment, Final Technical Report, Report to U.S. Department of Energy, Albuquerque Operations Office by Applied Concepts Corporation, Woodstock, Virginia, January 31, 1983.

12. Air Force Logistics Command (AFLC) Solar Thermal Plant, K10-01-83FR, Report to Jet Propulsion Laboratory, Applied Concepts Corporation, Woodstock, Virginia, April 15, 1983.

13. Kiceniuk, T., and Wingenbach, W., "Recent Tests on the Carter Small Reciprocating Steam Engines," Parabolic Dish Solar Thermal Annual Program Review Proc., DOE/JPL-1060-52, JPL Publication 82-66, Jet Propulsion Laboratory, Pasadena, California, pp. 123 to 145, July 15, 1982.

14. Parabolic Dish Module Experiment, Contract 58-100, Development Test Mode, Final Test Report, Sandia Report SAN 85-7007, Sanders Associates, Nashua, New Hampshire, September 11, 1985.

15. "Parabolic Dish Module Experiment, Critical Design Review," Sanders Associates, Inc., Merrimack, New Hampshire, June 12-13, 1984.

16. Owen, W.A., "Advanced Solar Receivers," Proc. Fifth Parabolic Dish Solar Thermal Power Program Annual Review, DOE/JPL-1060-69, JPL Publication 84-13, Jet Propulsion Laboratory, Pasadena, California, March 1, 1984.

17. Hanseth, E.J., "Development, Solar Test, and Evaluation of a High-Temperature Air Receiver for Point-Focusing Parabolic Dish Applications," Preprint 81-2532, AIAA, New York, December 1981.

18. Johnson, R.L., "Subatmospheric Brayton-Cycle Engine Program Review," Proc. Fifth Parabolic Dish Solar Thermal Power Program Annual Review, JPL Publication 84-13, DOE/JPL-1060-69, pp. 122 to 126, Jet Propulsion Laboratory, Pasadena, California, March 1, 1984.

19. "SAGT-1A Program Review," Doc. 31-5815, Garrett Turbine Engine Co., Phoenix, Arizona, March 21, 1985.

20. Washom, B.J., Hagen, T., Wells, D., and Willcox, W., Vanguard 1 Solar Parabolic Dish-Stirling Engine Module, Final Report, Report DOE-AL-16333-2 to U.S. Department of Energy, Advanco Corporation, El Segundo, California, September 30, 1984.

21. Advanco Corporation, "Solar Parabolic Dish Stirling Engine System Module," Project Status Report 32 to Department of Energy, Albuquerque Operations Office, January 1985.

22. Livingston, F.R., Activity and Accomplishments in Dish/Stirling Electric Power System Development, DOE/JPL-1060-82, JPL Publication 85-8, Jet Propulsion Laboratory, Pasadena, California, February 15, 1985.

23. Selcuk, M.K., "Dish Stirling Module Performance as Evaluated from Tests of Various Test Bed Concentrator Stirling Engine Configurations," JPL D-2637, Internal Report 5105-149, June 15, 1985.

24. Nelving, H.G., "Testing of the United Stirling 4-95 Solar Stirling Engine on Test Bed Concentrator," Proc. Fifth Parabolic Dish Solar Thermal Power Program Annual Review, DOE/JPL-1060-69, JPL Publication 84-13, Jet Propulsion Laboratory, Pasadena, California, pp. 102 to 108, March 1, 1984.

25. Nelving, H.G., "Testing of 4-95 Solar Stirling Engine in Concentrator at Edwards Air Force Base during period May 1982 - July 1983," United Stirling Co. 83-0033, September 7, 1983.

26. Haglund, R.A., "Non-Heat Pipe Receiver/P-40 Stirling Engine," Parabolic Dish Solar Thermal Power Annual Power Review Proc., DOE/JPL 1060-46, JPL Publication 81-44, Jet Propulsion Laboratory, Pasadena, California, May 1, 1981.

27. Starkey, D.J., "Characterization of Point Focusing Test Bed Concentrators at JPL," Parabolic Dish Solar Thermal Power Annual Program Review Proc., DOE/JPL 1060-46, JPL Publication 81-44, Jet Propulsion Laboratory, Pasadena, California, pp. 135 to 142.

28. Dennison, E.W., and Thostesen, T.O., Development and Testing of Parabolic Dish Concentrator No. 1, DOE/JPL-1060-81, JPL Publication 85-4, Jet Propulsion Laboratory, Pasadena, California, December 15, 1984.

29. Stallkamp, J.A., Control System for Parabolic Dish Concentrator No. 1, DOE/JPL-1060-86, JPL Publication 85-40, Jet Propulsion Laboratory, Pasadena, California, March 15, 1985.

30. Dennison, E.W., and Argoud, M.J., "Solar Concentrator Panel and Gore Testing in the JPL 25-Foot Space Simulator," AIAA Preprint 81-2584, December 1-3, 1981.

31. Overly, P., and Bedard, R., "Acurex Parabolic Dish Concentrator (PDC-2)", Parabolic Dish Solar Thermal Power Annual Review Proc., DOE/JPL 1060-52, JPL Publication 82-66, Jet Propulsion Laboratory, Pasadena, California, July 15, 1982.

32. Overly, P., "Reflective Panel Development," Detail Design Review, Low Cost Concentrator, Acurex Corp., Vol. 1, pp. 132 to 159, July 30, 1981.

33. Solar Systems Group, "A Conceptual Design Study of Point-Focusing Thin-Film Solar Concentrators," Final Report to JPL, Contract 955804, Boeing Engineering & Construction, November 11, 1981.

34. O'Neill, M.J., "A Transmittance-Optimized Point-Focus Fresnel Lens Solar Collector," Proc. Fifth Parabolic Dish Solar Thermal Power Program Annual Review, DOE/JPL-1060-69, JPL Publication 84-13, Jet Propulsion Laboratory, Pasadena, California, pp. 25 to 47, March 1, 1984.

35. Winston, R., and O'Gallagher, J., "Non-Imaging Secondary Concentrators," Proc. Fourth Parabolic Dish Solar Thermal Power Program Review, DOE/JPL-1060-58, JPL Publication 83-2, Jet Propulsion Laboratory, Pasadena, California, pp. 221 to 233, February 1, 1982.

36. Ortabasi, U., Gray, E., and O'Gallagher, J., "Development of a Secondary Concentrator to Increase the Intercept Factor of a Dish with Large Slope Errors," Proc. Fifth Parabolic Dish Solar Thermal Power Program Annual Review, DOE/JPL-1060-69, JPL Publication 84-13, Jet Propulsion Laboratory, Pasadena, California, pp. 170 to 178, March 1, 1984.

37. Jaffe, L.D., "Solar Tests of Aperture Plate Materials for Solar Thermal Dish Concentrators," Jnl. Solar Energy Engineering, Vol. 106, pp. 408 to 415, 1984. Also, DOE/JPL-1060-62, JPL Publication 83-68, Jet Propulsion Laboratory, Pasadena, California, August 15, 1983.

38. Percival, W., and Nelving, H.G., "First Phase Testing of Solar Thermal Engine at United Stirling," Parabolic Dish Solar Thermal Power Annual Program Review Proc., DOE/JPL-1060-46, JPL Publication 81-44, Jet Propulsion Laboratory, Pasadena, California, pp. 37 to 44, May 1, 1981.

39. Latta, A.F., et al, The Effects of Regional Insolation Differences Upon Advanced Solar Thermal Electric Power Plant Performance and Energy Costs, JPL Publication 79-39, DOE/JPL-1060-17, Rev. A, Jet Propulsion Laboratory, Pasadena, California, February 1, 1980.

40. Randall, C.M., and Whitson, M.E., Report No. ATR-78(7592)-1, The Aerospace Corporation, El Segundo, California, December 1, 1977.

41. Maynard, D.P., and Birur, C.G., Analytical Foundations/Computer Model for Dish-Brayton Power System, JPL Internal Report 5105-9, Jet Propulsion Laboratory, Pasadena, California, September 1980.

42. Bowyer, J.M., A Program for the Calculation of Paraboloidal-Dish Solar Thermal Power Plant Performance, JPL Publication 85-36, DOE/JPL-1060-85, Jet Propulsion Laboratory, Pasadena, California, April 15, 1986.

43. Mavis, C.L., and Smith, P.N., A Description and Assessment of Solar Central Receiver Systems Technology, SAND82-8023, Sandia National Laboratories, Livermore, California, to be published.

44. Garrett AiResearch Manufacturing Co., Steam Rankine Solar Receiver for Jet Propulsion Laboratory, Report No. 16349, (Contract No. 955157, JPL Report 9950-1122), Torrance, California, November 13, 1979.

45. Fairchild/Stratos Division, Dish Stirling Solar Receiver Program, Final Report, R.A. Haglund, (Contract No. 955400, JPL Report 9950-473), Manhattan Beach, California, December 15, 1980.

46. Sanders Asso., High Temperature Solar Receiver Final Report, (Contract No. 955120, JPL Report 9950-351), Nashua, New Hampshire, April 1980.

47. Rosenberg, L.S., and Revere, W.R., A Comparative Assessment of Solar Thermal Electric Power Plants in the 1-10 MWe Range, JPL Publication 81-53, DOE/JPL-1060-21, Jet Propulsion Laboratory, Pasadena, California, June 1981.

48. Fujita, T., et al, A Standard Description and Costing Methodology for the Balance-of-Plant Items of a Solar Thermal Electric Power Plant, JPL Publication 83-4, DOE/JPL-1060-59, Jet Propulsion Laboratory, Pasadena, California, January 1983.

49. Directory of Electric Utilities: 1978-1980, 88th Edition, Electric World, McGraw-Hill Publications Co., New York, New York, 1979.

50. Habib-agahi, H., and Jones, S.C., Irrigation Market for Solar Thermal Parabolic Dish Systems, JPL Publication 81-85, DOE/JPL-1060-49, Jet Propulsion Laboratory, Pasadena, California, September 1981.

51. The BDM Corporation, Military Applications for Point Focusing Distributed Receiver Solar Thermal Electric Power Systems, BDM/W-79-751-TR, McLean Virginia, December 1979.

52. Science Applications, Inc., "Task 17 - Systems Analysis of the Parabolic Dish Technology for Industrial Process Heat and Total Energy Applications," Contract No. 955238, for the Jet Propulsion Laboratory, Pasadena, California, March 4, 1981.

53. Gates, W.R., Solar Thermal Technology Development: Estimated Market Size and Energy Cost Savings, JPL Publication 83-14, DOE/JPL-1060-60, Jet Propulsion Laboratory, Pasadena, California, February 1983.

54. Annual Energy Outlook 1983, DOE/EIA-0383(83), Energy Information Administration, May 1984.

55. Energy Outlook, Vol. 6, No. 2, Data Resources, Inc., Lexington, Massachusetts, Summer 1982.

56. The EPRI Regional Systems, EPRI-P-1950-SR, Electric Power Research Institute, Palo Alto, California, July 1981.

57. Edelstein, R., and Flowers, L., "Final Presentation of the Solar Thermal Cost Goals Committee," presented to the U.S. Department of Energy, Solar Energy Research Institute, Golden, Colorado, February 26, 1982.